

**Continuum-based models and concepts for the transport of nanoparticles in saturated porous media: A state-of-the-science review**

BABAKHANI, Peyman, BRIDGE, Jonathan <<http://orcid.org/0000-0003-3717-519X>>, DOONG, Ruey-an and PHENRAT, Tanapon

Available from Sheffield Hallam University Research Archive (SHURA) at:

<https://shura.shu.ac.uk/16233/>

---

This document is the Accepted Version [AM]

**Citation:**

BABAKHANI, Peyman, BRIDGE, Jonathan, DOONG, Ruey-an and PHENRAT, Tanapon (2017). Continuum-based models and concepts for the transport of nanoparticles in saturated porous media: A state-of-the-science review. *Advances in Colloid and Interface Science*, 246, 75-104. [Article]

---

**Copyright and re-use policy**

See <http://shura.shu.ac.uk/information.html>

## Accepted Manuscript

Continuum-based models and concepts for the transport of nanoparticles in saturated porous media: A state-of-the-science review

Peyman Babakhani, Jonathan Bridge, Ruey-an Doong, Tanapon Phenrat



PII: S0001-8686(16)30295-0  
DOI: doi: [10.1016/j.cis.2017.06.002](https://doi.org/10.1016/j.cis.2017.06.002)  
Reference: CIS 1773

To appear in: *Advances in Colloid and Interface Science*

Revised date: ###REVISEDDATE###  
Accepted date: ###ACCEPTEDDATE###

Please cite this article as: Peyman Babakhani, Jonathan Bridge, Ruey-an Doong, Tanapon Phenrat , Continuum-based models and concepts for the transport of nanoparticles in saturated porous media: A state-of-the-science review, *Advances in Colloid and Interface Science* (2017), doi: [10.1016/j.cis.2017.06.002](https://doi.org/10.1016/j.cis.2017.06.002)

This is a PDF file of an unedited manuscript that has been accepted for publication. As a service to our customers we are providing this early version of the manuscript. The manuscript will undergo copyediting, typesetting, and review of the resulting proof before it is published in its final form. Please note that during the production process errors may be discovered which could affect the content, and all legal disclaimers that apply to the journal pertain.

# Continuum-Based Models and Concepts for the Transport of Nanoparticles in Saturated Porous Media: A State-of-the-Science Review

*Peyman Babakhani<sup>1,2</sup>, Jonathan Bridge<sup>3</sup>, Ruey-an Doong<sup>1,4\*</sup>, and Tanapon Phenrat<sup>5,6\*</sup>*

<sup>1</sup>Department of Biomedical Engineering and Environmental Sciences, National Tsing Hua University, No. 101, Section 2, Kuang Fu Road, Hsinchu, 30013, Taiwan

<sup>2</sup>Department of Civil Engineering and Industrial Design, School of Engineering, University of Liverpool, Liverpool, Merseyside L69 7ZX, UK

<sup>3</sup>Department of the Natural and Built Environment, Sheffield Hallam University, Sheffield UK S1 1WB

<sup>4</sup>Institute of Environmental Engineering, National Chiao Tung University, No. 1001, University Road, Hsinchu, 30010, Taiwan

<sup>5</sup>Research Unit for Integrated Natural Resources Remediation and Reclamation (IN3R), Department of Civil Engineering, Faculty of Engineering, Naresuan University, Phitsanulok, Thailand, 65000

<sup>6</sup>Center of Excellence for Sustainability of Health, Environment and Industry (SHE&I), Faculty of Engineering, Naresuan University, Phitsanulok, Thailand, 65000

To be submitted to

**Advances in Colloid and Interface Science**

\*Corresponding authors:

Ruey-an Doong (radoong@mx.nthu.edu.tw)

+886-3-5726785(ph) +886-3-5733555(fax)

Tanapon Phenrat (pomphenrat@gmail.com)

(6655)964057(ph) (6655)964002(fax)

## Abstract

Environmental applications of NP increasingly result in widespread NP distribution within porous media where they are subject to various concurrent transport mechanisms including irreversible

deposition, attachment/detachment (equilibrium or kinetic), agglomeration, physical straining, site-blocking, ripening, and size exclusion. Fundamental research in NP transport is typically conducted at small scale, and theoretical mechanistic modeling of particle transport in porous media faces challenges when considering the simultaneous effects of transport mechanisms. Continuum modeling approaches, in contrast, are scalable across various scales ranging from column experiments to aquifer. They have also been able to successfully describe the simultaneous occurrence of various transport mechanisms of NP in porous media such as blocking/straining or agglomeration/deposition/detachment. However, the diversity of model equations developed by different authors and the lack of effective approaches for their validation present obstacles to the successful robust application of these models for describing or predicting NP transport phenomena.

This review aims to describe consistently all the important NP transport mechanisms along with their representative mathematical continuum models as found in the current scientific literature. Detailed characterizations of each transport phenomenon in regards to their manifestation in the column experiment outcomes, i.e., breakthrough curve (BTC) and residual concentration profile (RCP), are presented to facilitate future interpretations of BTCs and RCPs. The review highlights two NP transport mechanisms, agglomeration and size exclusion, which are potentially of great importance in controlling the fate and transport of NP in the subsurface media yet have been widely neglected in many existing modeling studies.

A critical limitation of the continuum modeling approach is the number of parameters used upon application to larger scales and when a series of transport mechanisms are involved. We investigate the use of simplifying assumptions, such as the equilibrium assumption, in modeling the attachment/detachment mechanisms within a continuum modelling framework. While acknowledging criticisms about the use of this assumption for NP deposition on a mechanistic (process) basis, we found that its use as a description of dynamic deposition behavior in a continuum model yields broadly similar results to those arising from a kinetic model. Furthermore, we show that in two dimensional (2-D) continuum models the modeling efficiency based on the Akaike information criterion (AIC) is enhanced for equilibrium vs kinetic with no significant reduction in model performance. This is because fewer parameters are needed for the equilibrium model compared to the kinetic model.

Two major transport regimes are identified in the transport of NP within porous media. The first regime is characterized by higher particle-surface attachment affinity than particle-particle attachment affinity, and operative transport mechanisms of physicochemical filtration, blocking, and physical retention. The second regime is characterized by the domination of particle-particle attachment tendency over particle-surface affinity. In this regime although physicochemical filtration as well as straining may still be operative, ripening is predominant together with agglomeration and further subsequent retention. In both regimes careful assessment of NP fate and transport is necessary since certain combinations of concurrent transport phenomena leading to large migration distances are possible in either case.

Keywords: nanoparticle, continuum model, advection-dispersion, transport, attachment, porous media.

### **Highlights**

- Continuum models can successfully describe NP transport phenomena across scales
- Sixteen distinct types of continuum model have been applied to NP transport
- Agglomeration and size exclusion may be critically underrepresented in NP models
- Work needed to raise efficiency of continuum models by robust parameter reduction

### **Contents**

1. Introduction
2. Methodology
3. Transport mechanisms and their continuum modeling approaches
  - 3.1. Advection and dispersion
  - 3.2. Attachment and detachment
    - 3.2.1. Irreversible deposition
    - 3.2.2. Detachment

- 3.2.3. Coexistence of both irreversible deposition and reversible attachment/detachment
- 3.3. Straining
  - 3.3.1. Mechanism
  - 3.3.2. Criteria and manifestation
  - 3.3.3. Modeling approaches of straining
- 3.4. Site-blocking and ripening
  - 3.4.1. Site-blocking mechanism and related modeling approaches
  - 3.4.2. Ripening mechanism and related modeling approaches
- 3.5. Size exclusion
  - 3.5.1. Significance for NP
  - 3.5.2. Mechanism
  - 3.5.3. Continuum modeling approaches of size exclusion
- 3.6. Aggregation
  - 3.6.1. Definitions and observations
  - 3.6.2. Modelling considerations
- 4. Equilibrium vs kinetic terms in continuum models
- 5. Overview of the concurrent occurrence of multiple transport phenomena
  - 5.1. Conceptual model of transport for stable monodisperse dispersions
  - 5.2. Conceptual model of transport for stable poly-disperse dispersions
  - 5.3. Conceptual model of transport for unstable poly-disperse dispersions
  - 5.4. Experimental validation of model concepts

6. Upscaling of continuum models for NP transport
7. Conclusion

## 1. Introduction

Nanoparticles (NP) possess unique properties in engineered and environmental systems compared to their micron size counterparts [1, 2]. This leads to various novel applications in a wide variety of technology fields such as remediation of contaminants [3-6], catalysis [7], energy [8, 9] and many more [10]. NP released from various manufacturing or disposal points, such as landfill and wastewater treatment [10-12], may enter the environment and accumulate in soils and sediments [10, 13, 14]. NP can be mobilized from the topsoil zone to saturated zone due to infiltration driven by rainfall or irrigation. They can also enter aquifers via activities that intentionally inject NP into the subsurface media, e.g., for remediation of groundwater or for recovery enhancement of petroleum reservoir [10, 11, 14-20]. Growing concern about the unintentional migration and accumulation of NP in the subsurface environment, coupled with the aspirations for novel applications of nanotechnology in the subsurface, necessitate recognition of all the underlying mechanisms that possibly affect the behavior of NP in the subsurface porous media [15-23]. This knowledge will facilitate more effective and precise modeling tools for the description and prediction of NP fate and transport in porous media, thereby facilitating the development of necessary regulations to halt conversion of nanomaterial from an ‘emerging technology’ [24] to an ‘emerging contaminant’ [22, 25].

Modeling tools are an essential component of decision-making and design of the remediation strategies for the removal of groundwater contaminants and reducing the potential risks of contaminant remobilization, e.g., redistribution of non-aqueous phase liquids (NAPLs) [26, 27] and radionuclides [28, 29] in the groundwater. The unique behaviors of NP lead to complication in predicting unintended exposure and risk of NP [23, 30-33]. A wide range of physicochemical interactions impact NP transport in the subsurface. The relative significance of these processes for NP may differ from that of larger colloids. For instance, aggregation is potentially one of the most important phenomena that can occur for NP transported in porous media [21, 33, 34]. Depending on the scale of the assessment and the required resolution/precision of the outcomes, modeling tools deployed for assessing the behaviors of NP in porous media may be categorized in three major groups: 1) abstract models; 2) mechanistic models; and 3) continuum-scale models [30, 35-

37]. Selection of the most appropriate model for a given problem is a trade-off between simplicity and accuracy [12, 38].

Abstract models including material flow analysis (MFA) or multi-media models (MMM), are founded on the mass balance principle and assess the release and fate of NP in the environment from the global level down to the local levels [e.g., 10-12, 22, 23, 37, 39, 40-44]. Most of these models are intrinsically based on simple algebraic equations and may not sufficiently capture the phenomenology of the influential factors into the model [14, 45], although some attempts have been made to address this [13, 14, 18, 46]. These models typically rely on statistical and probabilistic approaches that incur unknown uncertainties in the total results or about individual parameters which require rigorous uncertainty analysis [11, 40, 41]. MFA-based models are basically top-down models [44] and there exists a lack of suitable analytical methods for quantification, detection and analysis of environmentally relevant data of NP distribution at relevant scales [12, 43].

Mechanistic models focus on the individual particles by considering the forces, torques, and energy of particle and interacting media [30, 36, 47-54]. These models become more difficult to apply when several phenomena occur simultaneously during transport of NP in porous media [21, 31, 33, 48, 55-64]. Moreover, the intrinsic complexities and heterogeneities prevalent in real environmental conditions, such as surface roughness [65-68], natural organic matter (NOM) [32, 47, 69], iron oxyhydroxide coating [70-72], silylation [73], extracellular polymeric substance, and biofilm [74-76] make it unfeasible to use models such as classical colloid filtration theory (CFT) [65-68], Derjaguin–Landau–Verwey–Overbeek (DLVO) theory [47, 77], and Maxwell model [78-80] which impose assumptions of uniformity. Mechanistic description of particle interactions with such heterogeneities at a range of scales, is a lively area of ongoing research [21, 81-84]. These models are yet to face the challenges related to the concurrent occurrence of various phenomena.

Continuum-based models are defined as partial-differential equations based on the continuity principle (either the mass conservation law (mass balance) or particle number/volume balance) over the bulk spatial and temporal domains of the system which are either continuous or numerically-discretized continuous domains [30, 35, 36, 85-87]. This definition contrasts with pore-scale models in which the domain has a discrete configuration of solid and fluid [87]. In this review, we narrow down the scope of the continuum-based models to Eulerian techniques and thus

exclude the particle tracking analysis (generally Lagrangian methods) [34, 57], since they consider particles as a separate constituent from the fluid phase. It should be noted that commonly “continuum” terminology has been used to designate a range of larger spatial scales of the model domain ( $\gg 1$  cm) in contrast to micro/pore-scale models (1-100  $\mu\text{m}$ ) [87]. From the present paper’s viewpoint not only the spatial scalability of continuum models but also their ability to provide information about the kinetics of phenomena, transient situations, and heterogeneities in the bulk spatial domain are considered unique features of continuum-based models.

Continuum models have been widely used for simulating miscible contaminants and classical colloid transport problems over the past decades and more recently they have been gaining popularity for modeling NP transport [12, 86, 88-90]. These models can be applied at various scales such as pore scale [91], column experiment [e.g., 21, 92-94], bench-scale experiments [21], mesocosm experiments [22, 95], and field scale operations [96, 97]. This allows continuum-based models to be applied not only for delineating the risk of NP release and the design of remediation strategies in the local scale but also for validating global assessment models of NP transport in the environment by applying them in tandem [35, 44].

In contrast to mechanistic approaches which deal with forces or energy, continuum models deal with rates. These models accommodate different types of data based on number concentration [e.g., 21, 92, 98-100] or mass concentration [e.g., 100, 101, 102]. They can be modified to transform the data internally [21, 34]. They can therefore be calibrated and validated against a wide variety of available data types obtained from various laboratory experiments or realistic field measurements [21, 96, 97, 103]. More noteworthy, is their capability to describe several transport phenomena simultaneously [e.g., 21, 92, 102, 104-111].

No one of the fate and transport modeling approaches precludes application in parallel with any other, as each offers different insights. Fig. 1 illustrates the concept of a comprehensive, multi-model analysis of engineered nanomaterials in the environment. For instance, continuum models of groundwater can be integrated with MFA to track the fate of NP in the subsurface where the required data for MFA is less available [44]. This class of models can be used to average the results of pore scale mechanistic simulations in order to obtain the one-dimensional concentration field and consequently estimate the values of the average deposition rate coefficients [91].

To date, there have been several informative review papers on the transport behaviors of NP [e.g., 12, 22, 23, 47, 48, 88, 112-114] and other colloids [e.g., 30, 36, 53, 68, 98, 100, 115-121]. Nevertheless, most of these reviews commit to investigate mechanistic approaches such as classical colloid filtration theory (CFT) and/or DLVO theory. Thus far, from continuum viewpoint, there is no comprehensive review on various phenomena taking place for NP in porous media. Furthermore, an overview of the concurrent impacts of different transport mechanisms is lacking. Therefore, the present study focuses on all the possible transport mechanisms of NP in porous media and their superposition within the context of continuum modelling. These mechanisms comprise reversible, irreversible and equilibrium interactions of NP with porous media, as well as agglomeration, straining, blocking, ripening, and size exclusion. In this review, we describe the basic conceptual model applied along with each mathematical model for these processes. The motives behind selecting the type of conceptual model and their limitations are also discussed. Further conceptual scenarios in which various transport mechanisms are acting together are proposed to resolve inconsistencies incurred in the interpretation of the experimental outcomes using one model only. Finally, we briefly discuss some issues of upscaling continuum models to multidimensional scales.

## 2. Methodology

In this review we categorize 16 types of continuum-based models which have been used to date for simulation of NP transport (Table 1). Information from almost 50 papers on NP transport column experiments and continuum modeling are summarized in Table 2, which highlights underlying mechanisms of transport together with the respective types of the applied continuum model. The main NP of concern in these data include: silver (AgNP), nanoscale zero zero-valent iron (NZVI), iron oxide, hydroxyapatite (HAP), graphene, graphene oxide (GO), cerium dioxide (CeO<sub>2</sub>), TiO<sub>2</sub>, zinc oxide (ZnO), quantum dots (QDs), carboxylate-modified latex (CML), and aluminum oxide (AlO) NP. In order to investigate various deposition mechanisms, we used the MT3DMS [89] code to produce breakthrough curves for various combinations of attachment and detachment parameters. We also used this model following [21] in an assessment of the validity of assuming an equilibrium term to describe NP attachment and concurrent

agglomeration/attachment in porous media. Full details of the model conditions and validation data are provided in Section 4.

### 3. Transport mechanisms and continuum modeling approaches

Figure 2 shows the result of a preliminary survey of literature on the major processes considered in transport of various NP in porous media. Aggregation (or agglomeration) is the most frequently-reported process across all NP types followed by straining, blocking, ripening, size exclusion, reversible deposition, and irreversible deposition, respectively. Despite this, aggregation and size exclusion in porous media have been widely neglected in continuum modeling studies of NP transport [21, 34], at least in comparison with straining [71, 92, 110, 111, 122-137], blocking [71, 102, 123, 124, 127, 128, 130, 131, 135, 138] and ripening [105-107, 110, 111] effects.

#### 3.1. Advection and dispersion

Advection and dispersion mechanisms of colloids/NP have been recognized to be broadly the same as those of solutes such as ionic species, organic compounds, radionuclides etc. [54, 115]. Advection is the mechanism of transport with the average velocity of flowing groundwater. Mechanical dispersion [89] acts to spread the solute or colloid suspension parallel with and normal to the direction of flow because of the difference between the real velocity of the water inside the pores and the mean groundwater velocity, which arises from microscale velocity variation both within and between pores of different sizes [87, 89, 139-144]. Adding the molecular diffusion to the mechanical dispersion will result in hydrodynamic dispersion [89].

In case of slow groundwater velocity, such as flow through compacted porous media, dispersion is of low significance but can nevertheless result from the molecular diffusion due to concentration gradients [84, 145]. Accordingly, the transport of solute and colloids/NP through porous media in the most simplified form might be described by the following basic partial differential ‘advection-dispersion’ equation (ADE) [84, 86, 119, 145-148]:

$$\frac{\partial C}{\partial t} + \frac{\rho_b}{\varepsilon} \frac{\partial S}{\partial t} = D \frac{\partial^2 C}{\partial x^2} - V \frac{\partial C}{\partial x} \quad (1)$$

where  $x$  is distance in the porous media [with the dimension of L];  $t$  is time elapsed [T];  $C$  [ $N L^{-3}$ ];  $N$  represents the particle number] and  $S$  [ $N M^{-1}$ ] are the particle number concentrations of fluid-phase particles and deposited phase particles, respectively [e.g., 21, 92, 98-100], or alternatively

$C$  [ $\text{ML}^{-3}$ ] and  $S$  [ $\text{MM}^{-1}$ ] are the particle mass concentrations of fluid-phase particles and deposited phase particles, respectively [e.g., 100, 101, 102];  $V$  [ $\text{L T}^{-1}$ ] is the pore water velocity (also known as real water velocity, linear groundwater flow velocity, seepage water velocity, interstitial velocity, or advection velocity). This is different from the Darcy velocity (also known as the superficial velocity or approach velocity) which is equal to the porosity times the pore water velocity [ $\text{LT}^{-1}$ ].  $D$  is the hydrodynamic dispersion or simply dispersion coefficient [ $\text{L}^2\text{T}^{-1}$ ];  $\varepsilon$  is the bed porosity [—]; and  $\rho_b$  is the porous medium bulk density [ $\text{ML}^{-3}$ ].

The dispersion in Eq. (1) is defined by analogy to Fick's law of diffusion and is linearly related to the pore water velocity. In a one-dimensional uniform flow field such as column experiments transverse dispersion is not considered and thus the dispersion coefficient has one longitudinal component related to pore water velocity [89, 149]:

$$D = \alpha_L V + D^* \quad (2)$$

where  $\alpha_L$  is longitudinal dispersivity [ $\text{L}$ ] and  $D^*$  is the effective molecular diffusion coefficient [ $\text{L}^2\text{T}^{-1}$ ].  $\alpha_L$  is typically an intrinsic property of the porous medium as well as a function of scale [94, 149-151]. Thus, the common practice for both colloid and reactive solute transport is to determine this coefficient based on the breakthrough curve (BTC) of nonreactive solute transport through any given porous media [94, 146, 149, 152]. However in the case of colloid transport, Chrysikopoulos and Katzourakis [94] in a meta-study of 48 different BTCs, found that the dispersivity can exhibit a positive correlation with the particle size and the pore water velocity. Therefore, they suggested that the dispersion coefficient should be obtained from the colloid breakthrough data rather than nonreactive solute transport due to the potential for particulate-specific dispersion mechanisms such as size exclusion and preferential flow (discussed in later sections) [92, 94, 141, 151]. Nonetheless, this approach can make the inverse modeling problematic when there are other parameters that must be estimated to represent other colloidal transport phenomena. Further research is needed to understand the uniqueness of estimated parameters based on fitting continuum model outputs to experimental data, especially when dispersivity is considered along with other NP transport parameters in the inverse modeling process.

Molecular diffusion is commonly neglected in colloid and solute transport studies with pore water velocities in the ranges of natural groundwater velocities [89, 151, 153]. However, it can become significant in very compact and fine porous media, fractured media with very low pore water velocities, or when there are other processes involved such as thermal or electrophoresis effects [89, 154-157]. The intrinsic diffusivity of colloidal particles decreases with increasing size according to the Stokes-Einstein equation and it is typically more than three orders of magnitude lower than the molecular diffusion for common solutes [94, 158-160]. For instance, the diffusivity of water is around  $2.3 \times 10^{-9} \text{ m}^2\text{s}^{-1}$  at 25 °C while for spherical particles with a diameter of 100 nm it is around  $4.9 \times 10^{-12} \text{ m}^2\text{s}^{-1}$  according to Stokes-Einstein. Nevertheless, NP differ from larger colloids since diffusion may remain a significant mechanism in their transport behaviors. Molnar et al. [30] recently identified the high diffusivity of NP as a barrier toward developing mechanistic modeling approaches for NP transport as well as a reason for the lack of distinction between solute and NP mobility properties. To date, NP diffusion has been rarely considered as a distinct parameter in the continuum models—only one study [157] has considered its effect via Stokes-Einstein equation in the numerical transport model. Yet, frequently mechanistic modelling approaches have recognized its potential influence on the deposition behavior of NP [31, 32, 67].

### **3.2. Attachment and detachment**

#### **3.2.1. Irreversible deposition**

Solute mass transfer from liquid to solid phases is generally dominated by sorption which is usually modelled as a reversible kinetic process [161]. However, colloids and NP interact with solid surfaces of porous media by a number of mechanisms which may yield attachment that is practically irreversible. In other words, solute retention which appears irreversible at short timescales can be considered reversible at larger time scales under the same conditions [161], whereas irreversibly attached colloids may not be detached unless a significant physical or chemical perturbation occurs in the conditions of the system [66]. Irreversible deposition or physicochemical filtration was well described by colloid filtration theory (CFT). This was performed initially by drawing analogy to the transport in flocculation process [65], later by trajectory analysis [162], and by using filtration mass balance equations in a sphere around a single collector [163]. Filtration theory needs estimation of two parameters, the single-collector

attachment efficiency,  $\alpha$ , and single-collector collision or contact efficiency,  $\eta_0$ . The first of these describes the probability of any collision between a particle and a collector resulting in attachment; the second describes the probability of that collision occurring in the first place. Although there has been a marked advancement in predicting  $\eta_0$  through use of correlation equations with controllable parameters such as Péclet number, particle:grain size ratio, and so on [31, 32, 67, 164], the estimation of  $\alpha$  still requires either empirical derivations, which may not be generalizable, or laboratory-column experiments [12, 31, 67, 88, 113]. This limitation has caused researchers to go as far as eliminating  $\alpha$  — replaced by a parameter for fractioning reversibly and irreversibly deposited particles [165].

In continuum-based models, the definition of the attachment term depends on the conceptualization of deposition phenomena. The simplified form of the governing ADE equation for colloid transport in porous media can be written with a first-order irreversible attachment term as model type (i), Table 1 [119, 148]. In this model,  $K_{att}$  is attachment rate coefficient [ $T^{-1}$ ] which can be related to the parameters of CFT via the following equation [67, 68, 146, 166-168]:

$$K_{att} = \frac{3(1-\varepsilon)}{2d_{50}} \alpha \eta_0 V \quad (3)$$

where  $d_{50}$  is the median porous media grain size [L] and  $\varepsilon$  is the porosity of porous media [—]. Although the parameter  $K_{att}$  can be expressed via the theoretical relationship of Eq. (3), determination of  $\alpha$  still requires experimental data. On this basis, throughout this paper we directly deal with the parameter  $K_{att}$  instead of  $\alpha$  [91, 93]. From the continuum modeling viewpoint, type (i) models only describe irreversible deposition and do not consider subsequent detachment. In experimental conditions where attachment is the only operative mechanism, increase in the value of  $K_{att}$  leads to a flat reduction of the BTC plateau as shown in Fig. 3. The curves in this figure are produced by numerical solution of type (i) model using the MT3DMS code [21].

Table 2 shows that 20% of NP continuum modelling studies used type (i) models. It is evident that most of these studies used very simplified experimental conditions, highlighting that this model and thereby CFT are strictly limited in scope of application to steady flow through idealized, uniform media. There have already been several excellent review papers [30, 48, 51-54, 56, 112, 115, 120] discussing the deposition mechanisms of NP and colloids in porous media. From the

perspective of continuum modelling, however, it is apparent that deposition cannot be considered in isolation except in the most artificial circumstances.

### 3.2.2. Detachment

When the colloid association with the solid surface is not strong enough to be permanently retained, particles can be subject to reversible deposition and thereby detachment. Particles can be maintained temporary when they are trapped at a shallow DLVO secondary minimum [31, 33] or as recently found even at a shallow primary minimum resulted from nanoscale surface heterogeneities [169, 170], or held at the surface by hydrodynamic forces. Depending on how fast the diffusion of the material is, the process of attachment-detachment can be considered in form of either fast forward—backward interactions of particles or discrete retention—re-entrainment of particles [102, 165, 167, 171]. In other words, if particle detachment is so fast that the net result of particle interactions with the solid surface is dominated by attachment, it is only the attachment that can be at last perceptible. On the other hand, if the detachment rate is low, for example in slow-diffusion regimes experienced by larger ( $> 1 \mu\text{m}$ ) colloid/aggregate sizes then particles may be first deposited and then be subject to detachment in time; this case is commonly termed ‘re-entrainment’ [165, 167].

Commonly among literature studies, three forms of detachments have been inferred: (1) detachment shown by tailing in the BTC; (2) detachment in form of retarded or delayed BTC; and (3) detachment or release in form of separated peaks following the BTC. The first type of detachment typically emerges where the feeding solution into the column inlet is switched from the injecting particle dispersion to the particle-free solution with the same ionic strength and pH (two-phase injection experiments). This is the most common reference to ‘detachment’ and has been observed for various NP such as NZVI [105, 136], carbon nanotubes [172], silica [102], nanoporous silicate [173], and Ag NP [174-176] (Table 2). This is also known as re-entrainment and has been observed as dramatically extended BTC tailing which has been observed for a wide variety of colloids [165, 167, 171, 177]. The underlying mechanism for this kind of detachment is commonly sought in the hydrodynamic forces [33, 104, 178, 179]. The governing set of transport equations considering kinetic detachment of this type is given as type (ii) models (Table 1) [100, 142], as well as types (iii) and (iv) models accounting for dual-site attachment/detachment. Using

the MT3DMS code [89], we numerically solved type (ii) set of equations. The outcomes, by holding  $K_{att}$  constant while varying  $K_{det}$ , are presented in Fig. 4a. This figure shows that rising  $K_{det}$  not only causes the emergence of tailing in BTC, but also this leads to an asymmetric rise in the plateau of BTC which is higher at the side of the descending limb. The plateau elevates until finally it becomes flat at the largest value of  $K_{det}$  where BTC resembles the conservative transport behavior.

In the second type of detachment, retardation appears as a horizontal shift in the colloid/NP BTC compared to conservative transport BTC (Fig. 4b). This has been observed for iron NP [180], Ag NP [138, 174, 175], carboxyl-modified latex NP [181], HAP NP [124], and QDs [182-184] (Table 2). The most pronounced occurrence of the retardation has been observed for NP with infinitesimally small size (<10 nm) such as QDs, particularly at elevated IS, decreased pH, [183-185], smaller sizes of porous media grains [183, 186] or increased temperature [182]. It should be noted that although here we categorize retardation as a kind of detachment, in several studies which have observed retardation, ‘detachment’ has been ruled out because of not observing the tailing in the BTC [181, 183-190]. Nevertheless, our view based on the sum of evidence is that retardation results from reversible interaction of particles with the porous media surfaces – attachment and detachment, therefore — the net result of which will control the final transport of particles [21]. In the case of QDs, the delay in the BTC may arise from the fast diffusive mass transfer rate of QDs from bulk solution to the sand surface and slower mass transfer of QD from the solid phase to the bulk phase [183]. Retardation in its linear form is mathematically related to the most common parameter in the literature of reactive transport modeling in groundwater known as distribution coefficient or partition coefficient  $K_d$ . The use of  $K_d$ , however, requires applying an assumption of equilibrium between the dissolved and sorbed phases of solute contaminant (or attached and mobile phases of particles as discussed in section 4). The respective model of this parameter is given in Table 1, as type (v). The solution to this model using MT3DMS code is shown in Fig. 4b. This figure elucidates how retardation (and acceleration as will be described in section 3.5, “Size exclusion”) of BTC can occur in combination with a significant amount of irreversible attachment ( $K_{att} = 1 \times 10^{-3} S^{-1}$ ).

The third type of detachment is related to the cases where after injection of the particle dispersion (first phase) and particle-free background solution (second phase), a solution with a lower IS or a

different pH is flushed through the porous media container. The released mass can be seen in the BTC in form of separated peak(s) following the primary breakthrough [63, 64, 187, 189, 191-194]. The model for simulating the release is given as type (vi) model in Table 1 [64, 115, 187]. This equation assumes that remobilized particles do not reattach again, with the rationale that conditions following a perturbation that causes release are less favorable for reattachment than the original conditions [64].

Overall, for very small NP that display high diffusivity, thereby more collisions, detachment typically emerges in form of retardation of the BTC [102, 183], whereas for larger particles, due to hydrodynamics of the system, detachment may emerge in the form of tailing of the BTC [33, 104, 178, 179]. We suggest that in future studies selecting an appropriate detachment model should be based on the aforementioned categorization. It should be mentioned, however, that the models listed in this paper for every transport mechanism are not strictly the only available approach, and there might be other alternatives, particularly in the field of colloid transport literature. For instance, there have been other modeling approaches to the release of attached colloidal particles under perturbation (third type of detachment) [195, 196]. There is clearly a need for further work to understand the thresholds or transitions between different detachment phenomena and relate these, if possible, to changes in the rates of competing underlying processes acting on particles.

### **3.2.3. Coexistence of both irreversible deposition and reversible attachment/detachment**

In many practical cases both kinds of interaction can exist in the same system together, resulting in both reversible and irreversible depositions. This has been frequently observed in studies with dual deposition sites or polydisperse NP dispersions (containing fractions of small and large particles) [e.g., 21, 31, 33, 197, 198, 199]. In these cases, neither equilibrium sorption nor non-equilibrium kinetic attachment/detachment models alone can satisfactorily describe NP transport, as none of them take into account the absolute irreversible deposition by themselves. In the case of the equilibrium model, the irreversibility is not taken into account because a physical relationship between the mobile-phase concentration and the immobile-phase concentration (sorption isotherms) is imposed upon the governing equation of the transport in porous media via the  $d\bar{C}/dt$  term [161]. Regarding the non-equilibrium model, absolute irreversibility cannot be reached, unless the detachment rate in type (ii) model, (Table 1) is considered equal to zero—in which case the model reduces to type (i), Table 1. It was clearly illustrated in Fig. 4a that any

increase in  $K_{\text{det}}$  value resulted in the emergence of tailing in BTC, as well as an asymmetric rise in the plateau of BTC, suggesting that absolute irreversibility cannot be achieved by model type (ii) alone. Therefore, both equilibrium and non-equilibrium attachment/detachment models are intrinsically reversible and cannot take into account the absolute irreversibility of colloidal particles in the transport problems.

Accordingly, there is a need for an additional term in the model to describe irreversible deposition. Commonly, if the  $K_d$  parameter can be used by invoking the equilibrium assumption, then description of irreversible deposition is made by addition of a sink term to decay the concentration of the fluid phase—similar to the simple irreversible deposition model explained already (model type (i), Table 1). This combination results in model type (v), Table 1. The BTC produced by such a model is shown in Fig. 4b. However, should the equilibrium assumption cannot be invoked, then kinetic model already has a term that decays the concentration of the fluid-phase, and no additional term can be added to decay the concentration of this phase. In this case a sink term that decays the concentration/population of the attached phase ( $-\lambda_2 \frac{\rho_b}{\epsilon} S$ ) may be added to the model in order to take account of irreversible deposition—as given in model type (vii), suggested by Babakhani et al. [21], Table 1. Thus, in future modeling practices, we propose using either of the aforementioned approaches whenever both reversible and irreversible attachments are suspected to be operative simultaneously, e.g., due to heterogeneity in the population of particles. For such cases, these approaches are believed to be more rigorous representations of real condition rather than dual-site deposition models, e.g., model types (iii) and (iv). Further research is required to test this assertion across a range of scales and systems.

### 3.3. Straining

#### 3.3.1. Mechanism

In addition to the filtration mechanisms which are driven by the interfacial forces between particles and the porous media surfaces, retention of particles in porous media can be driven by physical straining [62, 200]. Since straining has been identified recently as a key process of retention in the transport of NP in porous media [e.g., 75, 125, 126, 130-132, 134, 137, 192, 201-207], in this section we review this phenomenon from the very fundamental concepts.

Straining is defined as the process of physical trapping of particles in the pore throats which are narrower than the size of particles. In the case of high concentration of particles, straining is deemed to occur as a result of concurrent arrival of many particles at a pore opening. This can result in “jamming” and “arching”, and eventually lead to “clogging” of the filtration surface [56, 120]. In engineered filtration systems such physical straining results in a continuous compressible cake [208, 209] or a mat with holes on it [209]. But although observed in experimental micromodel by the aid of pore visualization [210] this is not considered common in natural aquifers unless it is encountered at the upper area of porous media [53, 211] or in the case of injecting engineered NP into subsurface media, in the near vicinity of the injection well [e.g., 212, 213-215]. Occasionally straining has been further subdivided into two mechanisms of wedging and bridging. Wedging is the trapping of particles at two bounding surfaces without interference of particles while bridging is the simultaneous arriving and accumulation of particles at the pore constriction [51, 216, 217].

### 3.3.2. Criteria and manifestation

In reality, even for ideal spherical and uniform grains and NP, the pores are not ideal flow channels for the transport of NP because of the existence of narrow spaces at the contact angle of the spheres. These angular spaces brings about a potential of straining for different sizes of NP. Herzig et al. [119] illustrated different retention sites for straining as (Fig. 5): (1) surface sites; (2) crevice sites; (3) constriction sites; and (4) cavern sites. This initiated the development and the use of a criterion for straining model selection by the ratio of particle diameter to grain diameter ( $dp/dg$ ) [107, 200, 218]. This critical ratio for straining as obtained from experimental results simultaneously under the influence of physicochemical filtration and straining retention was found to be 0.0017 [62, 92, 219-221]. The idea of a critical straining threshold is important in developing the conceptual model of NP transport in regards to straining, since many papers have attributed [74, 75, 125, 126, 130-134, 137, 192, 201-207] or rejected [129, 222-224] the influence of straining based on this criteria.

Physical straining has been recognized to contribute: (1) to the removal of CeO<sub>2</sub> NP, (with  $dp/dg$  of 0.0002) ascribed to the angular shape of the porous media grains (industrial mineral silica) [192]; (2) to the removal of Ag NP following aggregation (with initial  $dp/dg = 3 \times 10^{-5}$ ) [201], or heteroaggregation (with initial  $dp/dg$  ranging from 0.0001 to 0.0004) [202], or due to the

existence of a portion of pores smaller than the particle size (with overall  $dp/dg = 3 \times 10^{-4}$ ) [203]; (3) to removal of GO at high IS due to concurrent agglomeration in porous media with initial  $dp/dg$  in range of 0.003-0.009 [130, 131], or with initial  $dp/dg$  in range of 0.001-0.002 [133], or elevated  $dp/dg$  of 0.005 [132], and/or ascribed to increased surface roughness because of the biofilm-coated sand with initial  $dp/dg$  of 0.0005-0.0007 [74]; (4) to removal of TiO<sub>2</sub> NP because of straining caused by aggregation during flow in porous media (initial  $dp/dg$  ranging from 0.001 to 0.010) [134] or due to presence of initial aggregates since suspended aggregates are more prone to encountering smaller pore throat (initial  $dp/dg = 0.0005$ ) [204], or because of the smaller pores resulted from the clay content in the soil (initial  $dp/dg$  in range of 0.0003 to 0.001) [205]; (5) to removal of ZnO NP at the high IS (50 mM NaNO<sub>3</sub>) due to heteroaggregation with soil particles, due to the presence of surface charge heterogeneities (resulting in subsequent clogging of the pores) (initial  $dp/dg$  in range of 0.001 to 0.009) [137], or due to the concurrent aggregation [75, 206, 207] with initial  $dp/dg$  in range of 0.0006 to 0.0012. Straining has also been recognized to contribute to the removal of HAP NP and goethite particles when co-transported and heteroaggregated, with maximum  $dp/dg$  of 0.0046 [125] or for HAP NP and hematite particles with maximum  $dp/dg$  of 0.0027 [126] being larger than the literature threshold value (0.002). These figures show that the criteria of 0.0017 cannot be valid for NP mainly due to the interference of other mechanisms.

In addition to this criterion, another sign for identifying the straining is the shape of the retained colloid mass profile as function of distance from inlet (RCP). As such, a number of authors [109, 110, 122, 129, 172, 225-228] attributed the retention behavior to straining whenever they observed a hyper-exponential profile for the RCP; that is a marked decreasing rate of deposition with distance from inlet according to an inverse power law. This is in spite of the fact that hyper-exponential behavior of the RCP can also be attributed to other factors and mechanisms such as surface roughness [62, 92, 229, 230], concurrent aggregation [231-234], colloid population heterogeneity [194, 235], variations in the pore-scale velocity [127, 236, 237], and chemical heterogeneity [220, 238, 239]. Nevertheless, monotonic and/or non-monotonic RCPs can be observed when the straining is considered the dominant mechanism of retention [109, 200, 240, 241]. Non-monotonic RCP demonstrates a peak of concentration somewhere between the inlet and the outlet of the porous media domain [109]. Therefore, hyper-exponential behavior of RCP may not be a deterministic sign of the straining phenomenon.

Despite extensive allusions to the reflection of transport and deposition mechanisms in the RCP shape among literature studies [e.g., 109, 110, 122, 129, 172, 225-227], there have been fewer attempts to evaluate the slope of the BTC plateau in regards to the underlying mechanisms of transport. In this paper, the information about various BTC plateau shapes including flat, ascending, and descending in both forms of limited duration of particle injection and continuous injection (experiments without post-flush of particle-free dispersion) were collected in Table 2. Straining has been reported along with a flat shaped plateau of BTC for AgNP following aggregation [201], GO at intermediate IS [133], and ZnO in presence of biofilm or NOM [75, 206] and with an ascending-shaped plateau of BTC for nHAP [111], GO at high IS [133], and ZnO [206, 207]. More frequently, however, straining has evidently come with an ascending-BTC plateau, e.g., for AgNP [176, 242]. NZVI [136], GO [74, 130-132], CeO<sub>2</sub> [192], TiO<sub>2</sub> [134], and ZnO [137]. This suggests that potential sites for straining mostly have a limited capacity. Once this capacity is met, a decrease in the retention rate results, that appears as an ascending-BTC plateau. Hence, straining is a phenomena that should commonly occur along with other transport mechanisms, such as blocking.

### 3.3.3. Modeling approaches of straining

Generally, straining has been described either with a depth-dependent decaying exponential function [92] or with a concentration-dependent decaying exponential function [200, 218, 241] in the continuum-based modeling framework. The former includes one empirical parameter,  $\beta$ , standing for the shape of the colloid spatial distribution and one extra variable of  $x$  standing for the distance from the inlet. This function, given below, is in fact able to predict the depth dependent RCP [92]:

$$\psi_x = \left(\frac{d_c+x}{d_c}\right)^{-\beta} \quad (4)$$

where  $d_c$  is size of grains (collector) representing the pore length which is oftentimes considered as  $d_{50}$ , the median size of the porous media grains. The implementation of this function in the advection-dispersion model is its multiplication in the term for attachment (in  $K_{att}$ ) as given in model types (viii), (xi), (xii), (xiii), (xiv), and (xv) in Table 1. When  $\beta$  is equal to zero ( $\psi_x = 1$ ), the decrease of retained concentration with distance is exponential which is the case for clean bed filtration theory [110].

On the other hand, the concentration-dependent decaying exponential expression includes two parameters, a rate coefficient parameter,  $k_0$ , standing for straining kinetic rate coefficient [ $T^{-1}$ ] and the coefficient for the exponential decline in straining rates,  $\lambda$ , with the same unit as retained concentration variable,  $S$ , [ $NM^{-1}$  or  $MM^{-1}$ ] [200]:

$$\frac{\rho_b}{\varepsilon} \frac{\partial S}{\partial t} = k_0 C e^{-S/\lambda} \quad (5)$$

This equation is solved with the advection-dispersion equation. When  $S \approx 0$ , the equation becomes the same as that for clean bed colloid filtration theory.

The depth-dependent expression of Bradford et al. [92] has become more popular for simulation of colloid and NP straining to the extent that most of the recent literature studies on NP transport have utilized this expression to fit the BTC/ RCP of NP transport through column experiments, e.g., for hydroxyapatite NP [71, 111, 122-126] and silver NP [123, 127]. This expression only uses one parameter ( $\beta$ ) which can be estimated based on the observed shape of the RCP. In some studies a fixed value of 0.432 [71, 92, 110, 111, 122-124, 127-134] or 1.532 [e.g., 138] has been used. In most studies, however, this parameter has been considered as a free parameter to be estimated in the inverse modeling and the values obtained are highly variable: 0.302 and 1.234 for Ag NP [135], 0.609 for CMC-NZVI [136], in range of 0.02 to 0.33 for ZnO NP [137], ranges of 0.659-2.28 and 0.764-1.69 in co-transport of HAP NP and hematite particles, respectively [126], or ranges of 0.432-1.85 and 0.432-1.57 in co-transport of HAP NP and goethite particles, respectively [125].

The depth-dependent model of Bradford et al. considers a decaying attachment rate with distance which is favorable for capturing the hyper-exponential behavior of RCP, frequently witnessed in the transport of colloid and NP subjected to concurrent physicochemical filtration and straining. On the other hand, in studies which have used the concentration-dependent model, the effect of physicochemical filtration had been turned off, by thoroughly cleaning of the sand and the use of deionized water (DI) as the dispersant solution, in order to maximize electrostatic repulsion between the colloids and sand surface thereby to expect the mere influence of straining unambiguously [185, 200, 218, 240, 241]. This brought about nearly a monotonic shaped RCP in those studies. It is still not clear whether this model can fit the BTCs and RCPs for the conditions where concurrent influences of physicochemical filtration and straining exist. It should be noted that the straining model of Bradford et al. has been criticized for not having enough power to

describe the real straining phenomenon [243]. In other words, whenever the depth-dependent model has been fitted to the experimental data with hyper-exponential RCP, it is obscured, recalling the ambiguities of the relevancy of straining to the RCP behavior, whether in reality the model describes the straining phenomena or it just captures the depth-dependent behavior [243]. One key drawback of the depth-dependent model of Bradford et al. is that it is still unknown how the variable of depth or length should be treated when it comes to application of the model in two- and three-dimensional simulations [118]. Although recently Köber et al. [213] employed this model for field-scale simulations, the treatment of the variable,  $x$ , was not clarified by these authors. In addition to this difficulty in upscaling the depth-dependent model of Bradford et al., it is also unclear whether this model can be valid in the real condition of flow in larger scales where the effect of preferential flow paths is considerable [153, 199, 210, 244, 245]. To date, relatively very few studies have discussed the occurrence of straining, clogging or pore plugging in the porous medium during NP transport in multi-dimensional domains [96, 157, 213, 214], some of which even tried to rule out these phenomena. Therefore, there is a crucial need to develop more rigorous conceptual models that can consider the concurrent effect of various phenomena occurring with straining of NP during transport in porous media. This may help providing insight into the role of each underlying mechanism. The problem becomes even more convoluted when other phenomena such as blocking/ripening and size exclusion are also involved as addressed in the next sections.

### **3.4. Site-blocking and ripening**

#### **3.4.1. Site-blocking mechanism and related modeling approaches**

The surface of porous materials may have a limited capacity for the adsorption/attachment of solute/particles and once this capacity is filled, the adsorption/attachment of further solute/particles is hindered by the presence of previously sorbed/attached materials. The most well-known approach for modeling this quality, which is called site-blocking effect, is to use the Langmuir approach for solute/gas [246] and for colloid [247] adsorption onto solid surfaces. This is used to model the site-blocking effect of colloidal particle attachment during transport in porous media via the following relationship [102]:

$$\psi_b = \left(1 - \frac{S}{S_m}\right) \quad (6)$$

where  $\psi_b$  is the Langmuirian blocking function related to the fraction of porous medium available for deposition [—] and  $S_m$  is the maximum retained-particle phase concentration, i.e., colloidal retention capacity [ $\text{NM}^{-1}$  or  $\text{MM}^{-1}$ ]. When used in the advection-dispersion model, this expression will result in a second-order colloid deposition kinetics limited by aqueous phase as well as the solid phase concentrations [102, 248]. The BTC produced by this model does not maintain a plateau but instead gradually climbs toward the peak (ascending plateau). This gradual rising plateau is a sign of decline in the deposition rate with increasing the amount of attached phase particles, i.e., the blocking effect [102]. Accordingly, many papers by observing the gradual increasing plateau of the BTC, applied the Langmuirian approach into the continuum model (model types (ix), (x), (xi), (xii), (xiv), and (xv), Table 1) in order to simulate the transport of NP such as Ag NP [135, 203], GO [249-251], CeO<sub>2</sub> NP [192], TiO<sub>2</sub> NP [102, 222], QD [184-187], and CML [185]. Based on the satisfactory model fitting results, these studies proposed the blocking of the physicochemical attachment sites as an underlying phenomenon for transport of NP in porous media. However, the application of this model has not been only limited to the blocking due to physicochemical deposition but also has been widely applied for describing the depleting capacity of the straining sites over time via model types (xi) and (xii), Table 1, e.g., for AG NP [123, 127, 128, 135, 138], GO [130, 131], and several other colloids [e.g., 110]. In addition, in a few studies [71, 124], the Langmuirian type site-blocking function was combined with the depth-dependent model of straining in form of dual-deposition sites (model type (xi), Table 1)—one for time-dependent retention and another for depth-dependent deposition, without any mention of straining or blocking explicitly.

It is very important to note that a rising plateau of the BTC should not be always taken as a sign of site-blocking phenomenon. Recalling the BTC generated by using the simple non-equilibrium attachment/detachment model (model type (ii), Table 1) in Fig. 4a, ascending BTC plateaus can also emerge with increasing  $K_{det}$  values as described in Section 3.2. Nevertheless, these shapes of BTC, which result from simple attachment/detachment model, come with tailing which may not be the case when the underlying transport process is site blocking [e.g., 132, 133, 181, 186, 187, 203, 222, 249, 250] unless they occur simultaneously. In the latter case, both  $K_{det}$  and Langmuirian function should be included in the model at the same time [74, 105, 130] (Table 2).

From a mechanistic standpoint, the Langmuir function can be criticized for being a linear function of the surface coverage [252]. Therefore, a dynamic blocking function based on the non-equilibrium model of random sequential adsorption (RSA) mechanics as a nonlinear power law function of surface coverage was developed in order to account for the real surface exclusion effects introduced by larger colloids [252, 253]. Being a sort of mechanistic approach, this model obviated the need for parameter estimation. This model was even employed to simulate the transport of colloid in heterogeneous porous media [101]. Nevertheless, this type of modeling approach generally comes with the disadvantages of ignoring the specific interactions of attaching particles with interfaces and with previously deposited particles, as well as inefficiency of their application for non-spherical particles [36]. Furthermore, they have the limitation of being strictly valid for just the irreversible deposition [36]. Detailed discussion of this model can be found in [36]. Overall, the identification of blocking phenomena is clearer than other transport mechanisms, such as straining and agglomeration, e.g., a rising-plateau BTC without tailing appears to be a clear sign of blocking mechanism in the system. A Langmuir type model, in spite of emanating from solute transport literature, has generally been found effective for modeling the site-blocking aspect of NP transport in porous media across different scales [254, 255].

### **3.4.2. Ripening mechanism and related modeling approaches**

Ripening is the opposite of the blocking phenomenon, i.e. it is expected to occur when the particle-particle interactions/associations on the surface of porous media are stronger than the particle-surface interactions/associations. Also, in contrast to the blocking mechanism, in which the deposition rate decreases with time, ripening causes an increase in the deposition rate with time. This leads to a dropping plateau of the BTC in the case of ripening [51, 92, 98, 100, 106, 107, 111, 115, 126, 234, 256-261]. Ripening has been observed for NP such as NZVI [105, 106, 258, 260, 262, 263], HAP NP [71, 111, 125, 126], TiO<sub>2</sub> [256, 264, 265], nano- C<sub>60</sub> [266], CeO<sub>2</sub> NP [267], and ZnO NP [206, 207] typically at ISs in the range 10-20 mM NaCl or 1 mM CaCl<sub>2</sub> [e.g., 207, 256, 265]. Increase in the inflow concentration of NP strongly affects the ripening and can result in clogging of porous media [105, 106].

In the context of continuum-based modeling of NP, two modeling approaches have generally been applied for ripening. First, a more robust form of Eq. (6), already capable of modeling the blocking effect, was introduced to model the ripening phenomenon alternatively, given as Eq. (e) in model

type (xv), Table 1 [105-107]. This equation represents ripening when  $\beta_1 > 0$  and  $A_1 > 0$  or blocking when  $\beta_1 = 1$  and  $A_1 = -1/S_m$ . Second, ripening has been modeled by adding a second-order term between aqueous phase and the attached phase to the mass balance equation of the attached phase as given in Eq. (b) in model type (xiii), Table 1 [110, 111].

The complexity of concurrent occurrence of various transport phenomena, namely, site-blocking and ripening along with aggregation, straining, and size exclusion, aggravated by the lack of proper experimental detection techniques, has not only caused problematic selection and application of various types of modeling approaches but also has been extended to the applied terminology in the literature of the subject [30, 118, 143]. Since ripening takes place in physicochemical conditions also favorable for aggregation, these terms sometimes has been used alternatively, or in other words, aggregation in porous media has been alluded to as ripening [107, 264, 268]. Yet, it should be clarified that aggregation, by itself, can occur both in the aqueous phase and the attached or immobilized phase separately. In aqueous phase, aggregation results from three mechanisms: perikinetic aggregation, differential sedimentation, and orthokinetic aggregation [21, 68] whilst in the attached phase, aggregation can result from the movement and/or rolling of the particles weakly attached on the secondary minimum of the collector surface and translating along the surface due to hydrodynamic drag forces and eventually their accumulation near the rear of the collector or at grain-to-grain contact areas [109, 237, 249, 269]. On the other hand, ripening arises from the interactions of depositing particles, still in the aqueous phase, with previously deposited particles, in the retained phase, leading to multilayer accumulation of particles on the surface of the collector [100, 111, 126, 256, 261, 262]. This also gives physical meaning to the second type of ripening model outlined above in which ripening is described by a second-order term standing for the interactions between the fluid phase and the attached phase.

Chen et al. [256] provided an alternative explanation for the increased NP retention during transport. They indicated that enhancement in deposition rate can be also due to the appearance of more favorable surfaces for further deposition resulting from the alteration of the media surface charge distribution. Those authors, furthermore, proposed that collision of NP aggregates with sand surface can reconstruct the aggregates, i.e., change the particle arrangement in the structure of aggregates. This amounts to a consequent reduction in the sand-NP aggregate repulsion forces thereby enhancing the deposition rate [256]. Nevertheless, this observation was based upon

detecting a decrease in the particle size of the effluent samples, and no rigorous experimental evidence was provided. Countering this argument, similar behavior would be expected via the concurrent agglomeration of NP similar to the conceptual model proposed by [33] and numerically confirmed by [21]. In this interpretation, due to polydispersity of the injecting TiO<sub>2</sub> dispersion in the study of Chen et al., concurrent agglomeration of the middle and larger fractions of the particles during transport, resulted from their deeper energy wells [31, 33, 199], could cause the removal of the middle and larger fractions of particles via agglomeration and subsequent ripening. In this way, the average size of particles which could reach the outlet of the porous media was reduced [21, 111, 270]. This process has more recently been described as size selective retention [271]. Future experimental studies with measurement of particle size distribution inside the pore spaces and pore solid surfaces are required to find a better distinction among these phenomena and, therefore, verify the continuum model conceptual ground.

It should be mentioned that blocking and ripening are two mutually exclusive phenomena, i.e., when physicochemical conditions are favorable for one, the other one should not take place. However, in practice they can still occur simultaneously within the continuum domain because of spatial heterogeneity in the porous media [261, 272]. In addition to concomitant blocking and ripening behaviors, transition from blocking phenomenon to ripening phenomenon has also been observed [125, 126, 256, 264, 265, 273]. Such shifts in the conditions of experiment that brings about a switching of the transport behavior from blocking to ripening is important because this can also alter most of the other underlying transport phenomena and thus provide insights into the role of each individual phenomena when several mechanisms of NP transport are operating concomitantly (see Fig. 6 a,b).

Overall, two transport regimes can be encountered in the transport of NP in porous media. In the first regime, i.e., higher particle-surface attachment affinity than particle-particle attachment affinity, the major transport mechanisms are physicochemical filtration (describable by either kinetic or equilibrium attachment/detachment model), blocking (describable by Langmuir function), and perhaps together with physical retention, i.e., straining (describable with depth-dependent function). This regime can produce ascending BTC plateaus (Fig. 6a). In practice, this condition may bring about a considerable mobility of NP which needs careful assessment of NP transport in order to prevent unwanted subsurface migration. The second regime is when the

particle-particle attachment tendency becomes dominant. In this regime although physicochemical filtration as well as straining may still be operative, ripening is predominant together with agglomeration and further subsequent retention. This regime may create descending BTC plateaus (Fig. 6b). If the conditions of the experiment shift the transport behavior from blocking to ripening, then hazardous aspects of unwanted NP migration might be relieved to some extent because of the substantial amount of the retention resulted from ripening. However, it may also be possible that in this regime even with significant agglomeration of NP in the mobile phase, ripening would not be the case. For instance, due to the lower input concentration ripening might not be significant. According to Table 2 ripening has been mostly the case when injection concentration ranged from 100 mg/L to 20000 mg/L while the typical injection concentration of studies reviewed here was  $27.5 \pm 11.5$  mg/L. If ripening does not occur in this regime, agglomeration might promote size exclusion, which will be described next, thereby results in great migration distances. Should it be the case, the hazardous aspect of NP transport within subsurface will be much more serious than what has been hitherto believed.

### **3.5. Size exclusion**

#### **3.5.1. Significance for NP**

The importance of size exclusion was elucidated in considering the reasons for unexpected large migration distances of solute contaminants, such as radionuclides, in the subsurface because of their association with groundwater colloids, [59, 61, 274-281]. Size exclusion, also known in a more general concept as hydrodynamic chromatography, has been recognized as an underlying phenomenon for faster migration of particles compared to non-reactive solute in porous or fractured media [58-61, 100, 108, 117, 142, 151, 153, 280, 282-285]. Due to this mechanism, up to 4 - 5.5 times enhancement in colloid velocity compared to mean pore water velocity has been observed in micro-models [117, 153].

Recently, the number of studies identifying size exclusion as an underlying transport phenomena of various NP has increased. These NP thus far include AgNP [135, 202, 286, 287], TiO<sub>2</sub> [264, 288], NZVI [289], and carbon nanotubes [290]. Particularly, size exclusion is noticeable in two areas of NP transport research, namely biofilm coated porous media [286, 291] and co-transport/hetero-aggregation of NP [264, 273] even though these research areas are still at a

relatively early stage. For example, studies on the co-transport of Au NP with SWNT [273] or TiO<sub>2</sub> with multi-walled carbon nanotubes (MWCNT) [264] showed that heteroaggregation of these NP can facilitate their transport in porous media [47, 95, 292]. Intuitively, it is easy to dismiss size exclusion for NP relative to larger colloids for the simple reason of their small size. However, notwithstanding the scientific necessity of obtaining robust proof of any such assertion, the potential for NP aggregation into particles large enough to experience size exclusion (section 3.6) provides a strong rationale for consideration of size exclusion in the context of NP fate and transport modelling.

### 3.5.2. Mechanism

Detection of size exclusion based on BTC and RCP data is challenging especially when several transport mechanisms act together. In many modeling studies of colloid and NP transport in porous media this mechanism has been neglected because of not observing the early BTC [e.g., 130, 131, 190]. However, even though early BTC may not be observed, size exclusion can still be influential because its reflection in the BTC might be counterbalanced by other transport processes [92, 107, 151]. Size exclusion was suggested by Bradford et al. [92] to be influential in the depth-dependent behavior of colloid retention. Agglomeration of NP can promote particle size growth which may in turn enhance the chance of size exclusion whilst it can also elevate physicochemical retention or retention via straining [31, 33, 92, 139, 199]. Although a satisfactory quantitative analysis of these effects acting simultaneously is still lacking [21, 33, 202, 281, 293], in this section we try to express the potential conceptual models of NP and colloid transport when several transport processes operate concomitantly.

It should be clarified that herein size exclusion is considered as a mechanism of enhancing the transport of larger colloidal particles compared to smaller ones and nonreactive solute. This should be distinguished from some applications of the ‘exclusion’ terminology with the meaning of excluding colloids from all of pores (clogging) [62] or as a capture mechanism of colloid deposition [187, 294-296]. Size exclusion has been generally referenced in the context of colloid transport on two different scales [151, 283, 285]. First on a larger scale, i.e., bulk scale, the size exclusion concept has been referred to as the exclusion of particles larger than a portion of the pores that can be passed through by solute but not by the colloids [51, 54, 66, 92, 94, 98, 100, 110,

115, 283, 285, 297-300]. Second, at pore scale size exclusion has been attributed to migration of particles on flow paths which are close to the center of the pore channels where the velocity is theoretically 1.5 times larger than the mean pore water velocity—similar to the phenomena in solute transport context called "charge" or "anion exclusion", but with different underlying forces [58, 116, 139, 151, 153, 283].

On the larger scale, the concept of inaccessibility of pores to colloid rather than solute, which has also been termed as "pore exclusion" [301], in order to be significant, requires the threshold ratio of the pore throat to colloid diameter to be larger than 1.5, suggesting for many environmental porous media that the size of the colloid must be larger than 1-2  $\mu\text{m}$  [153]. Grolimund et al. [302] showed that the inaccessibility of small pores in the soil texture to colloidal particles did not change with variations of the pore water velocity and therefore exclusion of colloids from the margins of the pore throats was the main cause of the breakthrough acceleration. The observation of 4-5.5 times enhancement in the colloid velocity in a micromodel by Sirivithayapakorn and Keller [153], which was attributed to the preferential paths resulted from the selectivity of the pores, i.e., inaccessibility of the small pore to larger particles, as well as observation of detours in a micromodel by Auset and Keller [283] suggest that this type of size exclusion might be still considerable.

At the smaller scale, the velocity profile in an individual pore section, approximated as a cylinder, is expected to adopt a parabolic shape according to the Poiseuille flow profile, i.e., the velocity is zero at the wall and the maximum at the center [60, 139-142, 283]. Part of mass that resides at the center of these pipes will arrive at the end of the pipes sooner than the mean velocity of the flow. This part of mass may contain the larger size fraction of the colloids with lower Brownian diffusion compared to small particles or solute. Since materials with lower diffusion may be less distributed over the pore (or fracture) cross-section area and are less likely to reach areas near the pore (or fracture) walls, they are conceptually less prone to the movement with the sluggish velocities at the vicinity of the walls. This part of mass is also less likely to move with retardation or attachment/detachment that occur in the area near pore channel walls. As a result, larger particles according to this conceptual model can migrate faster than average pore water velocity.

The underlying reasons presented in the current literature regarding why the particles tend to keep far from pore channel walls are neither satisfactory nor generic. For instance, it has been mentioned that the large size of particles prevent their centers of mass from sampling the areas very close to the pore (or fracture) walls, and/or that the surface-charge-induced repulsion of particles prevent them from entering certain pore regions close to walls [58, 59, 61, 92, 94, 100, 108, 115-117, 140-142, 151, 153, 160, 279, 280, 282-285, 291, 302-304]. It has also been mentioned in co-transport of TiO<sub>2</sub> with MWCNT that the long arm of MWCNT impede the heteroaggregates to reach the vicinity of the porous media solid surfaces where they can be deposited [264]. These reasons, however, may not be sufficient to describe the significant acceleration of migration velocity observed for particles compared to conservative solute, e.g., 1.45 times velocity enhancement observed by Grolimund et al. [302], because reaching to these velocities necessitates the majority of colloids travel at an area very close to the centerline of the pore channels while in addition to diffusion several other mechanisms/forces such as gravitational sedimentation, interception, inertia, and momentum may tend to bring the particles to the surface of the pore (or fracture) wall or at least redistribute them across the pore space [31, 33, 67, 120, 305]. In addition, the limited influential distance range of repulsive forces to the vicinity of the pore walls as well as the change in the charge sign due to heterogeneity of the geological medium can downgrade the mere role of repulsion forces in keeping the colloids far from the pore walls [281]. This lack of recognition about the underlying mechanism of size exclusion might be a reason for the complexity in identifying the size exclusion when several other transport mechanisms are also engaged. This is also the case even in the mechanistic modeling framework in which very few papers thus far have attempted to capture the effect of size exclusion phenomenon [59, 60, 140, 282].

In a study by Malkovsky and Pek [281], it was suggested that a substantial enhancement in the particle velocity relative to the average groundwater velocity can only result from drift forces created by the “Magnus effect” (the hydrodynamic force resulting on a rotating sphere in a heterogeneous flow field). This force causes the translation of particles toward the centerline [60, 139]. Essential conditions for the Magnus effect to be functional are the rotation of colloidal particles and unequal velocities of particle and local groundwater streamlines [281]. However, it has been indicated that rotational component of particle is negligible for a range of ratios of particle diameter to pore throat (or aperture) width lower than 0.4 while typical ratios has been reported to

be far lower — $10^{-4}$  to  $10^{-2}$  [60, 284, 306, 307]. Nevertheless, Malkovsky and Pek asserted that the Magnus effect was still considerable for relatively small particles because of their significant oscillation resulting from Brownian motion. Other authors attributed the reason for cross-stream displacement of particles near a wall to the inertia in a laminar flow [60, 308-311]. Based on this analysis, Segre and Silberberg [309, 311] found that particles close to the centerline tended to drift towards the wall of the tube and particles at the vicinity of the wall tended to drift toward the center. This tendency led to an equilibrium position at a distance about 0.6 times of the tube radii from the centerline.

### 3.5.3. Continuum modeling approaches of size exclusion

To date, no specific parameter has been added to the advection-dispersion model to represent size exclusion. However, several different approaches have been applied in the continuum modeling framework to capture the impact of size exclusion by adapting the basic flow and transport parameters including partition coefficient ( $K_d$ ), pore water velocity, volumetric water content (or porosity), and dispersivity [92, 108, 141, 299, 312-314]. In the simple linear adsorption model, anion exclusion was taken into account by allowing the partition coefficient to become negative in the parameter estimation process [313]. This is equivalent to letting the retardation factor in the parameter estimation process to go lower than unity, that is then called "acceleration factor" [153] as was shown in Fig. 4b. For a non-equilibrium adsorption model, exclusion was incorporated by considering an equivalent exclusion distance from the pore wall where the concentration is effectively zero [312, 313]. Subsequently, an exclusion volume could be estimated by multiplying the exclusion distance in the specific surface area ( $L^2 M^{-1}$ ). This exclusion volume times the soil bulk density yielded an equivalent porosity that could be subtracted from the porosity of the immobile domain used in the non-equilibrium dual domain model [312, 313]. Likewise, Bradford et al. [92] in order to model size/charge exclusion, altered both porosity, based on the water content accessible to colloids, and Darcy velocity, based on the relative water permeability accessible to colloids.

Some continuum approaches to size exclusion have been based on a known spatial distribution of pore/aperture width which was mainly obtained by a stochastic approach [299, 314]. The influence of size exclusion was then assimilated in the model by eliminating both advection and dispersion

fluxes into the fracture elements of the numerical grid which had an aperture thickness smaller than  $15 \mu\text{m}$  [299] or 12 times the colloid diameter [314]. In effect, this type of model considered the size exclusion at the larger scale, i.e., bulk scale size exclusion or pore exclusion (first interpretation described in section 3.5.2) rather than pore scale type. James and Chrysikopoulos [141] modified the Taylor dispersion coefficient, originally developed for dissolved matter, in order to account for the finite size of the colloidal particles. This way, they demonstrated that size exclusion from the slowest moving portion of the velocity profile increased the effective particle velocity whereby decreasing the overall particle dispersion. Scheibe and Wood [108] argued that increasing the velocity as a parameter for simulating size exclusion can result in altering dispersion (assuming no change in dispersivity), which is not conceptually consistent with the fact that the overall variance of the pore-scale velocity in respect to the size exclusion phenomenon should be decreased due to a lower chance of particles accessing certain regions of low velocity. Therefore, they proposed truncating the lower velocities from the velocity distribution profile to take account of the very low velocities adjacent to the pore walls that were not experienced by the colloids. The advantage of their method was that the velocity field for particles was statistically similar to that of the pore water velocity distribution but slightly modified as a result of the truncation [108].

Overall, most of these modeling techniques are either based on a known (or a stochastically estimated) pore/aperture thickness distribution over the spatial domain [299, 314], or rely on modification of the other parameters and/or variables of the model such as velocity or dispersion [108, 141]. These issues can make the predictive power of the model less plausible when applied in larger scales. For instance, models which rely on the modification of the velocity field whereby estimating the parameters of model may not be applicable to real large-scale environmental problems in which the velocity field with its spatial and temporal variations in bulk scale is already unknown and might be affected by other factors as well when various phenomena such as straining and size exclusion coexist [92, 107]. This is also the case for the dispersivity parameter, which should be estimated based on the tracer breakthrough data in order to be determined as a property of the porous media and independent from the phenomenological mechanisms of particle transport [283].

Once the dispersivity parameter is estimated from tracer BTC, the total number of parameters required to be determined in the procedure of particle transport model calibration will be reduced.

Yet, recent findings of Chrysikopoulos and Katzourakis [94] on showing the dependency of dispersivity on particle size shows that there is the need for reformulation of the continuum-based models in order to take account of the particle size distribution and its dynamics resulted from size exclusion, agglomeration and other transport phenomena. Such a modelling approach may be accomplished if a multi-species model formulation can be adapted for different particle size classes in terms of mass concentration [85]. The potential of heterogeneous particle populations to complicate transport models, even when the initial input population is uniform, has been well documented. However, the mechanisms which underpin such effects – homo- and hetero-aggregation simultaneous with colloid transport and deposition – have been remarkably little studied in comparison to ‘static’ systems of flocculation and sedimentation.

### **3.6. Aggregation**

#### **3.6.1. Definitions and observations**

Homoaggregation or agglomeration of particles during transport within a porous media is one of the least understood phenomena relating to colloid and NP in the subsurface. It is of paramount importance because it causes change in the size and hence in the transport characteristics as well as the size-dependent functionality of NP. Understanding aggregation within porous media is therefore crucial to a range of environmental applications of NP, as well as assessments of environmental hazard. The terms 'aggregation' and 'stability' have been used interchangeably but they are two distinct processes; aggregation only considers the attachment of particles to each other, while stability considers both their attachment and their subsequent sedimentation and removal from the aqueous media [315-320]. This difference is more pronounced in the context of porous media. In particular, the restricted length scales for sedimentation to take place in pores and the fact that they are advecting through the pores may distinguish the aggregation in porous media from that in bulk liquids.

To date, the most common model for simulating the aggregation of colloid or NP is the Smoluchowski model [34, 45, 68, 104, 321-323]. This model is based on the superposition of three mechanisms: perikinetic, orthokinetic, and differential sedimentation. The perikinetic mechanism of aggregation involves particle-particle collisions caused by the Brownian motion of particles. Orthokinetic aggregation involves collisions arising from any motion or flow in a fluid that can cause shear stress. Differential sedimentation occurs when the particle sizes are so different that

larger particles settle faster than the smaller ones and collide with those in their paths [21, 68]. Detailed accounts of aggregation mechanisms, e.g., consideration of the fractal nature of aggregates or of gravitational sedimentation in aqueous media, are available elsewhere [324-326].

Aggregation of NP, in spite of being the focus of ongoing studies in aqueous media [45, 95, 322, 326-328] has been largely ignored by models of transport in porous media. Many modelling studies on NP transport reported to date have overlooked aggregation by assuming that in the selected experimental conditions aggregation might have not been operative. This rationale may be justified in several conditions: high experimental values of zeta potential or stability analysis based on critical coagulation concentration (CCC) or DLVO theory [182, 201, 222]; the lack of significant size change observed under equivalent conditions in batch experiments [70, 135, 181, 187, 192, 203, 329, 330]; or by observing no significant change in the concentration of suspended NP in such batch experiments, indicated the absence of sedimentation [e.g., 74]. Despite this, the formation of NP aggregates during transport in porous media has been experimentally demonstrated by a large number of studies for NP such as NZVI [21, 31, 33, 48, 104, 113, 180, 331, 332], HAP [111, 125, 126, 129], Graphene/GO [74, 130-133, 249], Ag NP [201-203], CeO<sub>2</sub> [267], TiO<sub>2</sub> [134, 204, 205, 288, 333], ZnO [75, 137, 206, 207, 224], and AlO NP [329, 330] (Table 2). The results of batch experiments may not be a real indicator of the particle conditions in porous media because aggregation in batch experiment in absence of flow can lack at least one of the main driving mechanisms of aggregation; that is orthokinetic aggregation [21, 45, 206, 249, 315]. This mechanism of agglomeration is very likely to be significant in porous media, because of the non-uniform distribution of the pore water velocity in pores which caused enhanced shear rate. Furthermore, enhanced local polydispersity in particle size distribution in pores can be responsible for accelerated agglomeration. This local polydispersity in the population of particles may arise from the complex multi-cascade processes of advective and diffusive transport [94, 141, 295, 334], tortuosity in porous media [150], detached agglomerates with different sizes arriving from the up-gradient pores [109, 167], and size selective deposition/preferential retention [111, 125, 135]. It is also worth mentioning that the observations in effluent samples that show no change in the size over time or as a function of the column length should not be used as evidence of no aggregation, because since aggregation tends to lead to large, more easily-deposited entities, it is preferentially the smaller, unaggregated particles which remain mobile as far as the column outlet [21, 111, 125, 135, 318, 319, 335].

Aggregation can affect the deposition of particles during their transport within porous media in a number of ways. Increase in size due to aggregation can reduce diffusivity thereby decreasing the frequency of collisions with pore surfaces [336]. The formation of porous aggregates can also alter their sedimentation velocity as well as collision rates with solid surfaces compared to those of impermeable spheres with equivalent mass and size [337]. The porosity and thus settling velocity of fractal aggregates can rise with growing their size because of the change in the fractal dimension that is an indication of their density [338-341]. For particles which collide with surfaces, increase in size of aggregates can increase the magnitude of the DLVO interaction energy secondary minimum, thereby increasing attachment rates [31-33, 199]. These interconnected and dynamic effects of change in particle size which occur differentially across a particle population render it complicated to develop a mechanistic approach for simulating the concurrent aggregation and transport of NP [21, 34, 57].

### **3.6.2. Modelling considerations**

Very few studies have attempted to develop a model for NP aggregation during transport in porous media in continuum framework [21, 57, 104]. These models were mostly developed specifically for NZVI because of its importance in remediation of groundwater contaminants and the need for designing field remediation strategies [21, 33, 34, 104, 199]. Phenrat et al. [31, 32] developed empirical attachment and contact efficiency relationships for predicting the sizes of aggregates and the subsequent deposition of formed aggregates based on a range of one-dimensional (1-D) column transport data of polymer-modified NZVI particles. These empirical correlations can be used along with continuum model to simulate NP aggregation and transport in porous media [342]. Raychoudhury et al. [104] combined the Smoluchowski model of aggregation with the CFT model within an advection-dispersion equation in order to simulate the aggregation and transport of polymer-modified NZVI. However, they did not explicitly obtain the particle-particle attachment efficiency within the porous media. Instead, they determined aggregation kinetic parameters from static batch experiments and used them for fitting the model against the breakthrough data. As noted above, there can be significant differences between static experiments with those conducted in a real dynamic environment of the porous media [88].

Taghavy et al. [34] used the Smoluchowski equation and CFT, all within a Lagrangian approach based on random-walk particle tracking to simulate the concurrent aggregation and transport of NZVI. Although they tackled the problem of binary collision in their probabilistic modeling

approach, the aggregation in that study was limited to perikinetic rather than orthokinetic aggregation [45, 315]. Furthermore, use of a Lagrangian approach limits the possibility of running a model in inverse mode and comes with consequent computational expenses when up-scaled [57, 88, 112].

Babakhani et al. [21] modified a widely-used solute transport model, MT3DMS, in order to incorporate the influence of aggregation together with other transport phenomena including attachment, detachment, and subsequent irreversible deposition of aggregates. They used a simple pseudo first-order reaction model to represent homoaggregation (Model type (vii), Table 1). The basis of common aggregation models such as the Smoluchowski model is a second-order rate equation [68, 343-345] although there is a limited number of studies which used a first-order formulation for aggregation [346-350]. Babakhani et al. showed that the use of a pseudo-first order model could describe the aggregation behavior of NP in porous media conditions of homogenous one dimensional and heterogeneous two-dimensional domains successfully. Interestingly, in the experimental cases where the conditions were favorable for disaggregation of NZVI, the model was still applicable by showing negative rates for the aggregation parameter [21]. Nevertheless, in that study, the effect of particle size distribution in porous media was not taken into consideration. Another approach to modelling aggregation was developed by Bradford et al. [109] that addressed hyper-exponential and non-monotonic trends of RCP. This was a dual-constituent model with the aim of capturing the transport and straining of pathogenic *E. coli*. The conceptual model assumed that *E. coli* could aggregate when a large number of mono-dispersed *E. coli* were deposited at straining sites. Then the aggregates of *E. coli* formed in the deposited phase could be released into the aqueous phase as a result of flow shear force after reaching a critical concentration. A two-constituent model (one constituent for the individual mono-disperse *E. coli*. and the other one for the released *E. coli*. aggregates) was developed. This model is presented as model type (xiv) in Table 1. The drawback of this model is the use of four extra parameters in comparison with a common model of straining and site-blocking, e.g., model type (xii), Table 1. Application of the Akaike information criterion (AIC) by Bradford et al. [109], described elsewhere in this paper, showed the two-species straining model performed better than the well-known first-order attachment-detachment model (type (ii), Table 1). However, it was not investigated whether this model could have been still better than the first-order attachment-detachment model with straining and blocking functions (model type (xii), Table 1). It should be noted that aggregation in the study

of Bradford et al. was assumed to occur at the deposited-particle phase, opposed to common consideration of aggregation process which takes place in the fluid phase [68]. Although this model distinguished the aggregating from non-aggregating species, still it did not consider the particle size distribution within the pores.

A substantial number of studies have attributed hyper-exponential RCPs to the aggregation process [75, 111, 203, 206, 207, 231-234, 264]. However, our review suggests two arguments against this possibility. The first reason is that the aggregation process is a time-dependent mechanism [21, 349, 350] and thus increase in particle size should occur progressively over the course of migration through the porous media. Therefore, the average size of retained aggregates should increase toward the outlet of the column; however observations of hyper-exponential RCP indicate typically a decrease in the size of the retained particles along the column length [125, 126, 206, 207]. The second reason, derived from experimental observations [127, 172, 200, 236], is that a decrease in the influent concentration causes greater hyper-exponential behavior. This is assumed to be because at low concentration of colloid/NP the capacity for straining will be exceeded only at the vicinity of the column inlet causing hyper-exponential shape while at high concentration, the capacity for straining will be uniformly met over the whole column length. On the other hand, aggregation is well known to be a concentration-dependent phenomenon [21, 31, 33, 104, 349, 351, 352] which typically increases with the population of particles by a second-order rate [68, 321, 345]. If aggregation is the reason for the hyper-exponential behavior, then the increase on the injecting concentration of NP must enhance the hyper-exponential pattern because of the ascended aggregation tendency. The outcomes of the aforementioned experimental studies show the opposite. One may attribute the hyper-exponential behavior to aggregation in the feeding reservoir of the NP upon injecting into the column experiment. Nonetheless, in the studies which carried out the ultra-sonication of the stock dispersion [125, 126, 131, 264, 353], still a hyper-exponential distribution emerged as well as a decrease in the retained particle size along the column length [125, 126], suggesting that the aggregation in the stock dispersion container cannot be responsible for hyper-exponential behavior.

Further carefully-designed experimental work is clearly required to better inform both conceptual and mathematical models of aggregation and its contribution to NP transport and fate in porous media. What is clear from the available evidence is that successful models must be validated against effluent breakthrough and perhaps retained mass profile data across a range of scales and

physicochemical conditions [293]. Future studies must be also directed to develop both continuum models and experimental techniques that can capture the effects of particle size distribution dynamics resulting from aggregation processes within pores. This can obviously give valuable insights into the roles of concurrent transport mechanisms.

#### 4. Equilibrium vs kinetic terms in continuum models

Incorporation of multiple transport mechanisms in continuum models and their application in complex, realistic domains and scales is not computationally efficient. The use of a partitioning (distribution) coefficient  $K_d$  in NP transport modeling is desirable because it reduces the number of parameters in the attachment/detachment process from two ( $K_{att}$  and  $K_{det}$ ) to one ( $K_d$ ), and more importantly facilitates the application of many analytical solutions and numerical tools for the governing equation [88, 354-356]. However, the use of  $K_d$  nominally requires the assumption of an equilibrium state between the suspended and attached phases which has been recently debated in the context of NP fate and transport [12, 88, 112, 114]. Conceptually the equilibrium assumption is invalid since  $K_d$  is physically based on the Gibb's energy and thermodynamic equilibrium assumption, while NP suspensions are thermodynamically unstable [114]. On the other hand, several authors have successfully utilized the concept of  $K_d$  in modeling NP transport, mostly in form of type (v) models (Tables 1 and 2) [146, 147, 180, 182, 190, 355, 357]. This is also in accordance with numerous experimental studies observing retarded BTCs [124, 138, 174, 175, 181-184]. Retardation factor is related to  $K_d$  as  $R = 1 + \rho_b K_d / \epsilon$ .

The equilibrium concept is increasingly popular in the context of NP adsorption to other surfaces in quiescent batch experiments [e.g., 358, 359-362]. Petersen et al. [360] obtained linear and nonlinear isotherms, respectively, for the sorption of regular and modified  $^{14}\text{C}$ -labeled multiwalled carbon nanotubes (MWCNTs) onto soil surfaces. Zhao et al. [357] found a linear adsorption isotherm fitted the attachment of GO NP saturated with Na and Ca ions onto the surface of goethite particles. Julich and Gäth [358] compared the sorption of copper oxide (CuO) NP with copper ions ( $\text{Cu}^{2+}$ ) onto soil and found out that the sorptivity of both of them followed the Freundlich isotherm with much stronger sorption obtained for CuO NP compared to  $\text{Cu}^{2+}$ . Abraham et al. [359] investigated the sorptivity of Ag NP onto model and environmental surfaces in stable and unstable systems and found that the sorption in the stable system followed the nonlinear Langmuir isotherm; however in the unstable system Ag NP sorption did not follow any classical models, suggesting NP aggregation plays a key role in modifying sorption phenomena. Nickel et al. [363] tested

whether the international standard guideline, OECD TG 106, for testing of nanomaterials adsorption/desorption, could be applicable for TiO<sub>2</sub> NP or not. The authors found that the guideline was not applicable because concurrent occurrence of agglomeration and adsorption was not accounted for.

While some, like Praetorius et al. [114] and subsequently Cornelis [112] have maintained criticism of the use of  $K_d$  in NP transport studies others (e.g. Dale et al. [12, 88]) suggest that although a theoretically-robust, mechanistic-based approach may perform better for controlled experimental conditions, when the complexity of the model domain and scale increases (i.e. in all environmentally-relevant conditions), more pragmatic approaches which ‘borrow’ entities such as  $K_d$  often turn out to be the more practical, and sometimes the only feasible solution. A fundamental part of the issue regarding the applicability of the equilibrium assumption must be related to the interference caused by co-acting aggregation phenomena in NP attachment to other surfaces. In this section, we demonstrate application of a type (vii) continuum model [21] to practically test the assumption of linear adsorption (equilibrium), by replacing the first-order, reversible, kinetic-reaction equation (non-equilibrium) attachment/detachment expression with linear adsorption partitioning. Can a one-parameter adsorption model ( $K_d$ ) be a surrogate for the two-parameter attachment/detachment deposition model across a range of scales and system conditions? The type (vii) model separately accounts for: (1) the attachment/detachment process; (2) the agglomeration of particles in the suspended phase; and (3) the irreversible deposition of aggregates. This model is described in detail in [21].

An iteration procedure was developed to optimize the transport parameters related to deposition and agglomeration ( $K_{att}$ ,  $K_{det}$ ,  $\lambda_1$  and  $\lambda_2$ ) against the observed concentration data presented in [21]. In summary, experimentally-observed BTCs which were available in mass concentration were fitted by using WinPEST model [364] in order to estimate model parameters. Internally, the mass concentration is converted to particle number concentration for agglomerating particles while the obtained parameters, are updated in the iterative procedure. Therefore, Eq. (e) in model type (vii), Table 1, is used to calculate the size of aggregates and, subsequently, Eq. (c) is used to calculate the population of aggregates (transformation of the mass concentration to the number particle concentration). Then, these transformed observation data are employed to recalibrate  $\lambda_1$  again. This procedure is iterated until the difference in  $\lambda_1$  values between two successive iterations is negligible (< 1 %). Here, in order to test the hypothesis of the linear adsorption isotherm

(equilibrium), Eqs. (a) and (b) in model type (vii) were substituted by the following single equation which is the standard equilibrium transport equation widely applied for the simulation of solute contaminants in the subsurface [54, 89, 90, 146, 190, 198]:

$$\frac{\partial C}{\partial t} \left(1 + \frac{\rho_b}{\varepsilon} K_d\right) = D \frac{\partial^2 C}{\partial x^2} - V \frac{\partial C}{\partial x} - \lambda_1 C - \lambda_2 \frac{\rho_b}{\varepsilon} S \quad (7)$$

where  $K_d$  is the partitioning or distribution coefficient between the aqueous and solid phases [ $L^3T^{-1}$ ] [356]. The MT3DMS code was used to solve the equations and one- and two-dimensional breakthrough data of polymer-modified NZVI [33, 199] were used for fittings as described previously [21]. Briefly, one dimensional transport data used here comprise a case of monodisperse suspension of polymer-modified NZVI (F3) at low concentration (30 mg/L) which was not an aggregating system as well as a polydisperse suspension (F1) at high concentration (6000 mg/L) which showed the highest aggregation according to the DLVO analysis reported in [33]. In addition, data of polymer-modified NZVI at high concentration (6000 mg/L) with removed excess polymer (washed-MRNIP2) and polymer-modified NZVI at low concentration (300 mg/L) (unwashed) from two dimensional (2-D) experiments were used from [199]. The 2-D experiments comprise a cell ( $30 \times 18 \times 2.5$  cm) containing three active layers: fine sand ( $d_{50} = 99 \mu\text{m}$ ), medium sand ( $d_{50} = 300 \mu\text{m}$ ), and coarse sand ( $d_{50} = 880 \mu\text{m}$ ). The NP dispersion was injected through the fine sand layer which was the middle one while a background groundwater flow had been set up through three side ports [199].

The results for 1-D simulations (Table 3) showed that incorporating  $K_d$  at low concentration (30 mg/L) in the case of F3 dispersion resulted in a just slightly poorer fit ( $r^2 = 0.977$ ,  $p = 0.59$ ) than the two-parameter kinetic model ( $r^2 = 0.987$ ,  $p = 0.43$ ). In the case of high concentration (6000 mg/L) for the F1 dispersion, however, the difference between the equilibrium and kinetic models was more pronounced. Final fitting statistics for the  $K_d$  model were  $r^2 = 0.971$ ,  $p = 0.18$ , while those of the 2-parameter approach were  $r^2 = 0.996$ ,  $p = 0.87$  (Table 3). The parameter values resulted from the equilibrium model simulation after 1% convergence of  $\lambda_I$  in the iteration procedure were  $4.75 \times 10^{-5}$  L/g,  $1.5 \times 10^{-3}$  s $^{-1}$ , and  $2.69 \times 10^{-3}$  s $^{-1}$  for  $K_d$ ,  $\lambda_I$ , and  $\lambda_2$ , respectively (Table 3). The obtained values for  $K_d$  in this study are comparable to those of He et al., [190], which ranged from  $1.9 \times 10^{-5}$  to  $7.1 \times 10^{-5}$  L/g. When the simulations were up-scaled to 2-D domains, the equilibrium model resulted in poorer performance, compared to the non-equilibrium model, at low concentration than at high concentration.  $r^2$  for the case at low concentration (unwashed) with non-equilibrium and equilibrium model fittings was 0.787 and

0.636, respectively, whereas for the case at high concentration (washed MRNIP2)  $r^2$  was 0.951 and 0.948 (Table 4). Yet,  $p$  values at both low and high concentrations increased when the non-equilibrium model was substituted by the equilibrium model, from 0.61 to 0.79 and from 0.58 to 0.92 at low and high concentrations, respectively. In [21], the reason for poorer model performance at low concentration than that at high concentration transport in 2-D domain was attributed to the existence of excess polymer in the dispersion of NZVI at low concentration which was not taken into account directly by the applied non-equilibrium model. Here, this deviation is even more obvious when a simpler model, i.e., equilibrium, is used.

In order to determine which model performs better, we calculated the Akaike information criterion (AIC) [365], which is commonly used as a model selection criteria in colloid and NP transport studies [63, 109, 172, 293, 366]. This criterion prefers the model with the best goodness-of-fit measure and at the same time with the least number of fitting parameters, corresponding to the lowest AIC value. This can be calculated as [63]:

$$\text{AIC} = n_{obs} \log(\sigma^2) + 2k_{par} + \frac{2k_{par}(k_{par} + 1)}{n_{obs} - k_{par} - 1} \quad (8)$$

where  $n_{obs}$  is the number of observation data,  $\sigma^2$  is the sum of squared residuals divided by  $n_{obs}$ , and  $k_{par}$  is the number of parameters estimated in the inverse modeling process.

The results of these calculations for both of the investigated cases in one dimensional domain showed that the lower AIC value was obtained when the non-equilibrium attachment/detachment model was applied—AIC values with non-equilibrium and equilibrium models for F3 at 0.03 g/L (no aggregation) were -97.8 and -94.2, respectively, and for F1 at 6 g/L (with aggregation) were 634 and 642, respectively (Table 3). This suggests that in one-dimensional simulations the kinetic attachment/detachment model is preferred rather than the linear adsorption partitioning model. Surprisingly, in two-dimensional simulations the equilibrium model was preferred by AIC instead of the non-equilibrium model—AIC values for non-equilibrium and equilibrium models at low concentration (0.3 g/L with free polymer) were -37.4 and -42.2, respectively, and at high concentration (6 g/L, without free polymer) were 609 and 582, respectively (Table 3). It should be noted that since AIC is a statistical model identification test, it is the final differences that matters not the magnitude. Both Praetorius et al. [114] and Cornelis [112] compare  $K_d$  with  $\alpha$ ,  $\eta_0$ , or  $K_{att}$ . However,  $K_d$  which considers the exchange between the two phases of suspended and attached mass, neither can be compared with  $\alpha$ , individually, which determines what portion of collisions

leads to attachment, nor with  $\eta_0$ , individually, which ascertains what flux of particles are colliding with the collector, nor with  $K_{att}$ , individually, which determines the rate of permanent removal without detachment. In practice,  $K_d$  might be only comparable with both  $K_{att}$  and  $K_{det}$  together, in a range that both equilibrium and kinetic model perform similarly [161]. If for a specific temporal and spatial scale we can use the assumption of instantaneous reaction (local equilibrium) [161], the concept of  $K_d$  can be defended, regardless of whether the system contains particles or solute, provided that the interfering role of other phenomena such as aggregation and subsequent irreversible removal will be accounted for by other terms in the model.

In other words, while strictly unjustifiable as a physical process for particle deposition in mechanistic models, nevertheless the equilibrium assumption may be an effective descriptor of reversible deposition behavior by concurrent attachment and detachment processes within a continuum modelling framework. Overall, in the experimental conditions simulated here, fairly similar model performance was obtained between the two modeling approaches in 1-D simulations. When the model was up-scaled to a 2-D stratigraphic, heterogeneous, experimental domain, the higher efficiency in terms of the number of model fitting parameter suggested that the equilibrium model is preferable in comparison to the kinetic model. This confirms the potential for use of the equilibrium assumption as a justified simplification for modelling NP in more complex porous media.

## **5. Overview of the concurrent occurrence of multiple transport phenomena**

### **5.1. Conceptual model of transport for stable monodisperse dispersions**

For stable monodisperse suspensions of larger sized colloids, the conceptual model of Bradford et al. [92], may best describe the transport phenomena in porous media. In this model it was hypothesized that straining caused filling of the pores at contact areas of grains and caused those small pores to become dead-end at the near vicinity of the column inlet thereby constraining the colloid to sample only the continuous pore channels. After passing this region of the porous media in the experimental packed column, particles would be mounted on the fast central streamlines of the pore channels with less interactions with the grain walls and narrow restrictions of pores at the grain-grain contacts due to the exclusion phenomena and thus the number of dead-end pores

experienced by particles reduces with distance from the inlet of the column. In this way, the concentration of the RCP reduces significantly along the column length [92]. This must be the most plausible explanation regarding the hyper-exponential behavior of the RCP for stable monodisperse dispersions.

## **5.2. Conceptual model of transport for stable poly-disperse dispersions**

When the particle population is poly-disperse but stable, the case which is more pronounced for NP dispersions [33], the hyper-exponential RCP as depicted in Fig. (7a) can still be developed as for monodisperse suspensions. At the entrance of the column all the particle size fractions have interactions with the surfaces of the porous media with higher chance of trapping larger particles due to the physical straining [62, 92] and/or physicochemical deposition resulted from their relatively deeper surface interaction energy minima [31, 33, 107]. As a proportion of large particles is irreversibly retained near the areas of the wall surfaces or grain-grain contacts at the entrance of the packed column, other survived large particles would less meet the close-to-wall regions during their travel through the rest of the column length thanks to the size exclusion. On the other hand, the particles from the smaller fraction of the size distribution spectrum can still have interaction with the wall. Yet, they exhibit shallow secondary minima [31, 33, 107, 139, 199] and thus are less subject to permanent deposition and also owing to their smaller size, they are less prone to straining all over the column length [62, 92, 107, 210]. Accordingly, neither significant deposition of small particles nor large particles can take place at the down-gradient of the column, in contrast to the entrance area. This concept is also compatible with blocking and ripening behaviors if one of them also occur. They can coincide with hyper-exponential shaped RCPs, because the retention process at the vicinity of the column entrance can be either straining or physicochemical filtration, regardless of whether the condition is favorable for blocking or ripening.

## **5.3. Conceptual model of transport for unstable poly-disperse dispersions**

One of the most complicated transport behaviors, observed more commonly in studies of NP than those of larger colloids, is non-monotonic retention [123, 225, 293]. Previous reports have ascribed the reason for this non-monotonic shape of the RCPs to a variety of phenomena such as the release of the attached particles from the region close to the column inlet and their re-entrapment in the

down-gradient regions of the column or their translation, flowing, or funneling in the attached phase as a third phase [109, 236, 268, 367, 368], presence of polymer competing with the NP for the adsorption sites at the inlet vicinity [127, 186, 265], surface heterogeneity [204, 369], and other system conditions such as grain types and size [109, 370]. Furthermore, ripening [371] and blocking are pointed out to be influential in causing non-monotonic shaped RCPs [127, 138]. Blocking can promote non-monotonic behavior via filling of  $S_m$  sites at higher loading concentrations, coarser sand grains, lower velocity, and higher IS [109, 127]. It has also been indicated that non-monotonic RCPs can also occur as a consequence of straining [109] and agglomeration [256, 265]. Dual-species [109], dual-permeability [367], dual-domain [236], and stochastic models [225] have been deployed successfully in reproducing the non-monotonic shape of the RCP

Considering the widespread evidence for the significance of aggregation processes in NP suspensions and during transport [109, 236, 367], we propose that agglomeration plays a key role in producing the non-monotonic shaped RCP. In contrast to the translation of attached mass of particles or aggregates on the surface of the grains [109, 236, 268, 367, 368], we assert it is agglomeration in the fluid phase that likely has the main contribution to bring about non-monotonic retention behavior in unstable suspensions, as illustrated in Fig. 7b (adapted from [21, 33, 270]). Essentially, at the immediate vicinity of the packed column entrance, the average size of particles is so small that they can neither be subject to irreversible deposition nor to size exclusion although there might be a delay in this area because of higher interaction of NP with walls due to their higher diffusion. Then all the particles, in this way, are transported toward the down-gradient of the column during which they are also agglomerating within the aqueous phase of the pores, as the condition is favorable for agglomeration. When the agglomerates are sufficiently grown in size their fate might be determined in two possible ways. First, those agglomerates closer to pore walls could be subject to straining and/or irreversible retention somewhere in the midst of the column length. This retention would potentially appear to be more pronounced as a result of ripening. Second, those agglomerates which are farther from pore walls by this time would be mounted on the faster central streamlines of the pores as a result of size exclusion. In this way they can potentially travel all the rest of the route to the column outlet and survive from retention although still their size may keep growing in this way and still be vulnerable

to the first possibility for retention as well. In combination, this aggregation-driven suite of processes leads to the appearance of a peak or a hotspot in the middle area of RCP. Clearly, assuming other factors to be held constant, the rate of aggregation should be a significant factor in determining the position of the non-monotonic peak as a function of distance from source.

#### **5.4 Experimental validation of model concepts**

We briefly reflect on recent developments in the experimental methods required to validate and test the models discussed. A crucial advance on standard column methods is represented by methods which 'open the box' on time-dependent changes within the porous medium. Recent advancement in real-time monitoring of transport in porous media include detecting solute transport by gamma imaging [372], colloid transport by fluorescence imaging [373-375], and NP transport by MRI [376]. X-ray computed tomography (XCT) has also been shown to have the potential for imaging the attached phase of NP, but its application at bulk scale is challenging because of interference at the grain/void interface and being limited to high electron density materials with high X-ray contrast [30]. Real-time monitoring of the attached phase of particles has been achieved by Roth et al. [377] via static light scattering (SLS) yielding important parameters such as permeability, the radius of gyration (analogous to the hydrodynamic radius), and the fractal dimension of deposited aggregates. SLS can obtain very small length scales (voxel resolution as low as 50 nm) at significantly lower cost than alternatives such as X-ray microtomography. Nevertheless, this technique requires a refractive index matched porous media which limits its ability to probe realistic environmental conditions in key parameters such as viscosity and surface properties [378]. The dynamics of the concurrent agglomeration and transport of NP in real porous media has not been monitored by any experimental technique within the literature reviewed here. Developing robust experimental evidence for validating models such as those proposed here, in particular where multiple processes are postulated and BTC/RCP interpretations are equivocal, remains a critical research priority.

#### **6. Upscaling of continuum models for NP transport**

In spite of large number of NP transport studies in 1-D column experiments, multidimensional transport reports are scarce [214, 244, 245, 379]. Likewise, multidimensional modeling tools are

still undeveloped [21, 96, 97, 103, 254, 255, 380, 381]. At larger scales, the nature of underlying phenomena can change compared to 1-D transport, due to the introduction of new impacts from nonuniform flow field, e.g. radial flow around injection wells [38, 382]. It is likely that the patterns of the BTC and RCP discussed throughout the present paper change significantly. In particular when the domain is heterogeneous, e.g. layered media [27, 199], multiple peaks can appear in the plateau of the BTC which cannot be modeled even when considering heterogeneous zones as discussed in [21]. Substantial differences may exist regarding the amount of pore space or solid surfaces available in 3-D porous media domain compared to that of simple ideal 1-D column domain. This can cause further deviations of column experiment outcomes compared to realistic environmental conditions.

Well-known, 3-D groundwater modeling packages such as HYDRUS and MODFLOW have been modified to capture some of the transport mechanisms of NP. To date, HYDRUS [383] has been adapted to simulate most of the NP transport mechanisms discussed in this paper, except aggregation [384]. A 2-D or 3-D application of HYDRUS for NP transport has not been reported thus far. In addition, capabilities of simulating variable density or variable viscosity characteristics of transport that can be influential in fate and transport of NP in porous media have not been reported for this package. On the other hand, the MODFLOW family of models, such as MT3DMS [89], SEAWAT [385], and RT3D [386] have been already applied for multidimensional transport simulations of NP with considering specific NP transport mechanisms including aggregation [21], density driven transport pattern [381], site blocking [254, 255], straining [213], and even reaction with groundwater contaminants [26]. Neither size exclusion as a specific phenomenon nor particle size distribution driven by aggregation, have not been considered in these models yet.

A MATLAB-based software called MNM1D was developed for capturing NP transport mechanisms [105]. This model is mainly expressed as model type (xv) in Table 1. Recently, this was combined with RT3D to simulate micro and nanoparticles transport in 3-D porous media [380]. However, this model, too, has not considered aggregation and size exclusion mechanisms of NP aggregates within porous media. Therefore, there exists the need for development of new 3-D modeling tools or further adaptation of current groundwater modeling package to take more of the NP transport mechanisms into account.

## 7. Conclusions

Continuum modeling can successfully describe a variety of NP transport phenomena and their concomitant effects and is able to work at various scales ranging from column experiments to aquifer and watershed. Its importance among other modeling approaches therefore lies in part in its ability to link with other modeling techniques to bridge the gaps across temporal and spatial scales and to be used as means of validation for those models.

On the other hand, there are a number of drawbacks with continuum models. First, continuum models have been criticized for being ‘descriptive’ or ‘backward models’ rather than being ‘predictive’ or ‘forward models’ [23, 30, 387]. Crucially, the parameters of the continuum-model, which are mostly rate-coefficient constants, require estimation for each specific problem they are applied to and cannot be measured simply from the given conditions of the problem. Second, continuum models can be applied regardless of whether the selected mathematical models really match the underlying physical mechanisms operating on NP. If the conceptual ground of continuum models are defined poorly, they can lack generalization and prediction power even though the mathematical model outputs fit the experimental data properly [293]. Third, simplifying assumptions in development of some of continuum models that can cause erroneous outcomes [112, 114]. For instance, the applicability of the equilibrium assumption to the number of interactions of NP with the porous media surfaces in the context of NP transport and aggregation has recently been debated by several research groups [12, 88, 112, 114, 388]. Fourth, most of the developed conceptual/mathematical models thus far only consider one or a few of the underlying mechanisms under oversimplified conditions where other phenomena are not operating or conducted only in the simplistic domain of the column experiment. This may lead to significant deviations when the models are up-scaled to more realistic conditions [12, 22, 88].

In addressing the first of these drawbacks, we have recently proposed a practical approach to predict the parameters of continuum models using an artificial neural network [342]. Such machine learning approaches, combined with continued advances in computing power, promise a significant advance in the use of continuum models for effective prediction of NP behavior. The objective of this paper has been to provide a systematic overview of the subject by which the significance and extent of the other three drawbacks can be rationally assessed.

In conclusion, we summarize here the key findings of this review:

- For NP as for larger colloids, the available literature to date recognizes several defined empirical trends consistent with the dominance of different transport processes. Hyper-exponential RCP is a sign of straining; ascending-plateau BTC indicates of blocking; descending-plateau BTC implies ripening, and early BTC is consistent with size exclusion. Furthermore, here we propose that non-monotonic RCP can result from agglomeration of NP. However, it is clear that multiple processes acting together concurrently on different fractions of the pore space or particle population may alter or mask these trends.
- The criteria used for identifying the underlying phenomena of colloid transport behavior, e.g., the use of particle size to grain size ratio in identifying straining, are not necessarily applicable for NP. In addition, there is obvious scope for misinterpretation in respect to the reflection of several transport phenomena in BTCs and RCPs. The ascertained underlying mechanisms based on these criteria may not hold true in many cases. There is a critical need for research into conceptual and computational models which not only acknowledge but systematically evaluate the simultaneous and variable operation of the whole range of processes able to act on NP during transport in porous media. It is time to recognize that uniform, steady conditions assumed by most standard mathematical approaches are the rare exception, rather than the rule, for colloidal systems in porous media even under apparently controlled experimental conditions.
- Two transport mechanisms, agglomeration during transport in porous media and size exclusion, have been widely neglected in the literature of NP transport modeling. Agglomeration results in size growth during the transport which can in turn trigger other mechanisms, especially, straining and size exclusion. Several literature evidences suggest that size exclusion might significantly contribute to transport behavior of NP aggregates even though it may not be shown up in the BTC and RCP, due to the concurrent operation of various transport phenomena. There exists the need for more rigorous investigations of the size exclusion mechanism in future NP transport studies.
- Two major transport regimes are identified in the transport of NP within porous media. The first regime is characterized by higher particle-surface attachment affinity than particle-particle attachment affinity, and operative transport mechanisms of physicochemical filtration, blocking, and physical retention. This regime can produce ascending BTC

plateaus. This condition may bring about a considerable mobility of NP in the subsurface and thus needs careful assessment. The second regime is characterized by the domination of particle-particle attachment tendency over particle-surface affinity. In this regime although physicochemical filtration as well as straining may still be operative, ripening is predominant together with agglomeration and further subsequent retention. This condition may create descending BTC plateaus. There is a need for further research in order to investigate how agglomeration affects the transport if in this regime ripening does not occur.

- When concurrent effects of agglomeration and deposition exist in the NP transport system, we found that employing a single equilibrium term to describe irreversible deposition within a continuum model yielded results that were close to those obtained using two kinetic terms (attachment and detachment rates). Furthermore, the equilibrium model turned out to be more efficient than kinetic model in terms of the number of fit parameters and goodness-of-fit criteria when the scale of the model and the level of complicity were augmented.
- Multidimensional continuum models which consider multiple transport phenomena represent the only conceptually feasible approach to predict transport behaviors of NP at environmentally-relevant scales in realistic 3-D domains. However, the present limitations of computational power mean that it is essential that work continues to define robust correlation relationships between measurable and unmeasurable parameters, and to validate the use of efficient continuum-scale parameters which represent multiple underlying mechanisms. Given the large number of datasets and experimental conditions evidenced in the literature presented here, machine learning approaches represent a promising tool for elicitation and prioritization of factors influencing NP transport, for use in continuum models. There are significant benefits to understanding and management of environmental NP arising from use of abstract and mechanistic models, and combinations of these with continuum approaches. However, further development of 3-D continuum modeling tools is of crucial importance in order to achieve the ambition of reliable, predictive forward modelling of the fate and transport of NP in subsurface environments.

## Acknowledgements

Financial support to P. B. through Dual-PhD program between the University of Liverpool and National Tsing Hua University is gratefully acknowledged. This work was also funded by the Taiwan's Ministry of Science and Technology (MOST) under the grant No. 104-2221-E-009-020-MY3 and by the National Research Council of Thailand (R2560B008). Payam Miri is acknowledged for help in production of figures. We gratefully acknowledge the insightful comments of the editor and anonymous reviewer which have enabled us to significantly improve the manuscript.

## **Figures and Tables:**

### **Figure Captions:**

**Figure 1.** The paradigm of various modeling approaches for simulating fate and transport of engineered nanomaterials (ENM) in the environment, showing the status of continuum-based models and their potential links with the available data sources and other modeling approaches

**Fig. 2.** Literature survey of various phenomena operative in the transport of nanoparticles based on the number of studies found in the Web of Science database in December, 2015 [389].

**Fig. 3.** Breakthrough curves generated by numerical solution of model Types (i) with MT3DMS model code following [21] for various  $K_{att}$  values ( $S^{-1}$ ). Other parameters of flow and porous media conditions were selected according to [21, 33] (or refer Table 2).

**Fig. 4.** Breakthrough curves generated by numerical solution of (a) model Type (ii) from Table 1, for various  $K_{det}$  values ( $S^{-1}$ ) and a fixed  $K_{att} = 0.001 S^{-1}$  and (b) model Type (v) from Table 1, for various retardation factors and a fixed  $K_{att} = 0.001 S^{-1}$  with MT3DMS model code following

[21]. Other parameters of flow and porous media conditions were selected according to [21, 33] (or refer Table 2).

**Fig. 5.** Possible retention sites for straining from [119].

**Fig. 6.** Possible regimes of transport mechanisms: (a) when particle-surface attachment tendency is higher than particle-particle attachment tendency and (b) when particle-particle attachment tendency is higher than particle-surface attachment tendency.

**Fig. 7.** The proposed conceptual models (a) for coupled effects of straining and size exclusion causing hyper-exponential shaped retention profile in the case of injecting poly-disperse particle dispersion into the experimental packed column and (b) for concurrent effects of agglomeration, deposition/straining, and size exclusion forming non-monotonic retention profile.

### **Tables:**

**Table 1.** List of continuum-based modeling types so far applied for the transport of nanoparticles in porous media. \*

<b>Model type No.</b>	<b>Colloid transport model equations</b>	<b>Modeled mechanisms other than advection and dispersion</b>	<b>Fitting parameters other than dispersion</b>	<b>Reference</b>
<b>i</b>	b) $\frac{\rho_b}{\varepsilon} \frac{\partial S}{\partial t} = K_{att} C$	attachment	$K_{att}$	[119, 148, 390]
<b>ii</b>	b) $\frac{\rho_b}{\varepsilon} \frac{\partial S}{\partial t} = K_{att} C - \frac{\rho_b}{\varepsilon} K_{det} S$	attachment/ detachment	$K_{att}, K_{det}$	[100, 142]
<b>iii</b>	b) $\frac{\rho_b}{\varepsilon} \frac{\partial S}{\partial t} = K_{att} C - \frac{\rho_b}{\varepsilon} f_r K_{det} S$	attachment and dual-site detachment	$K_{att}, K_{det}, f_r$	[206]

<b>iv</b>	b) $\frac{\partial S}{\partial t} = \frac{\partial S_1}{\partial t} + \frac{\partial S_2}{\partial t}$	dual-site attachment/	$K_{att,1}, K_{det,1},$	[391]
	c) $\frac{\rho_b}{\varepsilon} \frac{\partial S_1}{\partial t} = K_{att,1}C - \frac{\rho_b}{\varepsilon} K_{det,1}S_1$	detachment	$K_{att,2}, K_{det,2}$	
	d) $\frac{\rho_b}{\varepsilon} \frac{\partial S_2}{\partial t} = K_{att,2}C - \frac{\rho_b}{\varepsilon} K_{det,2}S_2$			
<b>v</b>	a) $\frac{\partial C}{\partial t} (1 + \frac{\rho_b}{\varepsilon} K_d) = D \frac{\partial^2 C}{\partial x^2} - V \frac{\partial C}{\partial x} - K_{att}C$	attachment, adsorption (retardation)	$K_{att}, K_d$	[146] [190]
	a) $\frac{\rho_b}{\varepsilon} \frac{\partial S}{\partial t} = K_{rel} \frac{\rho_b}{\varepsilon} (S - S_{eq}) H_0(S - S_{eq})$	Release after perturbation	$K_{rel}, f_{nr}$	[64, 115, 187]
	b) $S_{eq} = f_{nr} S_i$			
<b>vii</b>	a) $\frac{\partial C}{\partial t} + \frac{\rho_b}{\varepsilon} \frac{\partial S}{\partial t} = D \frac{\partial^2 C}{\partial x^2} - V \frac{\partial C}{\partial x} - \lambda_1 C - \lambda_2 \frac{\rho_b}{\varepsilon} S$	agglomeration, attachment/ detachment, and irreversible deposition	$K_{att}, K_{det}, \lambda_1, \lambda_2$	[21]
	b) $\frac{\rho_b}{\varepsilon} \frac{\partial S}{\partial t} = K_{att}C - \frac{\rho_b}{\varepsilon} K_{det}S$			
	c) $C = \frac{\hat{C}}{\frac{4}{3}\pi r^3 \rho_p}$			
	d) $S = \frac{\hat{S}}{\frac{4}{3}\pi r^3 \rho_p}$			
	e) $r = r_0 e^{\frac{\lambda_1 t}{3}}$			
<b>viii</b>	b) $\frac{\rho_b}{\varepsilon} \frac{\partial S}{\partial t} = K_{att} \psi_x C - \frac{\rho_b}{\varepsilon} K_{det} S$	depth-dependent (straining) attachment together with detachment	$K_{att}, K_{det}, \beta$	[92]
	c) $\psi_x = \left(\frac{d_c + x}{d_c}\right)^{-\beta}$			
<b>ix</b>	b) $\frac{\rho_b}{\varepsilon} \frac{\partial S}{\partial t} = K_{att} \psi_b C - \frac{\rho_b}{\varepsilon} K_{det} S$	site-blocking attachment together with detachment	$K_{att}, K_{det}, S_m$	[102]
	c) $\psi_b = \left(1 - \frac{S}{S_m}\right)$			

<b>x</b>	b) $\frac{\partial S}{\partial t} = \frac{\partial S_1}{\partial t} + \frac{\partial S_2}{\partial t}$	dual-site with site-	$K_{att,1}, K_{att,2},$	[181]
	c) $\frac{\rho_b}{\varepsilon} \frac{\partial S_1}{\partial t} + \frac{\rho_b}{\varepsilon} \frac{\partial S_2}{\partial t} = K_{att,1} \psi_{b,1} C + K_{att,2} \psi_{b,2} C$	blocking kinetic attachment for available and not available favorable sites	$S_{m,1}, S_{m,2}$	
	d) $\psi_{b,1} = \left(1 - \frac{S_1}{S_{m,1}}\right)$			
	e) $\psi_{b,2} = \left(1 - \frac{S_2}{S_{m,2}}\right)$			
<b>xi</b>	b) $\frac{\partial S}{\partial t} = \frac{\partial S_1}{\partial t} + \frac{\partial S_2}{\partial t}$	dual-site with site-	$K_{att,1}, K_{det,1},$	[124]
	c) $\frac{\rho_b}{\varepsilon} \frac{\partial S_1}{\partial t} = K_{att,1} \psi_b C - \frac{\rho_b}{\varepsilon} K_{det,1} S_1$	blocking attachment and depth-dependent (straining), together with detachment	$K_{att,2}, K_{det,2}, S_m,$ $\beta$	
	d) $\frac{\rho_b}{\varepsilon} \frac{\partial S_2}{\partial t} = K_{att,2} \psi_x C - \frac{\rho_b}{\varepsilon} K_{det,2} S_2$			
	e) $\psi_b = \left(1 - \frac{S_1}{S_m}\right)$			
	f) $\psi_x = \left(\frac{d_c+x}{d_c}\right)^{-\beta}$			
<b>xii</b>	b) $\frac{\rho_b}{\varepsilon} \frac{\partial S}{\partial t} = K_{att} \psi_b \psi_x C - \frac{\rho_b}{\varepsilon} K_{det} S$	site-blocking, depth-dependent (straining) attachment together with detachment	$K_{att}, K_{det}, S_m, \beta$	[110]
	c) $\psi_b = \left(1 - \frac{S}{S_m}\right)$			
	d) $\psi_x = \left(\frac{d_c+x}{d_c}\right)^{-\beta}$			
<b>xiii</b>	b) $\frac{\rho_b}{\varepsilon} \frac{\partial S}{\partial t} = K_{att} \psi_x C - \frac{\rho_b}{\varepsilon} K_{det} S + \rho_b K_{rip} S C$	ripening, depth-dependent (straining) attachment together with detachment	$K_{att}, K_{det}, K_{rip}, \beta$	[110, 111]
	c) $\psi_x = \left(\frac{d_c+x}{d_c}\right)^{-\beta}$			
<b>xiv</b>	a) $\frac{\partial C_1}{\partial t} + \frac{\rho_b}{\varepsilon} \frac{\partial S_1}{\partial t} = D \frac{\partial^2 C_1}{\partial x^2} - V \frac{\partial C_1}{\partial x} - \frac{\rho_b}{\varepsilon} K_{12} F_p$	dual-species for transport of aggregated and non-aggregated species	$K_{att,1}, K_{det,1},$ $K_{att,2}, K_{det,2}, S_m,$ $\beta, K_{12}, S_{crit1},$	[109]

	b)	$\frac{\partial C_2}{\partial t} + \frac{\rho_b}{\varepsilon} \frac{\partial S_2}{\partial t} = D \frac{\partial^2 C_2}{\partial x^2} - V \frac{\partial C_2}{\partial x} + \frac{\rho_b}{\varepsilon} K_{12} F_p$	with site-blocking attachment and depth- dependent (straining),		
	c)	$\frac{\rho_b}{\varepsilon} \frac{\partial S_1}{\partial t} = K_{att,1} \psi_b \psi_x C_1 - \frac{\rho_b}{\varepsilon} K_{det,1} S_1 - \frac{\rho_b}{\varepsilon} K_{12} F_p$	detachment		
	d)	$\frac{\rho_b}{\varepsilon} \frac{\partial S_2}{\partial t} = K_{att,2} C_2 - \frac{\rho_b}{\varepsilon} K_{det,2} S_2$			
	e)	$\psi_b = \left(1 - \frac{S_1}{S_m}\right)$			
	f)	$\psi_x = \left(\frac{d_c + x}{d_c}\right)^{-\beta}$			
	g)	$F_p = \max(S_1 - S_{crit1}, 0)$			
<b>xv</b>	b)	$\frac{\partial S}{\partial t} = \frac{\partial S_1}{\partial t} + \frac{\partial S_2}{\partial t}$	dual-site with site- blocking/ripening	$K_{att,1}, K_{det,1},$	[105, 106]
	c)	$\frac{\rho_b}{\varepsilon} \frac{\partial S_1}{\partial t} = K_{att,1} \psi_1 C - \frac{\rho_b}{\varepsilon} K_{det,1} S_1$	attachment and depth- dependent (straining),	$K_{att,2}, K_{det,2}, A_1,$ $\beta_1, \beta_2$	
	d)	$\frac{\rho_b}{\varepsilon} \frac{\partial S_2}{\partial t} = K_{att,2} \psi_2 C - \frac{\rho_b}{\varepsilon} K_{det,2} S_2$	detachment		
	e)	$\psi_1 = (1 + A_1 S_1^{\beta_1})$			
	f)	$\psi_2 = \left(\frac{d_c + x}{d_c}\right)^{\beta_2}$			
<b>xvi</b>	b)	$\frac{\partial S}{\partial t} = \frac{\partial S_1}{\partial t} + \frac{\partial S_2}{\partial t}$	dual-site with site- blocking attachment and straining at very high ionic strength	$K_{att,1}, K_{det,1},$	[133]
	c)	$\frac{\rho_b}{\varepsilon} \frac{\partial S_1}{\partial t} = K_{att,1} \psi_b C$		$K_{att,2}, K_{det,2}, S_m,$ $\beta$	
	d)	$\frac{\rho_b}{\varepsilon} \frac{\partial S_2}{\partial t} = K_{att,2} \psi_x C$			
	e)	$\psi_b = \left(1 - \frac{S_1}{S_m}\right)$			
	f)	$\psi_x = \max(1, S_2^{S_m'})$			

\* Wherever Eq. (a) is not presented it must be considered the same as Eq. (1) given in Section 3.1.  $x$  is distance in the porous media [with the dimension of L];  $t$  is time elapsed [T];  $C$  with dimension of  $[N L^{-3}]$ ;  $N$  represents the particle number, not a dimension] and  $S$  with dimension of  $[NM^{-1}]$  are the particle number concentrations of fluid-phase particles and deposited phase particles, respectively, according to a number of references [e.g., 21, 92, 98-100], or  $C$  with the dimension of  $[ML^{-3}]$  and  $S$  with dimension of

$[MM^{-1}]$  are the particle mass concentrations of fluid-phase particles and deposited phase particles according to other references [e.g., 100, 101, 102];  $V$  is the interstitial particle velocity or pore water velocity  $[LT^{-1}]$ ;  $D$  is the hydrodynamic dispersion coefficient  $[L^2T^{-1}]$ ;  $\varepsilon$  is the bed porosity  $[-]$ ;  $\rho_b$  is the porous medium bulk density  $[ML^{-3}]$ ;  $K_{att}$  and  $K_{det}$  are the attachment and detachment rate constants, respectively  $[T^{-1}]$ ;  $f_r$  is the fraction of reversibly retained particles  $[-]$ ;  $\psi_b$  is the Langmuirian blocking function related to the fraction of porous medium available for deposition  $[-]$ ;  $S_m$  is the maximum retained-particle phase concentration, i.e., colloidal retention capacity  $[NM^{-1}$  or  $MM^{-1}]$ ;  $\psi_x$  is the depth-dependent retention function commonly used for hyper-exponential retention profile modeling  $[-]$ ;  $d_c$  is the granular media average diameter  $[L]$ ;  $\beta$  is the empirical depth-dependent retention parameter  $[-]$ ;  $K_{rip}$  is the particle-particle interaction rate coefficient between fluid-phase particles and deposited phase particles  $[L^3 T^{-1}]$ ;  $F_p$  is the aggregated species production function  $[NM^{-1}]$ ;  $S_{crit1}$  is the critical concentration of  $S_1$  when production starts  $[NM^{-1}]$ ;  $K_{12}$  is the first-order production coefficient to account for the release rate of aggregated species  $[T^{-1}]$ ;  $A_1$  and  $\beta_1$  are the multiplier and exponent coefficients, respectively  $[-]$ , which define the interaction dynamics, i.e., ripening for  $A_1 > 0$  and  $\beta_1 > 0$  or blocking for  $\beta_1 = 1$  and  $A_1 = -1/S_m$ ;  $\psi_1$  is the expression for the effect of ripening or blocking which is equal to  $\psi_b$  when  $\beta_1 = 1$  and  $A_1 = -1/S_m$ ;  $\psi_2$  is the expression for the effect of straining, equal to  $\psi_x$  if assuming  $\beta_2 = -\beta$ ;  $\hat{C}$  is the mass concentration of fluid-phase particles  $[ML^{-3}]$ ;  $\hat{S}$  is the mass concentration of deposited-phase particles  $[MM^{-1}]$ ;  $r$  is the average radii of particles in the fluid phase and deposited phase  $[L]$ ;  $r_0$  is the average radius of particles (or agglomerates) at  $t = 0$   $[L]$ ;  $\rho_p$  is the average density of the particles or aggregates  $[ML^{-3}]$ ;  $\lambda_1$  is the pseudo-first-order reaction rate  $[T^{-1}]$ , which stands for the decay in population of particles due to agglomeration;  $\lambda_2$  is the pseudo-first-order reaction rate  $[T^{-1}]$ , which stands for the decay in the population of deposited, detachable particles and represents irreversible deposition;  $K_d$  is the well-known distribution coefficient of the nanoparticles between the aqueous and solid phases  $[L^3 M^{-1}]$ ;  $K_{rel}$  is the release rate constant,  $S_{eq}$   $[NM^{-1}$  or  $MM^{-1}]$  is the equilibrium value of  $S$  in the new steady state following perturbation;  $H_o(S-S_{eq})$  is the Heaviside function (acting as a cancelling function) which is equal to one when  $S > S_{eq}$  and zero when  $S \leq S_{eq}$ ;  $S_i$   $[NM^{-1}$  or  $MM^{-1}]$  is the value of  $S$  before the perturbation;  $f_{nr}$   $[-]$  is the fraction of deposited particles that are not released with the perturbation in the system conditions; and indexes 1 and 2 in dual-sites models (types (x), (iv), (xi), (xv), and (xvi)) stand for sites 1 and 2 and in dual species model (type (xiv)) stand for species 1 and 2. **Note:** Model type (xv) also includes modifications in the flow condition for change in the porosity and permeability due to clogging, which are not presented here.

**Table 2.** Summary of the NP transport studies experimental conditions and outcomes together with the major observed phenomena, the shapes of the breakthrough curve and residual concentration profile, and types of the applied continuum model.

No.	NP Type	Coating and free polymer	IS species	pH	IS (mM)	C <sub>0</sub> (mg/L)	dp/dg *	C/C <sub>0</sub> (%)	BTC plateau shape **	RP shape	Major underlying phenomena	Model Type(s) used	Ref.
1	AgNP	citrate; polyvinylpyrrolidone; branched polyethyleneimine	NaNO <sub>3</sub>	7	5	10	2.7E-05— 3.4E-05	20— 100	flat	NM	physicochemical filtration; straining following aggregation	ix without the term K <sub>det</sub>	El Badawy et al. [201]
2	AgNP	proteinate capping with bovine serum albumin	MgSO <sub>4</sub>	6.7	0—50	50	9.1E-05— 2.8E-04	0— 75.7	ascending	NM	straining	ix	Ren and Smith [242]
3	AgNP	two nonionic surfactants: polyoxyethylene glycerol trioleate and polyoxyethylene (20) sorbitan monolaurate	KNO <sub>3</sub>	6.5	1—10	1—10	8.6E-05	3.4 — 64.3	ascending	hyper-exponential	significant retardation	xii without the term K <sub>det</sub>	Liang et al. [138]
4	AgNP	Polyoxyethylene Glycerol Trioleate and Polyoxyethylene (20) Sorbitan monolaurate (Tween 20)	KNO <sub>3</sub>	6.5	1—5	1—10	7.4E-05— 1.9E-04	4.5 — 45.6	ascending	uniform, hyper-exponential or non-monotonic shapes	irreversible interactions in a primary minimum due to microscopic heterogeneity	xii without the term K <sub>det</sub>	Liang et al. [127]
5	AgNP	surfactant, polyoxyethylene glycerol trioleate and polyoxyethylene (20) sorbitan monolaurate (Tween 20)	NaNO <sub>3</sub> ; Ca(NO <sub>3</sub> ) <sub>2</sub> ; H <sub>2</sub> O	5.9— 6.5	0—50	60	7E-05— 5.8E-04	0— 100	ascending	non-monotonic	size selective filtration; reversible deposition of the AgNP due to secondary minimum interactions.	ix; ix without K <sub>det</sub> ; xii; i	Braun et al. [135]
6	AgNP	coating: PVP; free polymer: HA	KNO <sub>3</sub> ; Ca(NO <sub>3</sub> ) <sub>2</sub>	5.8	0.5— 100	10	5E-05— 4.3E-03	0— 88.3	ascending	non-monotonic	Increased aggregation of PVP- AgNP in presence of Ca <sup>2+</sup>	xii without the term K <sub>det</sub>	Wang et al. [128]
7	AgNP	PVP	KNO <sub>3</sub> ; Ca(NO <sub>3</sub> ) <sub>2</sub>	5.4— 6.1	0.1— 10	10	4.5E-05— 2.5E-04	0.4 — 36.5	ascending	hyper-exponential or non-monotonic	significant retardation, aggregation, irreversible deposition	xii without the term K <sub>det</sub> ; xiv without the term K <sub>det1</sub> ; xiv without the term K <sub>det1</sub> and K <sub>det2</sub>	Wang et al. [123]

No.	NP Type	Coating and free polymer	IS species	pH	IS (mM)	C <sub>0</sub> (mg/L)	dp/dg *	C/C <sub>0</sub> (%)	BTC plateau shape **	RP shape	Major underlying phenomena	Model Type(s) used	Ref.
8	AgNP	PVP	KNO <sub>3</sub>	4.5— 7.7	0.9— 2.6	1.7	1.3E-04— 3.6E-04	0.16 — 8.84	NC	depth-dependent	straining following heteroaggregation, size-exclusion	iv without K <sub>det2</sub>	Cornelis et al. [202]
9	AgNP	polyoxyethylene glycerol triolate and polyoxyethylene (20) sorbitan monolaurat, 4% w/w each and the unbounded surfactant of ~5% PAA	H <sub>2</sub> O; NaNO <sub>3</sub> ; Ca(NO <sub>3</sub> ) <sub>2</sub>	7.3	0—10	474— 800	2.3E-04— 2.8E-04	43— 100	ascending and rather flat	NM	blocking; physicochemical retention; aggregation; and probably straining	ix without K <sub>det</sub> ; i; ii;	Neukum et al. [176]
10	NZVI	PAA	NaClO <sub>4</sub>	8.6	1	200	3.1E-04— 3.5E-04	18— 70	continuous; flat	NM	aggregation; irreversible deposition	i	Laumann et al. [289]
11	Iron oxide NPs	PAA	NC	NC	NC	20— 500	2.7E-05— 4.7E-05	88— 97	continuous; flat	NM	irreversible deposition	i	Golzar et al., [392]
12	NZVI	CMC	NC	8.5	30— 160	100— 2500	5.4E-05— 1.3E-04	80	continuous; descending at low velocity	NM	aggregation and settling in the feeding stock dispersion	i with modified boundary condition	Kocur et al., [350]
13	NZVI	Pure PAA-nZVI; NOM; Lignin sulfonate; CMC; HA	NaHC O <sub>3</sub>	7.9— 8.3	1	200	1.6E-03— 1.9E-03	22— 53	continuous; flat	NM	irreversible deposition	i	Laumann et al. [393]
14	NZVI	CMC	KCl	8.1	15	200	1.6E-05— 5.8E-05	69— 99	symmetric, flat	NM	filtration due to Brownian diffusion and gravitational sedimentation	v	He et al. [190]
15	NZVI	CMC	NaHC O <sub>3</sub>	7.4	0.1	85— 1700	2.2E-04— 1.2E-03	55— 97	predominately ascending	hyper-exponential	Straining; detachment	xi without $\psi_b$ and K <sub>det2</sub>	Raychoudhury et al. [136]
16	NZVI	dispersed in xanthan solution	NC	NC	0—13	20000	1.0E-04	86— 90	flat	hyper-exponential	attachment, detachment (tailing), blocking, ripening, and clogging	xv	Tosco et al. [105]
17	NZVI	Cu	Natural ground water	7.2	40	8000	8.4E-05— 8.7E-05	61— 90	ascending at low concentration (2 g/L), descending at middle concentration (5 g/L), and multiple	NC	clogging after ripening	xv	Hosseini and Tosco [106]

No.	NP Type	Coating and free polymer	IS species	pH	IS (mM)	C <sub>0</sub> (mg/L)	dp/dg *	C/C <sub>0</sub> (%)	BTC plateau shape **	RP shape	Major underlying phenomena	Model Type(s) used	Ref.
18	NZVI	poly(styrene sulfonate) (PSS)	5 mM NaCl 5 mM NaHC O <sub>3</sub>	8	10	30—6000	1.6E-04—2.1E-3	61.5—97	peaks and tailing at very high concentrations (8 and 12 g/L) flat	NM	agglomeration and subsequent irreversible deposition of agglomerates; disaggregation identified by the model.	ii; vii	Babakhani et al. [21] and Phenrat et al. [33]
19	NZVI	CMC	NaHC O <sub>3</sub>	7.4	0.1	70—725	5.1E-04	55—72	continuous; ascending	NM	aggregation, detachment	vii	Babakhani et al. [21] and Raychoudhury et al. [104]
20	nHAP	Cu coated and humic acid as free polymer	NaCl; CaCl <sub>2</sub>	5.7—5.9	0—100	200	1.7E-04—2.3E-04	11—89	rather flat and ascending at the highest IS	hyper-exponential	aggregation	xi without considering $\psi_b$ and $K_{det2}$	Wang et al. [129]
21	nHAP	Cu	NaCl	6.2—9	0.1	200	1.7E-04	32—90	flat at various pH and water velocity but ascending by increasing the amount of Fe coating on the sand.	hyper-exponential	retardation; blocking	xi without $\psi_b$ ; xi without $K_{det}$	Wang et al. [124]
22	nHAP	Alizarin red S (ARS)-labeled (coated) NPs with humic acid as free polymer	NaCl	6—10.5	0.1	100	5E-04—6E-04	30.5—78.8	flat at various concentrations of HA, but descending at zero concentration of HA	hyper-exponential	blocking	xi without $\psi_b$ ; xi without $K_{det}$	Wang et al. [71]
23	nHAP	Alizarin red S (ARS)-labeled (coated) NPs with humic acid as free polymer	NaCl	7.2	0.1—50	100	4E-04—1.1E-03	7.8—78.8	flat	hyper-exponential	aggregation	xi without $\psi_b$ and $K_{det2}$	Wang et al. [122]
24	nHAP	Alizarin red S (ARS)-labeled (coated) NPs: in presence of SDBS and CTAB	NaCl	7	0.1	100	2.2E-04	0.8—78.6	descending	hyper-exponential	aggregation; ripening; straining; and size selective retention	xiii	Wang et al. [111]

No.	NP Type	Coating and free polymer	IS species	pH	IS (mM)	C <sub>0</sub> (mg/L)	dp/dg *	C/C <sub>0</sub> (%)	BTC plateau shape **	RP shape	Major underlying phenomena	Model Type(s) used	Ref.
25	GO	NA	NaCl	5.1	20—28	5—25	6E-04— 3.9E-03	0.2 — 56.9	ascending	exponential to uniform	aggregation; blocking	ix without K <sub>det</sub>	Sun et al. [249]
26	GO	NA	NaCl	6	1—100	5	1.3E-03	3.4 — 93.5	ascending	NM	blocking	ix without K <sub>det</sub>	Feriancikova and Xu [250]
27	GO	NA	NaCl	NC	1—100	12	5.5E-03	3— 99.4	ascending	NM	aggregation; blocking	i; ix without K <sub>det</sub>	Liu et al. [394]
28	graphene	SDBS and CTAB surfactants	DI water	NC	0.01	14— 16.5	9.1E-04— 9.9E-04	4.1 — 90.6	flat	NM	attachment	i	Liu et al. [251]
29	GO	NA	NaCl	7.1	50— 200	20	3E-03— 8.2E-3	22— 75	ascending	NM	straining due to concurrent agglomeration; blocking	xii	Fan et al. [130]
30	graphene	Carboxyl-functionalized	NC	5.6— 8.3	NC	12	1.1E-03	88.4 — 99.8	flat to slightly ascending	NM	attachment	i	Liu et al. [70]
31	GO	NA	various Ca <sup>2+</sup> /Na <sup>+</sup> ratios: 0; 0.15; 0.3; 0.6; 1; ∞	7	1—10	20	2.6E-03— 8.7E-03	1.8 — 80	ascending	NM	straining following agglomeration; blocking	xii	Fan et al. [131]
32	GO	NA	DI water; NaCl	4.8— 9	0—50	19.2— 21.7	9E-04— 2.5E-03	10.7 — 95.9	flat at intermediate IS and descending at high IS	Relatively flat low and moderate IS, elevated from inlet point at high IS (50 mM)	clogging and straining following agglomeration; blocking	xi without K <sub>det</sub>	Qi et al. [133]
33	GO	NA	NaCl	7.2	1—50	20	5.1E-04— 6.6E-04	24— 99.9	ascending	NC	aggregation; straining; blocking	xi with $\psi_x=1$ , without K <sub>det2</sub> , and by shifting the	He et al. [74]

No.	NP Type	Coating and free polymer	IS species	pH	IS (mM)	C <sub>0</sub> (mg/L)	dp/dg *	C/C <sub>0</sub> (%)	BTC plateau shape **	RP shape	Major underlying phenomena	Model Type(s) used	Ref.
												indexes 1 and 2	
34	GO	NA	DI water; NaCl; CaCl <sub>2</sub>	4—9	0—50	19.4—21.4	7.7E-04—3.8E-03	20.8—100	flat (in sand) or ascending (in soil) at high NaCl concentration, descending at high CaCl <sub>2</sub> concentration in soil	NM	aggregation; straining; blocking	xi without K <sub>det</sub> ; xvi	Qi et al. [132]
35	CeO <sub>2</sub>	HA	NaCl	7—10	1—100	200	6E-04—1.4E-03	9.9—74.8	flat	NM	Ripening in absence of HA due to aggregation	i	Lv et al. [267]
36	CeO <sub>2</sub>	NA	NaCl	3—9	1—100	10—50	2.1E-04	1.3—96.9	ascending	NM	aggregation; straining; blocking	ix	Li et al. [192]
37	TiO <sub>2</sub> , rutile	NA	KCl and KOH	10	5	50	1.7E-04	5—87	ascending	NM	blocking	ix without K <sub>det</sub>	Toloni et al. [222]
38	TiO <sub>2</sub> , anatase	NA	NaCl	2.6—9.6	0.1—50	35	1.2E-03—9.8E-03	0—94.1	continuous, flat at intermediate IS, ascending at high IS	NM	straining; aggregation; detachment	xi with $\psi_b=1$ and without K <sub>det2</sub>	Fang et al. [134]
39	ZnO	NA	NaNO <sub>3</sub>	8.5	1—50	34—430	1.3E-03—9E-03	2.1—81.2	continuous, ascending	hyper-exponential	clogging; straining; aggregation; detachment; blocking; irreversible attachment	xi with $\psi_x$ , $\psi_{b1}=\psi_x$ ; and without K <sub>det2</sub>	Sun et al. [137]
40, 41	ZnO	NA	NaCl; CaCl <sub>2</sub>	8	0.1—20	5	6E-04—1.2E-03	14.6—82.7	flat at low IS, descending at high IS; flat in presence of NOM, descending in absence of NOM at high IS	hyper-exponential	pore plugging; straining following the concurrent aggregation; detachment; blocking; irreversible attachment; and ripening	ii	Jiang et al. [206] and Jiang et al. [207]
42	ZnO	NA	NaCl; CaCl <sub>2</sub>	8	0.1—5	5	6E-04—9E-04	11.3—79	flat in all cases	hyper-exponential	straining following the concurrent aggregation	ii	Jiang et al. [75]

No.	NP Type	Coating and free polymer	IS species	pH	IS (mM)	C <sub>0</sub> (mg/L)	dp/dg *	C/C <sub>0</sub> (%)	BTC plateau shape **	RP shape	Major underlying phenomena	Model Type(s) used	Ref.
43	QD-CdSe/ZnS	COOHP; PAA-octylamine (PAA-OA); linoleic acid (LA)	NaCl	5—9.5	0—30	1.6E-03—2.3E-03	5e-05—2E-04	5.9—100	flat or spike like with retardation	NM	retardation	ix without K <sub>det</sub>	Wang et al. [184]
44	QD, CdSe/CdZnS	amphiphilic polymer, PAA-OA	NaCl	7	3	0.0016	8.7E-05—2.5E-04	0.4—75.3	flat to ascending and spike like	non-monotonic	blocking by polymer	ix without K <sub>det</sub>	Wang et al. [186]
45	CdSe QDs	nonionic ethoxylated alcohol surfactant-Neodol	synthetic seawater	8.5	550—1000	0.86	6.2E-05	91—96	flat	NM	retardation at elevated temperatures	v without K <sub>att</sub>	Kini et al. [182]
46	CdTe QDs	NA	NaCl; CaCl <sub>2</sub>	8	2—100	44.7	2E-04—3E-04	5—98	flat in NaCl solution and ascending in CaCl <sub>2</sub> solution	NM	blocking; release	ix without K <sub>det</sub>	Torkzaban et al. [187]
47	CML	NA	NaCl; CaCl <sub>2</sub>	7	0.5—60	3.13—25.0	2E-04—4E-04	30—100	ascending, delayed	NM	blocking; delay	x	Sasidharan et al. [181]
48	AIO	NA	NaCl	4.8	0—100	50—400	3E-04—1.3E-03	52.5—95.9	flat	NM	aggregation; blocking	x with $\psi_{b2}=1$	Rahman et al. [329] and Rahman et al. [330]
49	TiO <sub>2</sub> , anatase	NA	NaCl	4	1.1	100—1000	8E-05—7E-04	96.1—98.7	ascending	NM	irreversible deposition; blocking	ix without K <sub>det</sub>	Saiers et al. [102]
50	CdTe QDs and CML	NA	NaCl; CaCl <sub>2</sub>	8	0.5—100	40.2—250	2E-04—7E-04	1—99	ascending	NM	blocking	ix without detachment	Torkzaban et al. [185]

\*  $d_p/d_g$  is calculated based on the ratio of the average hydrodynamic diameter to the average grain size which might not be according to the what the authors reported, i.e., they might have calculated  $d_p/d_g$  based on other types of size measurement techniques than hydrodynamic diameter used here; \*\*BTC plateau shape mostly considered at intermediate or favorable retention condition.. NM: not measured; NA: not applicable; NC: not clear; PVP: polyvinylpyrrolidone; CMC: carboxy-methyl-cellulose; PAA: Polyacrylic acid; SDBS: anionic sodium dodecyl benzene sulfonate; CTAB: cationic cetyltrimethylammonium bromide; COOHP: carboxyl derivatized polymer.

**Table 3.** Parameter values and fitting results for cases of F3 at 30 mg/L and F1 at 6 g/L using non-equilibrium and equilibrium models.<sup>a</sup>

	<b>F3-0.03 g/L- Non-equilibrium<sup>b</sup></b>	<b>F3-0.03 g/L- Equilibrium<sup>b</sup></b>	<b>F1-6 g/L- Non-equilibrium<sup>c</sup></b>	<b>F1-6 g/L - Equilibrium<sup>c</sup></b>
<b>K<sub>d</sub> or K<sub>att</sub></b>	7.21E-03 <sup>d</sup>	4.99E-05 <sup>e</sup>	1.05E-02 <sup>d</sup>	4.75e-5 <sup>e</sup>
<b>K<sub>det</sub></b>	2.61E-02	NA	3.61E-02	NA
<b>λ<sub>1</sub></b>	NA	NA	8.89E-04	1.50e-3
<b>λ<sub>2</sub></b>	NA	NA	2.27E-03	2.69e-3
<b>R<sup>2</sup></b>	0.987	0.977	0.996	0.971
<b>P-Value</b>	0.43	0.59	0.87	0.18
<b>AIC</b>	-97.8	-94.2	634	642

<sup>a</sup>The unit of K<sub>d</sub> is m<sup>3</sup>/Kg and the units of other parameters are s<sup>-1</sup>. <sup>b</sup>Based on simple finite difference (FD) method. <sup>c</sup>Based on the total variation diminishing (TVD) method. <sup>d</sup>K<sub>att</sub>. <sup>e</sup>K<sub>d</sub>. NA: not applicable.

**Table 4.** Parameter values and fitting results for cases low concentration of 0.3 g/L and high concentration (washed-MRNIP2) of 6 g/L using non-equilibrium and equilibrium models.<sup>a</sup>

	<b>0.3 g/L- Non-equilibrium</b>	<b>0.3 g/L- Equilibrium</b>	<b>6 g/L- Non-equilibrium</b>	<b>6 g/L- Equilibrium</b>
<b>K<sub>d</sub> or K<sub>att</sub> fine</b>	6.82E-03 <sup>b</sup>	1.15E-05 <sup>c</sup>	2.34E-02 <sup>b</sup>	7.04E-05 <sup>c</sup>
<b>K<sub>d</sub> or K<sub>att</sub> medium</b>	2.78E-03 <sup>b</sup>	2.02E-03 <sup>c</sup>	3.67E-03 <sup>b</sup>	4.27E-04 <sup>c</sup>
<b>K<sub>d</sub> or K<sub>att</sub> coarse</b>	3.90E-03 <sup>b</sup>	8.00E-04 <sup>c</sup>	1.49E-01 <sup>b</sup>	1.08E-03 <sup>c</sup>
<b>K<sub>det</sub> fine</b>	4.88E-03	NA	5.02E-02	NA
<b>K<sub>det</sub> medium</b>	1.69E-05	NA	1.75E-04	NA
<b>K<sub>det</sub>coarse</b>	1.23E-03	NA	2.83E-02	NA
<b>λ<sub>1</sub> fine</b>	NA	NA	1.46E-04	7.04E-06
<b>λ<sub>1</sub> medium</b>	NA	NA	2.27E-03	1.32E-03
<b>λ<sub>1</sub>coarse</b>	NA	NA	9.87E-05	8.83E-05

$\lambda_2$ fine	NA	NA	2.48E-04	1.44E-04
$\lambda_2$ medium	NA	NA	3.08E-04	1.52E-03
$\lambda_2$ coarse	NA	NA	1.27E-04	1.55E-04
$R^2$	0.787	0.639	0.951	0.948
<b>P-Value</b>	0.61	0.79	0.58	0.92
<b>AIC</b>	-37.4	-42.2	609	582

<sup>a</sup>The unit of  $K_d$  is  $m^3/Kg$  and the units of other parameters are  $s^{-1}$ . <sup>b</sup> $K_{att}$ . <sup>c</sup> $K_d$ . NA: not applicable.

### References

- [1] Keane E. Fate, transport, and toxicity of nanoscale zero-valent iron (nZVI) used during superfund remediation. US Environmental Protection Agency. 2009.
- [2] Klaine SJ, Alvarez PJJ, Batley GE, Fernandes TF, Handy RD, Lyon DY, et al. Nanomaterials in the environment: behavior, fate, bioavailability, and effects. *Environmental Toxicology and Chemistry*. 2008;27:1825-51.
- [3] Doong R-a, Saha S, Lee C-h, Lin H-p. Mesoporous silica supported bimetallic Pd/Fe for enhanced dechlorination of tetrachloroethylene. *RSC Advances*. 2015;5:90797-805.
- [4] Lin F-h, Doong R-a. Highly efficient reduction of 4-nitrophenol by heterostructured gold-magnetite nanocatalysts. *Applied Catalysis A: General*. 2014;486:32-41.
- [5] Doong R-a, Liao C-Y. Enhanced visible-light-responsive photodegradation of bisphenol A by Cu, N-codoped titanate nanotubes prepared by microwave-assisted hydrothermal method. *Journal of hazardous materials*. 2016.
- [6] Li M, Hsieh T-C, Doong R-A, Huang CP. Tuning the adsorption capability of multi-walled carbon nanotubes to polar and non-polar organic compounds by surface oxidation. *Separation and Purification Technology*. 2013;117:98-103.
- [7] Chiang L-F, Doong R-a. Enhanced photocatalytic degradation of sulfamethoxazole by visible-light-sensitive TiO<sub>2</sub> with low Cu addition. *Separation and Purification Technology*. 2015;156:1003-10.
- [8] Chang P-Y, Bindumadhavan K, Doong R-A. Size Effect of Ordered Mesoporous Carbon Nanospheres for Anodes in Li-Ion Battery. *Nanomaterials*. 2015;5:2348-58.
- [9] Chang P-y, Huang C-h, Doong R-a. Ordered mesoporous carbon-TiO<sub>2</sub> materials for improved electrochemical performance of lithium ion battery. *Carbon*. 2012;50:4259-68.
- [10] Keller AA, McFerran S, Lazareva A, Suh S. Global life cycle releases of engineered nanomaterials. *Journal of Nanoparticle Research*. 2013;15:1-17.
- [11] Keller AA, Lazareva A. Predicted releases of engineered nanomaterials: from global to regional to local. *Environmental Science & Technology Letters*. 2013;1:65-70.
- [12] Dale A, Casman EA, Lowry GV, Lead JR, Viparelli E, Baalousha MA. Modeling nanomaterial environmental fate in aquatic systems. *Environmental Science & Technology*. 2015.
- [13] Liu HH, Cohen Y. Multimedia environmental distribution of engineered nanomaterials. *Environmental science & technology*. 2014;48:3281-92.
- [14] Meesters JAJ, Koelmans AA, Quik JTK, Hendriks AJ, Van de Meent D. Multimedia modeling of engineered nanoparticles with SimpleBox4nano: model definition and evaluation. *Environmental Science & Technology*. 2014;48:5726-36.

- [15] Yu H, He Y, Li P, Li S, Zhang T, Rodriguez-Pin E, et al. Flow enhancement of water-based nanoparticle dispersion through microscale sedimentary rocks. *Scientific reports*. 2015;5.
- [16] Bardos P, Bone B, Daly P, Elliott D, Jones S, Gregory, et al. A Risk/Benefit Appraisal for the Application of Nano-Scale Zero Valent Iron (nZVI) for the Remediation of Contaminated Sites, "Taking Nanotechnological Remediation Processes from Lab Scale to End User Applications for the Restoration of a Clean Environment". NANOREM, Supporting MS3, EU, 7th FP, NMP201212. 2014.
- [17] Tratnyek PG, Johnson RL. Nanotechnologies for environmental cleanup. *Nano today*. 2006;1:44-8.
- [18] Praetorius A, Scheringer M, Hungerbühler K. Development of environmental fate models for engineered nanoparticles • a case study of tio<sub>2</sub> nanoparticles in the rhine river. *Environmental Science & Technology*. 2012;46:6705-13.
- [19] Ehtesabi H, Ahadian MM, Taghikhani V, Ghazanfari MH. Enhanced heavy oil recovery in sandstone cores using tio<sub>2</sub> nanofluids. *Energy & Fuels*. 2013;28:423-30.
- [20] Hashemi R, Nassar NN, Pereira Almaso P. Enhanced Heavy Oil Recovery by in Situ Prepared Ultradispersed Multimetallic Nanoparticles: A Study of Hot Fluid Flooding for Athabasca Bitumen Recovery. *Energy & Fuels*. 2013;27:2194-201.
- [21] Babakhani P, Fagerlund F, Shamsai A, Lowry GV, Phenrat T. Modified MODFLOW-based model for simulating the agglomeration and transport of polymer-modified Fe nanoparticles in saturated porous media. *Environ Sci Pollut Res Int*. 2015:1-20.
- [22] Baalousha M, Cornelis G, Kuhlbusch T, Lynch I, Nickel C, Peijnenburg W, et al. Modeling Nanomaterials Fate and Uptake in the Environment: Current Knowledge and Future Trends. *Environmental Science: Nano*. 2016.
- [23] Peijnenburg W, Praetorius A, Scott-Fordsmand J, Cornelis G. Fate assessment of engineered nanoparticles in solids dominated media—Current insights and the way forward. *Environmental Pollution*. 2016.
- [24] Bottero J-Y, Auffan M, Borschnek D, Chaurand P, Labille J, Levard C, et al. Nanotechnology, global development in the frame of environmental risk forecasting. A necessity of interdisciplinary researches. *Comptes Rendus Geoscience*. 2015;347:35-42.
- [25] Tian Y, Gao B, Silvera-Batista C, Ziegler KJ. Transport of engineered nanoparticles in saturated porous media. *Journal of Nanoparticle Research*. 2010;12:2371-80.
- [26] Fagerlund F, Illangasekare TH, Phenrat T, Kim HJ, Lowry GV. PCE dissolution and simultaneous dechlorination by nanoscale zero-valent iron particles in a DNAPL source zone. *Journal of Contaminant Hydrology*. 2012;131:9-28.
- [27] Phenrat T, Fagerlund F, Illangasekare T, Lowry GV, Tilton RD. Polymer-Modified Fe<sub>0</sub> Nanoparticles Target Entrapped NAPL in Two Dimensional Porous Media: Effect of Particle Concentration, NAPL Saturation, and Injection Strategy. *Environmental Science & Technology*. 2011;45:6102-9.
- [28] U.S.EPA. OSWER. Selected Sites Using or Testing Nanoparticles for Remediation. : <http://clu-in.org/download/remed/nano-site-list.pdf>; 2011.
- [29] Vesilind PA, Peirce JJ, Weiner RF. *Environmental Engineering*: Butterworth-Heinemann; 1994.
- [30] Molnar IL, Johnson WP, Gerhard JI, Willson CS, O'Carroll DM. Predicting colloid transport through saturated porous media: A critical review. *Water Resources Research*. 2015.
- [31] Phenrat T, Kim H-J, Fagerlund F, Illangasekare T, Lowry GV. Empirical correlations to estimate agglomerate size and deposition during injection of a polyelectrolyte-modified Fe<sub>0</sub> nanoparticle at high particle concentration in saturated sand. *Journal of Contaminant Hydrology*. 2010;118:152-64.
- [32] Phenrat T, Song JE, Cisneros CM, Schoenfelder DP, Tilton RD, Lowry GV. Estimating Attachment of Nano- and Submicrometer-particles Coated with Organic Macromolecules in Porous Media: Development of an Empirical Model. *Environmental Science & Technology*. 2010;44:4531-8.
- [33] Phenrat T, Kim HJ, Fagerlund F, Illangasekare T, Tilton RD, Lowry GV. Particle size distribution, concentration, and magnetic attraction affect transport of polymer-modified Fe<sub>0</sub> nanoparticles in sand columns. *Environ Sci Technol*. 2009;43:5079-85.
- [34] Taghavy A, Pennell KD, Abriola LM. Modeling coupled nanoparticle aggregation and transport in porous media: A Lagrangian approach. *Journal of Contaminant Hydrology*. 2015;172:48-60.
- [35] Kelly RA, Jakeman AJ, Barreteau O, Borsuk ME, ElSawah S, Hamilton SH, et al. Selecting among five common modelling approaches for integrated environmental assessment and management. *Environmental Modelling & Software*. 2013;47:159-81.
- [36] Adamczyk Z, Nattich-Rak M, Sadowska M, Michna A, Szczepaniak K. Mechanisms of nanoparticle and bioparticle deposition—Kinetic aspects. *Colloids and Surfaces A: Physicochemical and Engineering Aspects*. 2013;439:3-22.

- [37] Mackay D, Webster E, Cousins I, Cahill T, Foster K, Gouin T. An introduction to multimedia models. CEMC Report. 2001:30.
- [38] Comba S, Braun J. A new physical model based on cascading column experiments to reproduce the radial flow and transport of micro-iron particles. *Journal of contaminant hydrology*. 2012;140:1-11.
- [39] Gottschalk F, Sonderer T, Scholz RW, Nowack B. Modeled environmental concentrations of engineered nanomaterials (TiO<sub>2</sub>, ZnO, Ag, CNT, fullerenes) for different regions. *Environmental science & technology*. 2009;43:9216-22.
- [40] Gottschalk F, Sonderer T, Scholz RW, Nowack B. Possibilities and limitations of modeling environmental exposure to engineered nanomaterials by probabilistic material flow analysis. *Environmental Toxicology and Chemistry*. 2010;29:1036-48.
- [41] Sun TY, Gottschalk F, Hungerbühler K, Nowack B. Comprehensive probabilistic modelling of environmental emissions of engineered nanomaterials. *Environmental Pollution*. 2014;185:69-76.
- [42] Mueller NC, Nowack B. Exposure modeling of engineered nanoparticles in the environment. *Environmental science & technology*. 2008;42:4447-53.
- [43] Gottschalk F, Sun T, Nowack B. Environmental concentrations of engineered nanomaterials: review of modeling and analytical studies. *Environmental Pollution*. 2013;181:287-300.
- [44] Nowack B, Baalousha M, Bornhöft N, Chaudhry Q, Cornelis G, Cotterill J, et al. Progress towards the validation of modeled environmental concentrations of engineered nanomaterials by analytical measurements. *Environmental Science: Nano*. 2015.
- [45] Quik JTK, van De Meent D, Koelmans AA. Simplifying modeling of nanoparticle aggregation–sedimentation behavior in environmental systems: A theoretical analysis. *Water Research*. 2014;62:193-201.
- [46] Arvidsson R, Molander S, Sandén BA, Hassellöv M. Challenges in exposure modeling of nanoparticles in aquatic environments. *Human and Ecological Risk Assessment*. 2011;17:245-62.
- [47] Hotze EM, Phenrat T, Lowry GV. Nanoparticle Aggregation: Challenges to Understanding Transport and Reactivity in the Environment. *J Environ Qual* 2010;39:1909–24.
- [48] Petosa AR, Jaisi DP, Quevedo IR, Elimelech M, Tufenkji N. Aggregation and deposition of engineered nanomaterials in aquatic environments: role of physicochemical interactions. *Environmental Science & Technology*. 2010;44:6532-49.
- [49] Adamczyk Z, Weroński P. Application of the DLVO theory for particle deposition problems. *Advances in Colloid and Interface Science*. 1999;83:137-226.
- [50] Grasso D, Subramaniam K, Butkus M, Strevett K, Bergendahl J. A review of non-DLVO interactions in environmental colloidal systems. *Reviews in Environmental Science and Biotechnology*. 2002;1:17-38.
- [51] Bradford SA, Torkzaban S. Colloid transport and retention in unsaturated porous media: A review of interface-, collector-, and pore-scale processes and models. *Vadose Zone Journal*. 2008;7:667-81.
- [52] Keir G, Jegatheesan V, Vigneswaran S. Deep bed filtration: modeling theory and practice. *Water and Wastewater Treatment Technologies*, V Saravanamuthu, ed, Eolss Publishers, Oxford, UK. 2009:263-307.
- [53] McDowell-Boyer LM, Hunt JR, Sitar N. Particle transport through porous media. *Water Resour Res*. 1986;22:1901-21.
- [54] Schijven JK, Hassanizadeh SM. Removal of viruses by soil passage: Overview of modeling, processes, and parameters. *Crit Rev Environ Sci Technol*. 2000;30:49 – 127.
- [55] Pan B, Xing B. Applications and implications of manufactured nanoparticles in soils: a review. *European Journal of Soil Science*. 2012;63:437-56.
- [56] Jegatheesan V, Vigneswaran S. Deep Bed Filtration: Mathematical Models and Observations. *Critical Reviews in Environmental Science and Technology*. 2005;35:515-69.
- [57] Taghavy A, Mittelman A, Wang Y, Pennell KD, Abriola LM. Mathematical modeling of the transport and dissolution of citrate-stabilized silver nanoparticles in porous media. *Environmental Science & Technology*. 2013;47:8499-507.
- [58] Albarran N, Missana T, Alonso U, García-Gutiérrez M, López T. Analysis of latex, gold and smectite colloid transport and retention in artificial fractures in crystalline rock. *Colloids and Surfaces A: Physicochemical and Engineering Aspects*. 2013;435:115-26.
- [59] Jen C-P, Li S-H. Effects of hydrodynamic chromatography on colloid-facilitated migration of radionuclides in the fractured rock. *Waste Management*. 2001;21:499-509.
- [60] Li S-H, Jen C-P. Modeling of hydrodynamic chromatography for colloid migration in fractured rock. *Nuclear technology*. 2001;133:253-63.

- [61] Xie J, Lu J, Lin J, Zhou X, Xu Q, Li M, et al. Insights into transport velocity of colloid-associated plutonium relative to tritium in porous media. *Scientific reports*. 2014;4.
- [62] Bradford SA, Yates SR, Bettahar M, Simunek J. Physical factors affecting the transport and fate of colloids in saturated porous media. *Water Resources Research*. 2002;38:63-1.
- [63] Bradford SA, Torkzaban S, Leij F, Simunek J. Equilibrium and kinetic models for colloid release under transient solution chemistry conditions. *Journal of contaminant hydrology*. 2015.
- [64] Torkzaban S, Bradford SA, Vanderzalm JL, Patterson BM, Harris B, Prommer H. Colloid release and clogging in porous media: Effects of solution ionic strength and flow velocity. *Journal of contaminant hydrology*. 2015.
- [65] Yao K-M, Habibian MT, O'Melia CR. Water and waste water filtration. Concepts and applications. *Environmental Science & Technology*. 1971;5:1105-12.
- [66] Ryan JN, Elimelech M. Colloid mobilization and transport in groundwater. *Colloids and Surfaces A*. 1996;107:1-56.
- [67] Tufenkji N, Elimelech M. Correlation equation for predicting single-collector efficiency in physicochemical filtration in saturated porous media. *Environmental Science & Technology*. 2004;38:529-36.
- [68] Elimelech M, Jia X, Gregory J, Williams R. Particle deposition and aggregation: measurement, modelling and simulation. Amsterdam: Elsevier; 1998.
- [69] Sirk KM, Saleh NB, Phenrat T, Kim H-J, Dufour B, Ok J, et al. Effect of adsorbed polyelectrolytes on nanoscale zero valent iron particle attachment to soil surface models. *Environmental science & technology*. 2009;43:3803-8.
- [70] Liu L, Gao B, Wu L, Yang L, Zhou Z, Wang H. Effects of pH and surface metal oxyhydroxides on deposition and transport of carboxyl-functionalized graphene in saturated porous media. *Journal of nanoparticle research*. 2013;15:1-8.
- [71] Wang D, Bradford SA, Harvey RW, Gao B, Cang L, Zhou D. Humic acid facilitates the transport of ARS-labeled hydroxyapatite nanoparticles in iron oxyhydroxide-coated sand. *Environmental science & technology*. 2012;46:2738-45.
- [72] Tian Y, Gao B, Wang Y, Morales VL, Carpena RM, Huang Q, et al. Deposition and transport of functionalized carbon nanotubes in water-saturated sand columns. *Journal of hazardous materials*. 2012;213:265-72.
- [73] Elimelech M, Nagai M, Ko C-H, Ryan JN. Relative insignificance of mineral grain zeta potential to colloid transport in geochemically heterogeneous porous media. *Environmental science & technology*. 2000;34:2143-8.
- [74] He J-Z, Li C-C, Wang D-J, Zhou D-M. Biofilms and extracellular polymeric substances mediate the transport of graphene oxide nanoparticles in saturated porous media. *Journal of hazardous materials*. 2015;300:467-74.
- [75] Jiang X, Wang X, Tong M, Kim H. Initial transport and retention behaviors of ZnO nanoparticles in quartz sand porous media coated with *Escherichia coli* biofilm. *Environmental Pollution*. 2013;174:38-49.
- [76] Li Z, Hassan AA, Sahle-Demessie E, Sorial GA. Transport of nanoparticles with dispersant through biofilm coated drinking water sand filters. *Water research*. 2013;47:6457-66.
- [77] Phenrat T, Saleh N, Sirk K, Kim H-J, Tilton RD, Lowry GV. Stabilization of aqueous nanoscale zerovalent iron dispersions by anionic polyelectrolytes: adsorbed anionic polyelectrolyte layer properties and their effect on aggregation and sedimentation. *Journal of Nanoparticle Research*. 2008;10:795-814.
- [78] Zhang W, Crittenden J, Li K, Chen Y. Attachment efficiency of nanoparticle aggregation in aqueous dispersions: modeling and experimental validation. *Environmental science & technology*. 2012;46:7054-62.
- [79] Marmor A. A kinetic theory approach to primary and secondary minimum coagulations and their combination. *Journal of Colloid and Interface Science*. 1979;72:41-8.
- [80] Wu L, Liu L, Gao B, Muñoz-Carpena R, Zhang M, Chen H, et al. Aggregation kinetics of graphene oxides in aqueous solutions: experiments, mechanisms, and modeling. *Langmuir*. 2013;29:15174-81.
- [81] Soltanian MR, Ritzi R, Huang CC, Dai Z, Deng H. A note on upscaling retardation factor in hierarchical porous media with multimodal reactive mineral facies. *Transport in Porous Media*. 2014;108:355-66.
- [82] Soltanian MR, Ritzi RW, Huang CC, Dai Z. Relating reactive solute transport to hierarchical and multiscale sedimentary architecture in a Lagrangian-based transport model: 2. Particle displacement variance. *Water Resources Research*. 2015;51:1601-18.
- [83] Allaire SE, Roulier S, Cessna AJ. Quantifying preferential flow in soils: A review of different techniques. *Journal of Hydrology*. 2009;378:179-204.
- [84] Huang PM, Li Y, Sumner ME. Handbook of soil sciences: properties and processes. New York, US: CRC Press Taylor and Francis Group an informa business; 2011.
- [85] Jacobson MZ. Fundamentals of atmospheric modeling: Cambridge university press; 2005.

- [86] Van Genuchten MT, Wierenga PJ. Mass transfer studies in sorbing porous media I. Analytical solutions. *Soil Science Society of America Journal*. 1976;40:473-80.
- [87] Mehmani Y, Balhoff MT. Mesoscale and hybrid models of fluid flow and solute transport. *Rev Mineral Geochem*. 2015;80:433-59.
- [88] Dale AL, Lowry GV, Casman EA. Much ado about  $\alpha$ : reframing the debate over appropriate fate descriptors in nanoparticle environmental risk modeling. *Environmental Science: Nano*. 2015.
- [89] Zheng C, Wang PP. A modular three-dimensional multi-species transport model for simulation of advection, dispersion and chemical reactions of contaminants in groundwater systems; documentation and user's guide. US Army Engineer Research and Development Center Contract Report SERDP-99-1, Vicksburg, Mississippi, USA. 1999.
- [90] Saiers JE, Hornberger GM. Migration of  $^{137}\text{Cs}$  through quartz sand: experimental results and modeling approaches. *Journal of Contaminant Hydrology*. 1996;22:255-70.
- [91] Seetha N, Majid Hassanizadeh S, Kumar M, Raoof A. Correlation equations for average deposition rate coefficients of nanoparticles in a cylindrical pore. *Water Resources Research*. 2015;51:8034-59.
- [92] Bradford SA, Simunek J, Bettahar M, van Genuchten MT, Yates SR. Modeling colloid attachment, straining, and exclusion in saturated porous media. *Environmental science & technology*. 2003;37:2242-50.
- [93] Bradford SA, Torkzaban S. Determining parameters and mechanisms of colloid retention and release in porous media. *Langmuir*. 2015;31:12096-105.
- [94] Chrysikopoulos CV, Katzourakis VE. Colloid particle size-dependent dispersivity. *Water Resources Research*. 2015.
- [95] Therezien M, Thill A, Wiesner MR. Importance of heterogeneous aggregation for NP fate in natural and engineered systems. *Science of The Total Environment*. 2014;485:309-18.
- [96] Cullen E, O'Carroll DM, Yanful EK, Sleep B. Simulation of the subsurface mobility of carbon nanoparticles at the field scale. *Advances in Water Resources*. 2010;33:361-71.
- [97] Krol MM, Oleniuk AJ, Kocur CM, Sleep BE, Bennett P, Xiong Z, et al. A field-validated model for in situ transport of polymer-stabilized nZVI and implications for subsurface injection. *Environmental science & technology*. 2013;47:7332-40.
- [98] Bradford SA, Simunek J, Bettahar M, van Genuchten MT, Yates SR. Significance of straining in colloid deposition: Evidence and implications. *Water Resour Res*. 2006;42:W12S5.
- [99] Song L, Elimelech M. Dynamics of colloid deposition in porous media: modeling the role of retained particles. *Colloids and Surfaces A*. 1993;73:49-63.
- [100] Kretzschmar R, Borkovec M, Grolimund D, Elimelech M. Mobile subsurface colloids and their role in contaminant transport. *Advances in agronomy*. 1999;66:121-93.
- [101] Sun N, Elimelech M, Sun N-Z, Ryan JN. A novel two-dimensional model for colloid transport in physically and geochemically heterogeneous porous media. *Journal of contaminant hydrology*. 2001;49:173-99.
- [102] Saiers JE, Hornberger GM, Liang L. First-and second-order kinetics approaches for modeling the transport of colloidal particles in porous media. *Water Resources Research*. 1994;30:2499-506.
- [103] Chowdhury AIA, Krol MM, Kocur CM, Boparai HK, Weber KP, Sleep BE, et al. NZVI injection into variably saturated soils: Field and modeling study. *Journal of Contaminant Hydrology*. 2015;183:16-28.
- [104] Raychoudhury T, Tufenkji N, Ghoshal S. Aggregation and deposition kinetics of carboxymethyl cellulose-modified zero-valent iron nanoparticles in porous media. *Water Research*. 2012;46:1735-44.
- [105] Tosco T, Sethi R. Transport of non-Newtonian suspensions of highly concentrated micro-and nanoscale iron particles in porous media: a modeling approach. *Environmental Science & Technology*. 2010;44:9062-8.
- [106] Hosseini SM, Tosco T. Transport and retention of high concentrated nano-Fe/Cu particles through highly flow-rated packed sand column. *Water Research*. 2013;47:326-38.
- [107] Shen C, Huang Y, Li B, Jin Y. Effects of solution chemistry on straining of colloids in porous media under unfavorable conditions. *Water resources research*. 2008;44.
- [108] Scheibe TD, Wood BD. A particle-based model of size or anion exclusion with application to microbial transport in porous media. *Water resources research*. 2003;39.
- [109] Bradford SA, Simunek J, Walker SL. Transport and straining of *E. coli* O157: H7 in saturated porous media. *Water Resources Research*. 2006;42.
- [110] Bradford SA, Bettahar M. Concentration dependent transport of colloids in saturated porous media. *Journal of Contaminant Hydrology*. 2006;82:99-117.

- [111] Wang D, Su C, Liu C, Zhou D. Transport of fluorescently labeled hydroxyapatite nanoparticles in saturated granular media at environmentally relevant concentrations of surfactants. *Colloids and Surfaces A: Physicochemical and Engineering Aspects*. 2014;457:58-66.
- [112] Cornelis G. Fate descriptors for engineered nanoparticles: the good, the bad, and the ugly. *Environmental Science: Nano*. 2015;2:19-26.
- [113] O'Carroll D, Sleep B, Krol M, Boparai H, Kocur C. Nanoscale zero valent iron and bimetallic particles for contaminated site remediation. *Advances in Water Resources*. 2013;51:104-22.
- [114] Praetorius A, Tufenkji N, Goss K-U, Scheringer M, von der Kammer F, Elimelech M. The road to nowhere: equilibrium partition coefficients for nanoparticles. *Environmental Science: Nano*. 2014;1:317-23.
- [115] Bradford SA, Wang Y, Kim H, Torkzaban S, Šimůnek J. Modeling microorganism transport and survival in the subsurface. *Journal of environmental quality*. 2014;43:421-40.
- [116] Ginn TR. A brief review of bacterial transport in natural porous media. Pacific Northwest Lab., Richland, WA (United States); 1995.
- [117] Keller AA, Auset M. A review of visualization techniques of biocolloid transport processes at the pore scale under saturated and unsaturated conditions. *Advances in Water Resources*. 2007;30:1392-407.
- [118] Massoudieh A, Ginn TR. Colloid-facilitated contaminant transport in unsaturated porous media. *Modelling of pollutants in complex environmental systems*. 2010;2:263-86.
- [119] Herzig JP, Leclerc DM, Goff PL. Flow of Suspensions through Porous Media—Application to Deep Filtration. *Industrial & Engineering Chemistry*. 1970;62:8-35.
- [120] Ives KJ. Rapid filtration. *Water Research*. 1970;4:201-23.
- [121] Tufenkji N. Modeling microbial transport in porous media: Traditional approaches and recent developments. *Advances in Water Resources*. 2007;30:1455-69.
- [122] Wang D, Bradford SA, Harvey RW, Hao X, Zhou D. Transport of ARS-labeled hydroxyapatite nanoparticles in saturated granular media is influenced by surface charge variability even in the presence of humic acid. *Journal of hazardous materials*. 2012;229:170-6.
- [123] Wang D, Ge L, He J, Zhang W, Jaisi DP, Zhou D. Hyperexponential and nonmonotonic retention of polyvinylpyrrolidone-coated silver nanoparticles in an Ultisol. *Journal of contaminant hydrology*. 2014;164:35-48.
- [124] Wang D, Bradford SA, Paradelo M, Peijnenburg WJGM, Zhou D. Facilitated transport of copper with hydroxyapatite nanoparticles in saturated sand. *Soil Science Society of America Journal*. 2012;76:375-88.
- [125] Wang D, Jin Y, Jaisi DP. Effect of Size-Selective Retention on the Cotransport of Hydroxyapatite and Goethite Nanoparticles in Saturated Porous Media. *Environmental science & technology*. 2015;49:8461-70.
- [126] Wang D, Jin Y, Jaisi D. Cotransport of Hydroxyapatite Nanoparticles and Hematite Colloids in Saturated Porous Media: Mechanistic Insights from Mathematical Modeling and Phosphate Oxygen Isotope Fractionation. *Journal of Contaminant Hydrology*. 2015.
- [127] Liang Y, Bradford SA, Šimunek J, Vereecken H, Klumpp E. Sensitivity of the transport and retention of stabilized silver nanoparticles to physicochemical factors. *water research*. 2013;47:2572-82.
- [128] Wang D, Jaisi DP, Yan J, Yan Jin a, Zhou D. Transport and Retention of Polyvinylpyrrolidone-Coated Silver Nanoparticles in Natural Soils. *Vadose Zone J*. 2015.
- [129] Wang D, Paradelo M, Bradford SA, Peijnenburg WJGM, Chu L, Zhou D. Facilitated transport of Cu with hydroxyapatite nanoparticles in saturated sand: Effects of solution ionic strength and composition. *water research*. 2011;45:5905-15.
- [130] Fan W, Jiang X, Lu Y, Huo M, Lin S, Geng Z. Effects of surfactants on graphene oxide nanoparticles transport in saturated porous media. *Journal of Environmental Sciences*. 2015.
- [131] Fan W, Jiang XH, Yang W, Geng Z, Huo MX, Liu ZM, et al. Transport of graphene oxide in saturated porous media: Effect of cation composition in mixed Na–Ca electrolyte systems. *Science of The Total Environment*. 2015;511:509-15.
- [132] Qi Z, Zhang L, Chen W. Transport of graphene oxide nanoparticles in saturated sandy soil. *Environmental Science: Processes & Impacts*. 2014;16:2268-77.
- [133] Qi Z, Zhang L, Wang F, Hou L, Chen W. Factors controlling transport of graphene oxide nanoparticles in saturated sand columns. *Environmental toxicology and chemistry*. 2014;33:998-1004.
- [134] Fang J, Xu M-j, Wang D-j, Wen B, Han J-y. Modeling the transport of TiO<sub>2</sub> nanoparticle aggregates in saturated and unsaturated granular media: effects of ionic strength and pH. *water research*. 2013;47:1399-408.
- [135] Braun A, Klumpp E, Azzam R, Neukum C. Transport and deposition of stabilized engineered silver nanoparticles in water saturated loamy sand and silty loam. *Science of The Total Environment*. 2014.

- [136] Raychoudhury T, Tufenkji N, Ghoshal S. Straining of Polyelectrolyte-Stabilized Nanoscale Zero Valent Iron Particles during Transport through Granular Porous Media. *Water Research*. 2014;50:80-90.
- [137] Sun P, Shijirbaatar A, Fang J, Owens G, Lin D, Zhang K. Distinguishable Transport Behavior of Zinc Oxide Nanoparticles in Silica Sand and Soil Columns. *Science of The Total Environment*. 2015;505:189-98.
- [138] Liang Y, Bradford SA, Simunek J, Heggen M, Vereecken H, Klumpp E. Retention and remobilization of stabilized silver nanoparticles in an undisturbed loamy sand soil. *Environmental science & technology*. 2013;47:12229-37.
- [139] Prieve DC, Hoysan PM. Role of colloidal forces in hydrodynamic chromatography. *Journal of Colloid and Interface Science*. 1978;64:201-13.
- [140] Fallah H, Fallah A, Rahmani A, Afkhami M, Ahmadi A. Size Exclusion Mechanism, Suspension Flow through Porous Medium. *International Journal of Modern Nonlinear Theory and Application*. 2012;1:113.
- [141] James SC, Chrysikopoulos CV. Effective velocity and effective dispersion coefficient for finite-sized particles flowing in a uniform fracture. *Journal of colloid and interface science*. 2003;263:288-95.
- [142] de Marsily G. *Quantitative hydrogeology; groundwater hydrology for engineers*. Academic Press, New York, NY. 1986.
- [143] Howington SE, Peters JF, Illangasekare TH. Discrete network modeling for field-scale flow and transport through porous media. DTIC Document; 1997.
- [144] Mehmani Y, Balhoff MT. Eulerian network modeling of longitudinal dispersion. *Water Resources Research*. 2015;51:8586-606.
- [145] Zheng C, Wang P. MT3DMS, A modular three-dimensional multi-species transport model for simulation of advection, dispersion and chemical reactions of contaminants in groundwater systems; documentation and user's guide. US Army Corps Engineers, Engineer Research and Development Center, Contract Report SERDP-99-1, Vicksburg, MS. 1999:202.
- [146] Harvey RW, Garabedian SP. Use of colloid filtration theory in modeling movement of bacteria through a contaminated sandy aquifer. *Environmental Science & Technology*. 1991;25:178-85.
- [147] Zhang W, Jianzhi N, Morales VL, Chen X, Hay AG, Lehmann J, et al. Transport and retention of biochar particles in porous media: effect of pH, ionic strength, and particle size. *Ecohydrology*. 2010;3:497-508.
- [148] Iwasaki T, Slade JJ, Jr., Stanley WE. SOME NOTES ON SAND FILTRATION [with Discussion]. *Journal (American Water Works Association)*. 1937;29:1591-602.
- [149] Wang HF, Anderson MP. *Introduction to groundwater modeling: finite difference and finite element methods*: Academic Press; 1995.
- [150] Illangasekare TH, Frippiat CC, Fučík R. *Dispersion and Mass Transfer Coefficients in Groundwater of Near-Surface Geologic Formations*: CRC Press/Taylor and Francis Group; 2010.
- [151] Keller AA, Sirivithayapakorn S, Chrysikopoulos CV. Early breakthrough of colloids and bacteriophage MS2 in a water-saturated sand column. *Water Resources Research*. 2004;40.
- [152] Parker JC, Van Genuchten T, Virginia Agricultural Experiment S. *Determining Transport Parameters from Laboratory and Field Tracer Experiments*: Virginia Agricultural Experiment Station; 1984.
- [153] Sirivithayapakorn S, Keller A. Transport of colloids in saturated porous media: A pore-scale observation of the size exclusion effect and colloid acceleration. *Water Resources Research*. 2003;39.
- [154] Chowdhury AIA, O'Carroll DM, Xu Y, Sleep BE. Electrophoresis enhanced transport of nano-scale zero valent iron. *Advances in Water Resources*. 2012;40:71-82.
- [155] Darbha GK, Fischer C, Luetzenkirchen J, Schäfer T. Site-specific retention of colloids at rough rock surfaces. *Environmental science & technology*. 2012;46:9378-87.
- [156] Reiche T, Noseck U, Schäfer T. Migration of Contaminants in Fractured-Porous Media in the Presence of Colloids: Effects of Kinetic Interactions. *Transport in Porous Media*. 2015:1-28.
- [157] Salama A, Negara A, El Amin M, Sun S. Numerical investigation of nanoparticles transport in anisotropic porous media. *Journal of contaminant hydrology*. 2015;181:114-30.
- [158] Batchelor GK. Brownian diffusion of particles with hydrodynamic interaction. *Journal of Fluid Mechanics*. 1976;74:1-29.
- [159] Sharma M, Yashonath S. Size dependence of solute diffusivity and Stokes-Einstein relationship: Effect of van der Waals interaction. *Diffusion Fundamentals*. 2007;6:35-1.
- [160] Zheng Q, Dickson SE, Guo Y. Differential transport and dispersion of colloids relative to solutes in single fractures. *Journal of colloid and interface science*. 2009;339:140-51.
- [161] Limousin G, Gaudet JP, Charlet L, Szenknect S, Barthès V, Krimissa M. Sorption isotherms: A review on physical bases, modeling and measurement. *Applied Geochemistry*. 2007;22:249-75.

- [162] Rajagopalan R, Tien C. Trajectory analysis of deep-bed filtration with the sphere-in-cell porous media model. *AIChE Journal*. 1976;22:523-33.
- [163] Logan BE, Jewett DG, Arnold RG, Bouwer EJ, O'Melia CR. Clarification of clean-bed filtration models. *Journal of Environmental Engineering*. 1995;121:869-73.
- [164] Li J, Xie X, Ghoshal S. Correlation Equation for Predicting the Single-Collector Contact Efficiency of Colloids in a Horizontal Flow. *Langmuir*. 2015;31:7210-9.
- [165] Landkamer LL, Harvey RW, Scheibe TD, Ryan JN. Colloid transport in saturated porous media: Elimination of attachment efficiency in a new colloid transport model. *Water Resources Research*. 2013;49:2952-65.
- [166] O'Carroll D, Sleep B, Krol M, Boparai H, Kocur C. Nanoscale zero valent iron and bimetallic particles for contaminated site remediation. *Advances in Water Resources*. 2012:1-19.
- [167] Johnson WP, Li X, Assemi S. Deposition and re-entrainment dynamics of microbes and non-biological colloids during non-perturbed transport in porous media in the presence of an energy barrier to deposition. *Advances in Water Resources*. 2007;30:1432-54.
- [168] O'Carroll DM, Bradford SA, Abriola LM. Infiltration of PCE in a system containing spatial wettability variations. *Journal of Contaminant Hydrology*. 2004;73:39-63.
- [169] Torkzaban S, Bradford SA. Critical role of surface roughness on colloid retention and release in porous media. *Water research*. 2016;88:274-84.
- [170] Wang Z, Jin Y, Shen C, Li T, Huang Y, Li B. Spontaneous Detachment of Colloids from Primary Energy Minima by Brownian Diffusion. *PLoS one*. 2016;11.
- [171] Zhang P, Johnson WP, Piana MJ, Fuller CC, Naftz DL. Potential Artifacts in Interpretation of Differential Breakthrough of Colloids and Dissolved Tracers in the Context of Transport in a Zero-Valent Iron Permeable Reactive Barrier. *Groundwater*. 2001;39:831-40.
- [172] Kasel D, Bradford SA, Šimůnek J, Heggen M, Vereecken H, Klumpp E. Transport and retention of multi-walled carbon nanotubes in saturated porous media: Effects of input concentration and grain size. *water research*. 2013;47:933-44.
- [173] Shang J, Liu C, Wang Z. Transport and retention of engineered nanoporous particles in porous media: effects of concentration and flow dynamics. *Colloids and Surfaces A: Physicochemical and Engineering Aspects*. 2013;417:89-98.
- [174] Flory J, Kanel SR, Racz L, Impellitteri CA, Silva RG, Goltz MN. Influence of pH on the transport of silver nanoparticles in saturated porous media: laboratory experiments and modeling. *Journal of nanoparticle research*. 2013;15:1-11.
- [175] Kanel SR, Flory J, Meyerhoefer A, Fraley JL, Sizemore IE, Goltz MN. Influence of natural organic matter on fate and transport of silver nanoparticles in saturated porous media: laboratory experiments and modeling. *Journal of Nanoparticle Research*. 2013;17:1-13.
- [176] Neukum C, Braun A, Azzam R. Transport of engineered silver (Ag) nanoparticles through partially fractured sandstones. *Journal of contaminant hydrology*. 2014;164:181-92.
- [177] Zhang P, Johnson WP, Scheibe TD, Choi KH, Dobbs FC, Mailloux BJ. Extended tailing of bacteria following breakthrough at the Narrow Channel Focus Area, Oyster, Virginia. *Water Resources Research*. 2001;37:2687-98.
- [178] Bergendahl J, Grasso D. Prediction of colloid detachment in a model porous media: hydrodynamics. *Chemical Engineering Science*. 2000;55:1523-32.
- [179] Torkzaban S, Bradford SA, Walker SL. Resolving the Coupled Effects of Hydrodynamics and DLVO Forces on Colloid Attachment in Porous Media. *Langmuir*. 2007;23:9652-60.
- [180] Harendra S, Vipulanandan C. Fe/Ni bimetallic particles transport in columns packed with sandy clay soil. *Industrial & Engineering Chemistry Research*. 2010;50:404-11.
- [181] Sasidharan S, Torkzaban S, Bradford SA, Dillon PJ, Cook PG. Coupled effects of hydrodynamic and solution chemistry on long-term nanoparticle transport and deposition in saturated porous media. *Colloids and Surfaces A: Physicochemical and Engineering Aspects*. 2014;457:169-79.
- [182] Kini GC, Yu J, Wang L, Kan AT, Biswal SL, Tour JM, et al. Salt-and temperature-stable quantum dot nanoparticles for porous media flow. *Colloids and Surfaces A: Physicochemical and Engineering Aspects*. 2014;443:492-500.
- [183] Torkzaban S, Kim Y, Mulvihill M, Wan J, Tokunaga TK. Transport and deposition of functionalized CdTe nanoparticles in saturated porous media. *Journal of contaminant hydrology*. 2010;118:208-17.
- [184] Wang Y, Zhu H, Becker MD, Englehart J, Abriola LM, Colvin VL, et al. Effect of surface coating composition on quantum dot mobility in porous media. *Journal of nanoparticle research*. 2013;15:1-16.

- [185] Torkzaban S, Wan J, Tokunaga TK, Bradford SA. Impacts of bridging complexation on the transport of surface-modified nanoparticles in saturated sand. *Journal of contaminant hydrology*. 2012;136:86-95.
- [186] Wang Y, Becker MD, Colvin VL, Abriola LM, Pennell KD. Influence of Residual Polymer on Nanoparticle Deposition in Porous Media. *Environmental Science & Technology*. 2014;48:10664-71.
- [187] Torkzaban S, Bradford SA, Wan J, Tokunaga T, Masoudih A. Release of Quantum Dot Nanoparticles in Porous Media: Role of Cation Exchange and Aging Time. *Environmental Science & Technology*. 2013;47:11528-36.
- [188] Treumann S, Torkzaban S, Bradford SA, Visalakshan RM, Page D. An explanation for differences in the process of colloid adsorption in batch and column studies. *Journal of contaminant hydrology*. 2014;164:219-29.
- [189] Torkzaban S, Kim HN, Simunek J, Bradford SA. Hysteresis of colloid retention and release in saturated porous media during transients in solution chemistry. *Environmental science & technology*. 2010;44:1662-9.
- [190] He F, Zhang M, Qian T, Zhao D. Transport of carboxymethyl cellulose stabilized iron nanoparticles in porous media: Column experiments and modeling. *Journal of Colloid and Interface Science*. 2009;334:96-102.
- [191] Lanphere JD, Luth CJ, Walker SL. Effects of solution chemistry on the transport of graphene oxide in saturated porous media. *Environmental science & technology*. 2013;47:4255-61.
- [192] Li Z, Sahle-Demessie E, Hassan AA, Sorial GA. Transport and deposition of CeO<sub>2</sub> nanoparticles in water-saturated porous media. *Water research*. 2011;45:4409-18.
- [193] Godinez IG, Darnault CJG. Aggregation and transport of nano-TiO<sub>2</sub> in saturated porous media: effects of pH, surfactants and flow velocity. *Water research*. 2011;45:839-51.
- [194] Jones EH, Su C. Fate and transport of elemental copper (Cu<sup>0</sup>) nanoparticles through saturated porous media in the presence of organic materials. *water research*. 2012;46:2445-56.
- [195] Grolimund D, Borkovec M. Release of colloidal particles in natural porous media by monovalent and divalent cations. *Journal of Contaminant Hydrology*. 2006;87:155-75.
- [196] Tiraferri A, Sethi R, Tosco TAE. Ionic Strength Dependent Transport of Microparticles in Saturated Porous Media: Modeling Mobilization and Immobilization Phenomena under Transient Chemical Conditions. 2009.
- [197] Tufenkji N. Application of a dual deposition mode model to evaluate transport of *Escherichia coli* D21 in porous media. *Water resources research*. 2006;42.
- [198] Zhang W, Niu J, Morales VL, Chen X, Hay AG, Lehmann J, et al. Transport and retention of biochar particles in porous media: effect of pH, ionic strength, and particle size. *Ecohydrology*. 2010;3:497-508.
- [199] Phenrat T, Cihan A, Kim H-J, Mital M, Illangasekare T, Lowry GV. Transport and deposition of polymer-modified Fe<sup>0</sup> nanoparticles in 2-D heterogeneous porous media: Effects of particle concentration, Fe<sup>0</sup> content, and coatings. *Environmental Science & Technology*. 2010;44:9086-93.
- [200] Xu S, Gao B, Saiers JE. Straining of colloidal particles in saturated porous media. *Water Resources Research*. 2006;42.
- [201] El Badawy AM, Aly Hassan A, Scheckel KG, Suidan MT, Tolaymat TM. Key factors controlling the transport of silver nanoparticles in porous media. *Environmental science & technology*. 2013;47:4039-45.
- [202] Cornelis G, Pang L, Doolette C, Kirby JK, McLaughlin MJ. Transport of silver nanoparticles in saturated columns of natural soils. *Science of the Total Environment*. 2013;463:120-30.
- [203] Neukum C, Braun A, Azzam R. Transport of stabilized engineered silver (Ag) nanoparticles through porous sandstones. *Journal of contaminant hydrology*. 2014;158:1-13.
- [204] Choy CC, Wazne M, Meng X. Application of an empirical transport model to simulate retention of nanocrystalline titanium dioxide in sand columns. *Chemosphere*. 2008;71:1794-801.
- [205] Fang J, Shan X-q, Wen B, Lin J-m, Owens G. Stability of titania nanoparticles in soil suspensions and transport in saturated homogeneous soil columns. *Environmental pollution*. 2009;157:1101-9.
- [206] Jiang X, Tong M, Kim H. Influence of natural organic matter on the transport and deposition of zinc oxide nanoparticles in saturated porous media. *Journal of colloid and interface science*. 2012;386:34-43.
- [207] Jiang X, Tong M, Lu R, Kim H. Transport and deposition of ZnO nanoparticles in saturated porous media. *Colloids and Surfaces A: Physicochemical and Engineering Aspects*. 2012;401:29-37.
- [208] Cleasby JL, Baumann ER. Selection of sand filtration rates. *Journal (American Water Works Association)*. 1962:579-602.
- [209] Ives KJ. Simplified Rational Analysis of Filter Behaviour. *ICE Proceedings*. Vol. 25. 3 ed: Thomas Telford; 1963. p. 345-64.
- [210] Auset M, Keller AA. Pore-scale visualization of colloid straining and filtration in saturated porous media using micromodels. *Water resources research*. 2006;42.

- [211] Wei Y-T, Wu S-C, Chou C-M, Che C-H, Tsai S-M, Lien H-L. Influence of nanoscale zero-valent iron on geochemical properties of groundwater and vinyl chloride degradation: A field case study. *Water Research*. 2010;44:131-40.
- [212] Elliott DW, Zhang W-X. Field assessment of nanoscale bimetallic particles for groundwater treatment. *Environmental Science & Technology*. 2001;35:4922-6.
- [213] Köber R, Hollert H, Hornbruch G, Jekel M, Kamptner A, Klaas N, et al. Nanoscale zero-valent iron flakes for groundwater treatment. *Environmental Earth Sciences*. 2014;72:3339-52.
- [214] Edmiston PL, Osborne C, Reinbold KP, Pickett DC, Underwood LA. Pilot scale testing composite swellable organosilica nanoscale zero-valent iron—Iron-Osorb®—for in situ remediation of trichloroethylene. *Remediation Journal*. 2011;22:105-23.
- [215] Rosansky S, Condit W, Sirabian R. Best practices for injection and distribution of amendments. Technical Report TR-NAVFAC-EXWC-EV; 2013.
- [216] Zhang L, Hou L, Wang L, Kan AT, Chen W, Tomson MB. Transport of fullerene nanoparticles (n C60) in saturated sand and sandy soil: controlling factors and modeling. *Environmental science & technology*. 2012;46:7230-8.
- [217] Dong H, Zeng G, Zhang C, Liang J, Ahmad K, Xu P, et al. Interaction between Cu 2+ and different types of surface-modified nanoscale zero-valent iron during their transport in porous media. *Journal of Environmental Sciences*. 2015;32:180-8.
- [218] Xu S, Liao Q, Saiers JE. Straining of nonspherical colloids in saturated porous media. *Environmental science & technology*. 2008;42:771-8.
- [219] Foppen JWA, Mporokoso A, Schijven JF. Determining straining of *Escherichia coli* from breakthrough curves. *Journal of contaminant hydrology*. 2005;76:191-210.
- [220] Li X, Scheibe TD, Johnson WP. Apparent decreases in colloid deposition rate coefficients with distance of transport under unfavorable deposition conditions: A general phenomenon. *Environmental Science & Technology*. 2004;38:5616-25.
- [221] Tan Y, Gannon JT, Baveye P, Alexander M. Transport of bacteria in an aquifer sand: Experiments and model simulations. *Water resources research*. 1994;30:3243-52.
- [222] Toloni I, Lehmann F, Ackerer P. Modeling the effects of water velocity on TiO<sub>2</sub> nanoparticles transport in saturated porous media. *Journal of contaminant hydrology*. 2014;171:42-8.
- [223] Jones EH, Su C. Transport and retention of zinc oxide nanoparticles in porous media: Effects of natural organic matter versus natural organic ligands at circumneutral pH. *Journal of hazardous materials*. 2014;275:79-88.
- [224] Kurlanda-Witek H, Ngwenya BT, Butler IB. Transport of bare and capped zinc oxide nanoparticles is dependent on porous medium composition. *Journal of contaminant hydrology*. 2014;162:17-26.
- [225] Bradford SA, Toride N. A stochastic model for colloid transport and deposition. *Journal of environmental quality*. 2007;36:1346-56.
- [226] Gargiulo G, Bradford S, Šimůnek J, Ustohal P, Vereecken H, Klumpp E. Bacteria transport and deposition under unsaturated conditions: The role of the matrix grain size and the bacteria surface protein. *Journal of contaminant hydrology*. 2007;92:255-73.
- [227] Gargiulo G, Bradford SA, Šimunek J, Ustohal P, Vereecken H, Klumpp E. Bacteria transport and deposition under unsaturated flow conditions: The role of water content and bacteria surface hydrophobicity. *Vadose Zone Journal*. 2008;7:406-19.
- [228] Ben-Moshe T, Dror I, Berkowitz B. Transport of metal oxide nanoparticles in saturated porous media. *Chemosphere*. 2010;81:387-93.
- [229] Shellenberger K, Logan BE. Effect of molecular scale roughness of glass beads on colloidal and bacterial deposition. *Environmental science & technology*. 2002;36:184-9.
- [230] Yoon JS, Germaine JT, Culligan PJ. Visualization of particle behavior within a porous medium: Mechanisms for particle filtration and retardation during downward transport. *Water Resources Research*. 2006;42.
- [231] Chen KL, Elimelech M. Aggregation and deposition kinetics of fullerene (C60) nanoparticles. *Langmuir*. 2006;22:10994-1001.
- [232] Chen KL, Elimelech M. Influence of humic acid on the aggregation kinetics of fullerene (C 60) nanoparticles in monovalent and divalent electrolyte solutions. *Journal of Colloid and Interface Science*. 2007;309:126-34.
- [233] Chatterjee J, Gupta SK. An agglomeration-based model for colloid filtration. *Environmental Science & Technology*. 2009;43:3694-9.
- [234] Chatterjee J, Abdulkareem S, Gupta SK. Estimation of colloidal deposition from heterogeneous populations. *water research*. 2010;44:3365-74.

- [235] Tong M, Johnson WP. Colloid population heterogeneity drives hyperexponential deviation from classic filtration theory. *Environmental science & technology*. 2007;41:493-9.
- [236] Bradford SA, Torkzaban S, Simunek J. Modeling colloid transport and retention in saturated porous media under unfavorable attachment conditions. *Water Resources Research*. 2011;47.
- [237] Bradford SA, Torkzaban S, Wiegmann A. Pore-scale simulations to determine the applied hydrodynamic torque and colloid immobilization. *Vadose Zone Journal*. 2011;10:252-61.
- [238] Bolster CH, Mills AL, Hornberger GM, Herman JS. Spatial distribution of deposited bacteria following miscible displacement experiments in intact cores. *Water Resources Research*. 1999;35:1797-807.
- [239] Tufenkji N, Elimelech M. Spatial distributions of *Cryptosporidium* oocysts in porous media: Evidence for dual mode deposition. *Environmental science & technology*. 2005;39:3620-9.
- [240] Porubcan AA, Xu S. Colloid straining within saturated heterogeneous porous media. *Water research*. 2011;45:1796-806.
- [241] Xu S, Saiers JE. Colloid straining within water-saturated porous media: Effects of colloid size nonuniformity. *Water resources research*. 2009;45.
- [242] Ren D, Smith JA. Protein-capped silver nanoparticle transport in water-saturated sand. *Journal of Environmental Engineering*. 2012;139:781-7.
- [243] Johnson WP, Ma H, Pazmino E. Straining credibility: a general comment regarding common arguments used to infer straining as the mechanism of colloid retention in porous media. *Environmental science & technology*. 2011;45:3831-2.
- [244] Johnson RL, Nurmi JT, O'Brien Johnson GS, Fan D, O'Brien Johnson RL, Shi Z, et al. Field-Scale Transport and Transformation of Carboxymethylcellulose-Stabilized Nano Zero-Valent Iron. *Environmental science & technology*. 2013;47:1573-80.
- [245] Kocur CM, Chowdhury AI, Sakulchaicharoen N, Boparai HK, Weber KP, Sharma P, et al. Characterization of nZVI mobility in a field scale test. *Environmental Science & Technology*. 2014;48:2862-9.
- [246] Langmuir I. THE ADSORPTION OF GASES ON PLANE SURFACES OF GLASS, MICA AND PLATINUM. *Journal of the American Chemical Society*. 1918;40:1361-403.
- [247] Adamczyk Z, Siwek B, Zembala M, Belouschek P. Kinetics of localized adsorption of colloid particles. *Advances in Colloid and Interface Science*. 1994;48:151-280.
- [248] Skopp J. Analysis of time-dependent chemical processes in soils. *Journal of environmental quality*. 1986;15:205-13.
- [249] Sun Y, Gao B, Bradford SA, Wu L, Chen H, Shi X, et al. Transport, retention, and size perturbation of graphene oxide in saturated porous media: Effects of input concentration and grain size. *Water research*. 2015;68:24-33.
- [250] Feriencikova L, Xu S. Deposition and remobilization of graphene oxide within saturated sand packs. *Journal of hazardous materials*. 2012;235:194-200.
- [251] Liu L, Gao B, Wu L, Sun Y, Zhou Z. Effects of surfactant type and concentration on graphene retention and transport in saturated porous media. *Chemical Engineering Journal*. 2015;262:1187-91.
- [252] Johnson PR, Elimelech M. Dynamics of colloid deposition in porous media: Blocking based on random sequential adsorption. *Langmuir*. 1995;11:801-12.
- [253] Schaaf P, Talbot J. Surface exclusion effects in adsorption processes. *The Journal of chemical physics*. 1989;91:4401-9.
- [254] Becker MD, Wang Y, Paulsen JL, Song Y-Q, Abriola LM, Pennell KD. In situ measurement and simulation of nano-magnetite mobility in porous media subject to transient salinity. *Nanoscale*. 2015;7:1047-57.
- [255] Bai C, Li Y. Modeling the transport and retention of nC 60 nanoparticles in the subsurface under different release scenarios. *Journal of contaminant hydrology*. 2012;136:43-55.
- [256] Chen G, Liu X, Su C. Transport and retention of TiO<sub>2</sub> rutile nanoparticles in saturated porous media under low-ionic-strength conditions: measurements and mechanisms. *Langmuir*. 2011;27:5393-402.
- [257] Deshpande PA, Shonnard DR. Modeling the effects of systematic variation in ionic strength on the attachment kinetics of *Pseudomonas fluorescens* UPER-1 in saturated sand columns. *Water resources research*. 1999;35:1619-27.
- [258] Basnet M, Di Tommaso C, Ghoshal S, Tufenkji N. Reduced transport potential of a palladium-doped zero valent iron nanoparticle in a water saturated loamy sand. *Water research*. 2015;68:354-63.
- [259] Gastone F, Tosco T, Sethi R. Guar gum solutions for improved delivery of iron particles in porous media (Part 1): Porous medium rheology and guar gum-induced clogging. *Journal of contaminant hydrology*. 2014;166:23-33.

- [260] Tosco T, Gastone F, Sethi R. Guar gum solutions for improved delivery of iron particles in porous media (Part 2): Iron transport tests and modeling in radial geometry. *Journal of contaminant hydrology*. 2014;166:34-51.
- [261] Nascimento AG, Totola MR, Souza CS, Borges MT, Borges AC. Temporal and spatial dynamics of blocking and ripening effects on bacterial transport through a porous system: A possible explanation for CFT deviation. *Colloids and Surfaces B: Biointerfaces*. 2006;53:241-4.
- [262] Basnet M, Ghoshal S, Tufenkji N. Rhamnolipid biosurfactant and soy protein act as effective stabilizers in the aggregation and transport of palladium-doped zerovalent iron nanoparticles in saturated porous media. *Environmental science & technology*. 2013;47:13355-64.
- [263] Tiraferri A, Sethi R. Enhanced transport of zerovalent iron nanoparticles in saturated porous media by guar gum. *Journal of Nanoparticle Research*. 2009;11:635-45.
- [264] Wang X, Cai L, Han P, Lin D, Kim H, Tong M. Cotransport of multi-walled carbon nanotubes and titanium dioxide nanoparticles in saturated porous media. *Environmental Pollution*. 2014;195:31-8.
- [265] Chen G, Liu X, Su C. Distinct effects of humic acid on transport and retention of tio<sub>2</sub> rutile nanoparticles in saturated sand columns. *Environmental Science & Technology*. 2012;46:7142-50.
- [266] Cheng X, Kan AT, Tomson MB. Study of C 60 transport in porous media and the effect of sorbed C 60 on naphthalene transport. *Journal of Materials Research*. 2005;20:3244-54.
- [267] Lv X, Gao B, Sun Y, Shi X, Xu H, Wu J. Effects of Humic Acid and Solution Chemistry on the Retention and Transport of Cerium Dioxide Nanoparticles in Saturated Porous Media. *Water, Air, & Soil Pollution*. 2014;225:1-9.
- [268] Tong M, Ma H, Johnson WP. Funneling of flow into grain-to-grain contacts drives colloid- colloid aggregation in the presence of an energy barrier. *Environmental science & technology*. 2008;42:2826-32.
- [269] Kuznar ZA, Elimelech M. Direct microscopic observation of particle deposition in porous media: Role of the secondary energy minimum. *Colloids and Surfaces A: Physicochemical and Engineering Aspects*. 2007;294:156-62.
- [270] Babakhani P, Fagerlund F, Shamsai A, Lowry GV, Phenrat T. Supplementary Material for "Modified MODFLOW-based model for simulating the agglomeration and transport of polymer-modified Fe nanoparticles in saturated porous media". *Environ Sci Pollut Res Int*. 2015:1-20.
- [271] !!! INVALID CITATION !!!
- [272] Camesano TA, Unice KM, Logan BE. Blocking and ripening of colloids in porous media and their implications for bacterial transport. *Colloids and Surfaces A: Physicochemical and Engineering Aspects*. 1999;160:291-307.
- [273] Afroz ARMN, Das D, Murphy CJ, Vikesland P, Saleh NB. Co-transport of gold nanospheres with single-walled carbon nanotubes in saturated porous media. *Water research*. 2016;99:7-15.
- [274] McCarthy JF, Zachara JM. Subsurface transport of contaminants. *Environmental Science & Technology*. 1989;23:496-502.
- [275] Smith PA, Degueudre C. Colloid-facilitated transport of radionuclides through fractured media. *Journal of contaminant hydrology*. 1993;13:143-66.
- [276] Kersting AB, Efurud DW, Finnegan DL, Rokop DJ, Smith DK, Thompson JL. Migration of plutonium in ground water at the Nevada Test Site. *Nature*. 1999;397:56-9.
- [277] Xie J, Lin J, Wang Y, Li M, Zhang J, Zhou X, et al. Colloid-associated plutonium aged at room temperature: evaluating its transport velocity in saturated coarse-grained granites. *Journal of contaminant hydrology*. 2015;172:24-32.
- [278] Xie J, Wang Y, Lin J, Li M, Zhang J, Zhou X, et al. Trace-level plutonium (IV) polymer stability and its transport in coarse-grained granites. *Chemical Geology*. 2015;398:1-10.
- [279] Grindrod P. The impact of colloids on the migration and dispersal of radionuclides within fractured rock. *Journal of contaminant hydrology*. 1993;13:167-81.
- [280] Kurosawa S, James SC, Yui M, Ibaraki M. Model analysis of the colloid and radionuclide retardation experiment at the Grimsel Test Site. *Journal of colloid and interface science*. 2006;298:467-75.
- [281] Malkovsky VI, Pek AA. Effect of elevated velocity of particles in groundwater flow and its role in colloid-facilitated transport of radionuclides in underground medium. *Transport in porous media*. 2009;78:277-94.
- [282] Li S-H, Yang H-T, Jen C-P. Modeling of colloid transport mechanisms facilitating migration of radionuclides in fractured media. *Nuclear technology*. 2004;148:358-68.
- [283] Auset M, Keller AA. Pore-scale processes that control dispersion of colloids in saturated porous media. *Water Resources Research*. 2004;40.
- [284] Small H, Saunders FL, Solc J. Hydrodynamic chromatography a new approach to particle size analysis. *Advances in Colloid and Interface Science*. 1976;6:237-66.

- [285] Dong H, Onstott TC, DeFlaun MF, Fuller ME, Scheibe TD, Streger SH, et al. Relative dominance of physical versus chemical effects on the transport of adhesion-deficient bacteria in intact cores from South Oyster, Virginia. *Environmental science & technology*. 2002;36:891-900.
- [286] Mitzel MR, Tufenkji N. Transport of industrial PVP-stabilized silver nanoparticles in saturated quartz sand coated with *Pseudomonas aeruginosa* PAO1 biofilm of variable age. *Environmental science & technology*. 2014;48:2715-23.
- [287] Sagee O, Dror I, Berkowitz B. Transport of silver nanoparticles (AgNPs) in soil. *Chemosphere*. 2012;88:670-5.
- [288] Solovitch N, Labille Jrm, Rose Jrm, Chaurand P, Borschneck D, Wiesner MR, et al. Concurrent aggregation and deposition of TiO<sub>2</sub> nanoparticles in a sandy porous media. *Environmental science & technology*. 2010;44:4897-902.
- [289] Laumann S, Micić V, Lowry GV, Hofmann T. Carbonate minerals in porous media decrease mobility of polyacrylic acid modified zero-valent iron nanoparticles used for groundwater remediation. *Environmental Pollution*. 2013;179:53-60.
- [290] Jaisi DP, Elimelech M. Single-Walled Carbon Nanotubes Exhibit Limited Transport in Soil Columns. *Environmental Science & Technology*. 2009;43:9161-6.
- [291] Golmohamadi M, Clark RJ, Veinot JGC, Wilkinson KJ. The role of charge on the diffusion of solutes and nanoparticles (silicon nanocrystals, nTiO<sub>2</sub>, nAu) in a biofilm. *Environmental Chemistry*. 2013;10:34-41.
- [292] Kim H-J, Phenrat T, Tilton RD, Lowry GV. Effect of kaolinite, silica fines and pH on transport of polymer-modified zero valent iron nano-particles in heterogeneous porous media. *Journal of Colloid and Interface Science*. 2012;370:1-10.
- [293] Goldberg E, Scheringer M, Bucheli TD, Hungerbühler K. Critical assessment of models for transport of engineered nanoparticles in saturated porous media. *Environmental science & technology*. 2014;48:12732-41.
- [294] Torkzaban S, Bradford SA, Vanderzalm JL, Patterson BM, Harris B, Prommer H. Colloid release and clogging in porous media: Effects of solution ionic strength and flow velocity. *Journal of contaminant hydrology*. 2015;181:161-71.
- [295] Shapiro AA, Bedrikovetsky PG. A stochastic theory for deep bed filtration accounting for dispersion and size distributions. *Physica A: Statistical Mechanics and its Applications*. 2010;389:2473-94.
- [296] You Z, Bedrikovetsky P, Kuzmina L. Exact solution for long-term size exclusion suspension-colloidal transport in porous media. Hindawi Publishing Corporation; 2013.
- [297] Sen TK, Khilar KC. Review on subsurface colloids and colloid-associated contaminant transport in saturated porous media. *Advances in colloid and interface science*. 2006;119:71-96.
- [298] Harter T, Wagner S, Atwill ER. Colloid transport and filtration of *Cryptosporidium parvum* in sandy soils and aquifer sediments. *Environmental science & technology*. 2000;34:62-70.
- [299] Abdel-Salam A, Chrysikopoulos CV. Modeling of colloid and colloid-facilitated contaminant transport in a two-dimensional fracture with spatially variable aperture. *Transport in porous media*. 1995;20:197-221.
- [300] Wang Y, Bradford SA, Šimůnek J. Transport and fate of microorganisms in soils with preferential flow under different solution chemistry conditions. *Water Resources Research*. 2013;49:2424-36.
- [301] Ginn TR. A travel time approach to exclusion on transport in porous media. *Water resources research*. 2002;38:12-1.
- [302] Grolimund D, Elimelech M, Borkovec M, Barmettler K, Kretzschmar R, Sticher H. Transport of in Situ Mobilized Colloidal Particles in Packed Soil Columns. *Environmental Science & Technology*. 1998;32:3562-9.
- [303] Ginn TR. Comment on "Stochastic analysis of virus transport in aquifers," by Linda L. Campbell Rehmann, Claire Welty, and Ronald W. Harvey. *Water Resources Research*. 2000;36:1981-2.
- [304] Weisbrod N, Meron H, Walker S, Gitis V. Virus transport in a discrete fracture. *Water research*. 2013;47:1888-98.
- [305] Chrysikopoulos CV, Syngouna VI. Effect of gravity on colloid transport through water-saturated columns packed with glass beads: Modeling and experiments. *Environmental science & technology*. 2014;48:6805-13.
- [306] DiMarzio EA, Guttman CM. Separation by flow. *Journal of Polymer Science Part B: Polymer Letters*. 1969;7:267-72.
- [307] DiMarzio EA, Guttman CM. Separation by Flow. *Macromolecules*. 1970;3:131-46.
- [308] Cox RG, Hsu SK. The lateral migration of solid particles in a laminar flow near a plane. *International journal of multiphase flow*. 1977;3:201-22.
- [309] Segre G, Silberberg A. Behaviour of macroscopic rigid spheres in Poiseuille flow Part 2. Experimental results and interpretation. *Journal of fluid mechanics*. 1962;14:136-57.

- [310] Cox RG, Brenner H. The lateral migration of solid particles in Poiseuille flow—I Theory. *Chemical Engineering Science*. 1968;23:147-73.
- [311] Segre G, Silberberg A. Behaviour of macroscopic rigid spheres in Poiseuille flow Part 1. Determination of local concentration by statistical analysis of particle passages through crossed light beams. *Journal of Fluid Mechanics*. 1962;14:115-35.
- [312] Krupp HK, Biggar JW, Nielsen DR. Relative flow rates of salt and water in soil. *Soil Science Society of America Journal*. 1972;36:412-7.
- [313] Van Genuchten MT. Non-equilibrium transport parameters from miscible displacement experiments. 1981.
- [314] Chrysikopoulos CV, Abdel-Salam A. Modeling colloid transport and deposition in saturated fractures. *Colloids and Surfaces A: Physicochemical and Engineering Aspects*. 1997;121:189-202.
- [315] Risovic D, Martinis M. The role of coagulation and sedimentation mechanisms in the two-component model of sea-particle size distribution. *Fizika*. 1994;3:103-18.
- [316] Tang P, Raper JA. Modelling the settling behaviour of fractal aggregates—a review. *Powder technology*. 2002;123:114-25.
- [317] Friedlander SK. On the particle-size spectrum of atmospheric aerosols. *Journal of Meteorology*. 1960;17:373-4.
- [318] Friedlander SK. Similarity considerations for the particle-size spectrum of a coagulating, sedimenting aerosol. *Journal of Meteorology*. 1960;17:479-83.
- [319] Jeffrey DJ. Quasi-stationary approximations for the size distribution of aerosols. *Journal of the Atmospheric Sciences*. 1981;38:2440-3.
- [320] Abel JS, Stangle GC, Schilling CH, Aksay IA. Sedimentation in flocculating colloidal suspensions. *Journal of materials research*. 1994;9:451-61.
- [321] Smoluchowski M. Versuch einer mathematischen Theorie der Koagulationskinetik kolloider Lösungen. *Zeitschrift fuer Physikalische Chemie* 92. 1917;129-68.
- [322] Quik JTK, Velzeboer I, Wouterse M, Koelmans AA, Van de Meent D. Heteroaggregation and sedimentation rates for nanomaterials in natural waters. *Water research*. 2014;48:269-79.
- [323] Hunt JR. Self-similar particle-size distributions during coagulation: theory and experimental verification. *Journal of Fluid Mechanics*. 1982;122:169-85.
- [324] Lee DG, Bonner JS, Garton LS, Ernest ANS, Autenrieth RL. Modeling coagulation kinetics incorporating fractal theories: a fractal rectilinear approach. *Water Research*. 2000;34:1987-2000.
- [325] Lee DG, Bonner JS, Garton LS, Ernest ANS, Autenrieth RL. Modeling coagulation kinetics incorporating fractal theories: comparison with observed data. *Water Research*. 2002;36:1056-66.
- [326] Liu HH, Surawanvijit S, Rallo R, Orkoulas G, Cohen Y. Analysis of nanoparticle agglomeration in aqueous suspensions via constant-number Monte Carlo simulation. *Environmental Science & Technology*. 2011;45:9284-92.
- [327] Yu H, Fu J, Dang L, Cheong Y, Tan H, Wei H. Prediction of the Particle Size Distribution Parameters in a High Shear Granulation Process Using a Key Parameter Definition Combined Artificial Neural Network Model. *Industrial & Engineering Chemistry Research*. 2015;54:10825-34.
- [328] Goudeli E, Eggersdorfer ML, Pratsinis SE. Coagulation–Agglomeration of fractal-like particles: Structure and self-preserving size distribution. *Langmuir*. 2015;31:1320-7.
- [329] Rahman T, George J, Shipley HJ. Transport of aluminum oxide nanoparticles in saturated sand: Effects of ionic strength, flow rate, and nanoparticle concentration. *Science of The Total Environment*. 2013;463–464:565-71.
- [330] Rahman T, Millwater H, Shipley HJ. Modeling and sensitivity analysis on the transport of aluminum oxide nanoparticles in saturated sand: Effects of ionic strength, flow rate, and nanoparticle concentration. *Science of The Total Environment*. 2014;499:402-12.
- [331] Wei Y-T, Wu S-c, Yang S-W, Che C-H, Lien H-L, Huang D-H. Biodegradable surfactant stabilized nanoscale zero-valent iron for in situ treatment of vinyl chloride and 1, 2-dichloroethane. *Journal of hazardous materials*. 2012;211:373-80.
- [332] Wang Q, Lee J-H, Jeong S-W, Jang A, Lee S, Choi H. Mobilization and deposition of iron nano and sub-micrometer particles in porous media: A glass micromodel study. *Journal of hazardous materials*. 2011;192:1466-75.
- [333] Dunphy Guzman KA, Finnegan MP, Banfield JF. Influence of surface potential on aggregation and transport of titania nanoparticles. *Environmental Science & Technology*. 2006;40:7688-93.
- [334] Klimentko AY, Saulov DN, Massarotto P, Rudolph V. Conditional model for sorption in porous media with fractal properties. *Transport in porous media*. 2012;92:745-65.

- [335] Phenrat T, Kim HJ, Fagerlund F, Illangasekare T, Tilton RD, Lowry GV. Supporting Information for "Particle size distribution, concentration, and magnetic attraction affect transport of polymer-modified FeO nanoparticles in sand columns". *Environ Sci Technol*. 2009;43:5079-85.
- [336] Lin S, Wiesner MR. Deposition of Aggregated Nanoparticles • A Theoretical and Experimental Study on the Effect of Aggregation State on the Affinity between Nanoparticles and a Collector Surface. *Environmental science & technology*. 2012;46:13270-7.
- [337] Li X, Logan BE. Collision frequencies of fractal aggregates with small particles by differential sedimentation. *Environmental science & technology*. 1997;31:1229-36.
- [338] Li X-Y, Logan BE. Permeability of fractal aggregates. *Water research*. 2001;35:3373-80.
- [339] Meng Z, Hashmi SM, Elimelech M. Aggregation rate and fractal dimension of fullerene nanoparticles via simultaneous multiangle static and dynamic light scattering measurement. *Journal of colloid and interface science*. 2013;392:27-33.
- [340] Chakraborti RK, Gardner KH, Atkinson JF, Van Benschoten JE. Changes in fractal dimension during aggregation. *Water Research*. 2003;37:873-83.
- [341] Johnson CP, Li X, Logan BE. Settling Velocities of Fractal Aggregates. *Environmental Science & Technology*. 1996;30:1911-8.
- [342] Babakhani P, Bridge J, Doong R-a, Phenrat T. Parameterisation and Prediction of Nanoparticles Transport in Porous Media: a Reanalysis using Artificial Neural Network. *Water Resources Research*. In Press.
- [343] Holthoff H, Egelhaaf SU, Borkovec M, Schurtenberger P, Sticher H. Coagulation rate measurements of colloidal particles by simultaneous static and dynamic light scattering. *Langmuir*. 1996;12:5541-9.
- [344] Holthoff H, Schmitt A, Fernández-Barbero A, Borkovec M, Ángel Cabrerizo-Vilchez M, Schurtenberger P, et al. Measurement of absolute coagulation rate constants for colloidal particles: comparison of single and multiparticle light scattering techniques. *Journal of colloid and interface science*. 1997;192:463-70.
- [345] Szilagyi I, Szabo T, Desert A, Trefalt G, Oncsik T, Borkovec M. Particle aggregation mechanisms in ionic liquids. *Physical Chemistry Chemical Physics*. 2014;16:9515-24.
- [346] Birkner FB, Morgan JJ. Polymer flocculation kinetics of dilute colloidal suspensions. *Journal (American Water Works Association)*. 1968:175-91.
- [347] Swift DL, Friedlander SK. The coagulation of hydrosols by Brownian motion and laminar shear flow. *Journal of colloid science*. 1964;19:621-47.
- [348] Logan BE, Passow U, Alldredge AL, Grossart H-P, Simont M. Rapid formation and sedimentation of large aggregates is predictable from coagulation rates (half-lives) of transparent exopolymer particles (TEP). *Deep Sea Research Part II: Topical Studies in Oceanography*. 1995;42:203-14.
- [349] Baalousha M. Aggregation and disaggregation of iron oxide nanoparticles: Influence of particle concentration, pH and natural organic matter. *Science of The Total Environment*. 2009;407:2093-101.
- [350] Kocur CM, O'Carroll DM, Sleep BE. Impact of nZVI stability on mobility in porous media. *Journal of Contaminant Hydrology*. 2013;145:17-25.
- [351] Phenrat T, Saleh N, Sirk K, Tilton RD, Lowry GV. Aggregation and sedimentation of aqueous nanoscale zerovalent iron dispersions. *Environmental Science & Technology*. 2007;41:284-90.
- [352] Baalousha M, Sikder M, Prasad A, Lead J, Merrifield R, Chandler GT. The concentration-dependent behaviour of nanoparticles. *Environmental Chemistry*. 2015;13:1-3.
- [353] Han Y, Hwang G, Kim D, Bradford SA, Lee B, Eom I, et al. Transport, retention, and long-term release behavior of ZnO nanoparticle aggregates in saturated quartz sand: Role of solution pH and biofilm coating. *Water research*. 2016;90:247-57.
- [354] Weerts AH, Leij FJ, Toride N, Van Genuchten MT. Analytical models for contaminant transport in soils and groundwater. *Personal Communication*. 1995.
- [355] Zhang P, Fan C, Lu H, Kan AT, Tomson MB. Synthesis of crystalline-phase silica-based calcium phosphonate nanomaterials and their transport in carbonate and sandstone porous media. *Industrial & Engineering Chemistry Research*. 2011;50:1819-30.
- [356] EPA U. Understanding variation in partition coefficient,  $K_d$ , values. Office of Air and Radiation, United States Environmental Protection Agency, . 1999;EPA 402-R-99-004B:1-341.
- [357] Zhao J, Liu F, Wang Z, Cao X, Xing B. Heteroaggregation of graphene oxide with minerals in aqueous phase. *Environmental science & technology*. 2015;49:2849-57.
- [358] Julich D, Gäth S. Sorption behavior of copper nanoparticles in soils compared to copper ions. *Geoderma*. 2014;235:127-32.

- [359] Abraham PM, Barnikol S, Baumann T, Kuehn M, Ivleva NP, Schaumann GE. Sorption of silver nanoparticles to environmental and model surfaces. *Environmental science & technology*. 2013;47:5083-91.
- [360] Petersen EJ, Pinto RA, Zhang L, Huang Q, Landrum PF, Weber Jr WJ. Effects of polyethyleneimine-mediated functionalization of multi-walled carbon nanotubes on earthworm bioaccumulation and sorption by soils. *Environmental science & technology*. 2011;45:3718-24.
- [361] Zhang L, Petersen EJ, Huang Q. Phase distribution of <sup>14</sup>C-labeled multiwalled carbon nanotubes in aqueous systems containing model solids: Peat. *Environmental science & technology*. 2011;45:1356-62.
- [362] Forouzangohar M, Kookana RS. Sorption of nano-C 60 clusters in soil: hydrophilic or hydrophobic interactions? *Journal of Environmental Monitoring*. 2011;13:1190-4.
- [363] Nickel C, Gabsch S, Hellack B, Nogowski A, Babick F, Stintz M, et al. Mobility of coated and uncoated TiO<sub>2</sub> nanomaterials in soil columns—Applicability of the tests methods of OECD TG 312 and 106 for nanomaterials. *Journal of environmental management*. 2015;157:230-7.
- [364] Watermark Numerical Computing & Waterloo Hydrogeologic I. WinPEST User's Manual: Non-linear Parameter Estimation and Predictive Analysis Program 1999.
- [365] Akaike H. A new look at the statistical model identification. *Automatic Control, IEEE Transactions on*. 1974;19:716-23.
- [366] Bai C, Li Y. Time series analysis of contaminant transport in the subsurface: Applications to conservative tracer and engineered nanomaterials. *Journal of contaminant hydrology*. 2014;164:153-62.
- [367] Yuan H, Shapiro AA. A mathematical model for non-monotonic deposition profiles in deep bed filtration systems. *Chemical Engineering Journal*. 2011;166:105-15.
- [368] Li X, Lin C-L, Miller JD, Johnson WP. Role of grain-to-grain contacts on profiles of retained colloids in porous media in the presence of an energy barrier to deposition. *Environmental science & technology*. 2006;40:3769-74.
- [369] Li Y, Wang Y, Pennell KD, Abriola LM. Investigation of the transport and deposition of fullerene (C<sub>60</sub>) nanoparticles in quartz sands under varying flow conditions. *Environmental science & technology*. 2008;42:7174-80.
- [370] Tong M, Camesano TA, Johnson WP. Spatial variation in deposition rate coefficients of an adhesion-deficient bacterial strain in quartz sand. *Environmental science & technology*. 2005;39:3679-87.
- [371] Wang Y, Li Y, Costanza J, Abriola LM, Pennell KD. Enhanced mobility of fullerene (C<sub>60</sub>) nanoparticles in the presence of stabilizing agents. *Environmental science & technology*. 2012;46:11761-9.
- [372] Corkhill CL, Bridge JW, Chen XC, Hillel P, Thornton SF, Romero-Gonzalez ME, et al. Real-Time Gamma Imaging of Technetium Transport through Natural and Engineered Porous Materials for Radioactive Waste Disposal. *Environmental science & technology*. 2013;47:13857-64.
- [373] Bridge JW, Banwart SA, Heathwaite AL. Noninvasive quantitative measurement of colloid transport in mesoscale porous media using time lapse fluorescence imaging. *Environmental science & technology*. 2006;40:5930-6.
- [374] Bridge JW, Banwart SA, Heathwaite AL. High-resolution measurement of pore saturation and colloid removal efficiency in quartz sand using fluorescence imaging. *Environmental science & technology*. 2007;41:8288-94.
- [375] Bridge JW, Heathwaite AL, Banwart SA. Measurement of colloid mobilization and redeposition during drainage in quartz sand. *Environmental science & technology*. 2009;43:5769-75.
- [376] Ramanan B, Holmes WM, Sloan WT, Phoenix VR. Investigation of nanoparticle transport inside coarse-grained geological media using magnetic resonance imaging. *Environmental science & technology*. 2011;46:360-6.
- [377] Roth EJ, Gilbert B, Mays DC. Colloid deposit morphology and clogging in porous media: Fundamental insights through investigation of deposit fractal dimension. *Environmental science & technology*. 2015;49:12263-70.
- [378] Byron ML, Variano EA. Refractive-index-matched hydrogel materials for measuring flow-structure interactions. *Experiments in fluids*. 2013;54:1-6.
- [379] Su C, Puls RW, Krug TA, Watling MT, O'Hara SK, Quinn JW, et al. Travel distance and transformation of injected emulsified zerovalent iron nanoparticles in the subsurface during two and half years. *Water research*. 2013;47:4095-106.
- [380] Bianco C, Tosco T, Sethi R. A 3-dimensional micro-and nanoparticle transport and filtration model (MNM3D) applied to the migration of carbon-based nanomaterials in porous media. *Journal of Contaminant Hydrology*. 2016;193:10-20.

- [381] Kanel SR, Goswami RR, Clement TP, Barnett MO, Zhao D. Two dimensional transport characteristics of surface stabilized zero-valent iron nanoparticles in porous media. *Environmental Science & Technology*. 2007;42:896-900.
- [382] Comba S, Braun J. An empirical model to predict the distribution of iron micro-particles around an injection well in a sandy aquifer. *Journal of Contaminant Hydrology*. 2012;132:1-11.
- [383] Šimunek J, Šejna M, Saito H, Sakai M, Van Genuchten MT. The HYDRUS-1D software package for simulating the one-dimensional movement of water, heat, and multiple solutes in variably-saturated media, version 4.08. University of California, Riverside, Dept of Environmental Sciences HYDRUS Software Series. 2009;3:330.
- [384] Šimunek J, van Genuchten MT, Šejna M. Recent Developments and Applications of the HYDRUS Computer Software Packages. *Vadose Zone Journal*. 2016;15.
- [385] Langevin CD, Thorne Jr DT, Dausman AM, Sukop MC, Guo W. SEAWAT Version 4: a computer program for simulation of multi-species solute and heat transport. Geological Survey (US); 2008.
- [386] Clement TP. A Modular Computer Code for Simulating Reactive Multispecies Transport in 3-Dimensional Groundwater Systems. The US Department of Energy. 1997:1-59.
- [387] Goldberg E, Scheringer M, Bucheli TD, Hungerbühler K. Prediction of nanoparticle transport behavior from physicochemical properties: machine learning provides insights to guide the next generation of transport models. *Environmental Science: Nano*. 2015;2:352-60.
- [388] Westerhoff P, Nowack B. Searching for global descriptors of engineered nanomaterial fate and transport in the environment. *Accounts of chemical research*. 2012;46:844-53.
- [389] Web of Science™, <http://apps.webofknowledge.com/>.
- [390] Tufenkji N, Elimelech M. Deviation from the Classical Colloid Filtration Theory in the Presence of Repulsive DLVO Interactions. *Langmuir*. 2004;20:10818-28.
- [391] Schijven JF, Hassanizadeh SM, de Bruin RHAM. Two-site kinetic modeling of bacteriophages transport through columns of saturated dune sand. *Journal of Contaminant Hydrology*. 2002;57:259-79.
- [392] Golzar M, Saghravani SF, Azhdari Moghaddam M. Experimental Study and Numerical Solution of Poly Acrylic Acid Supported Magnetite Nanoparticles Transport in a One-Dimensional Porous Media. *Advances in Materials Science and Engineering*. 2014;2014.
- [393] Laumann S, Micić V, Hofmann T. Mobility enhancement of nanoscale zero-valent iron in carbonate porous media through co-injection of polyelectrolytes. *Water research*. 2014;50:70-9.
- [394] Liu L, Gao B, Wu L, Morales VL, Yang L, Zhou Z, et al. Deposition and transport of graphene oxide in saturated and unsaturated porous media. *Chemical Engineering Journal*. 2013;229:444-9.

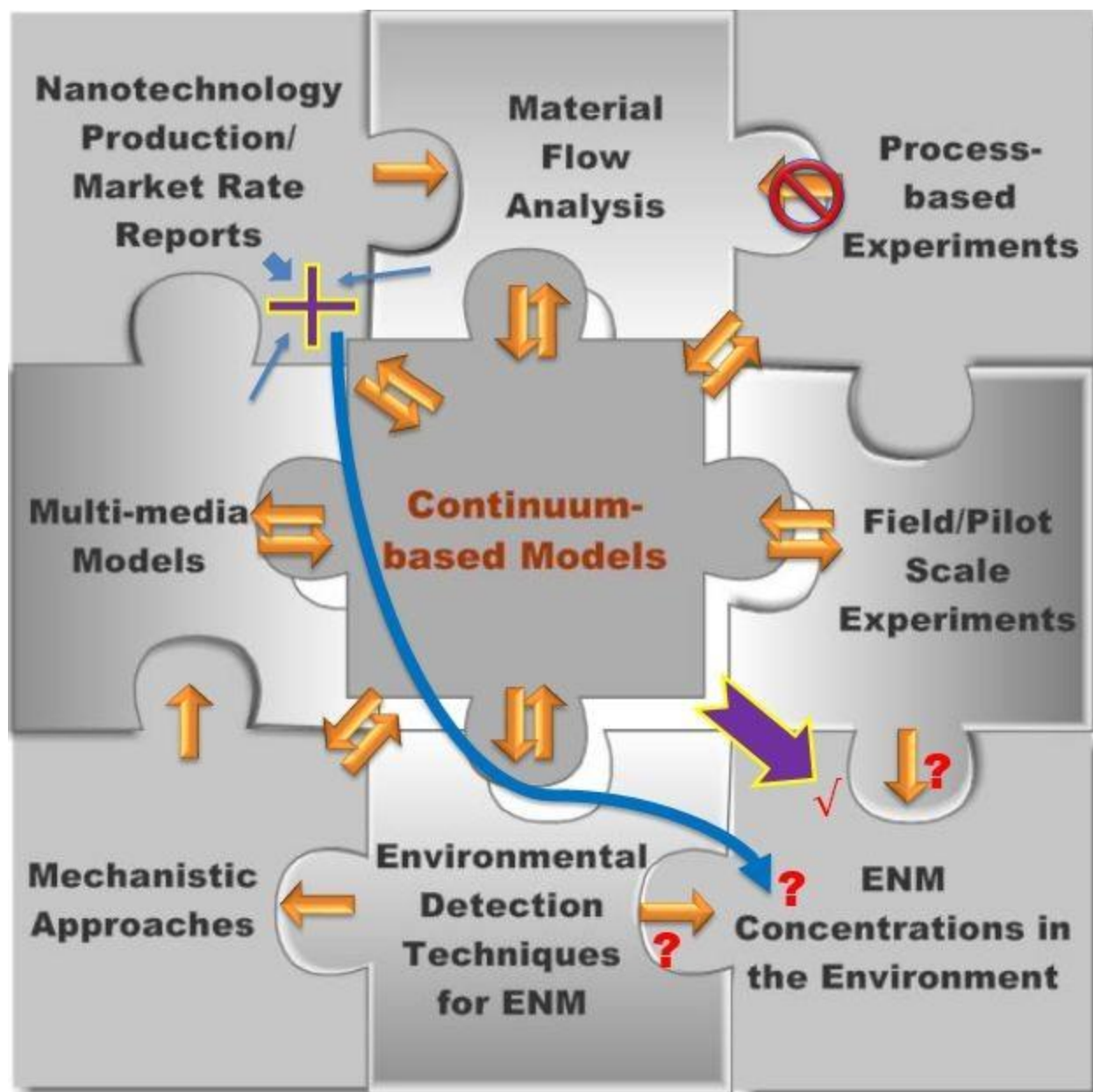


Figure 1

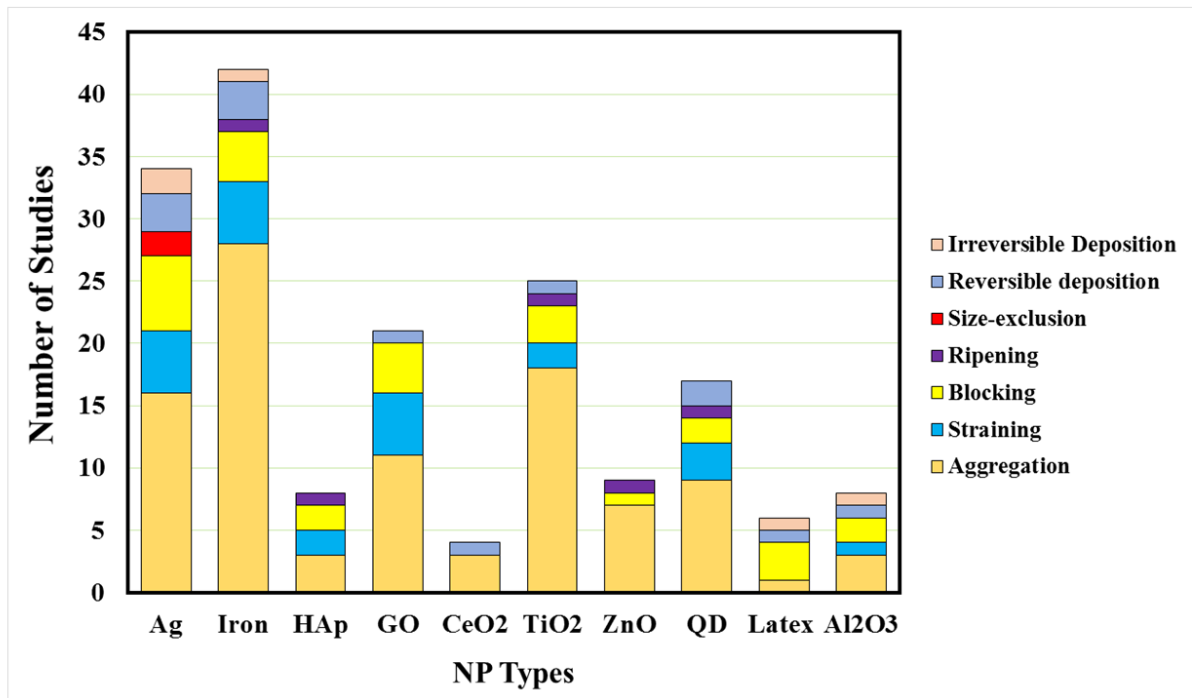


Figure 2

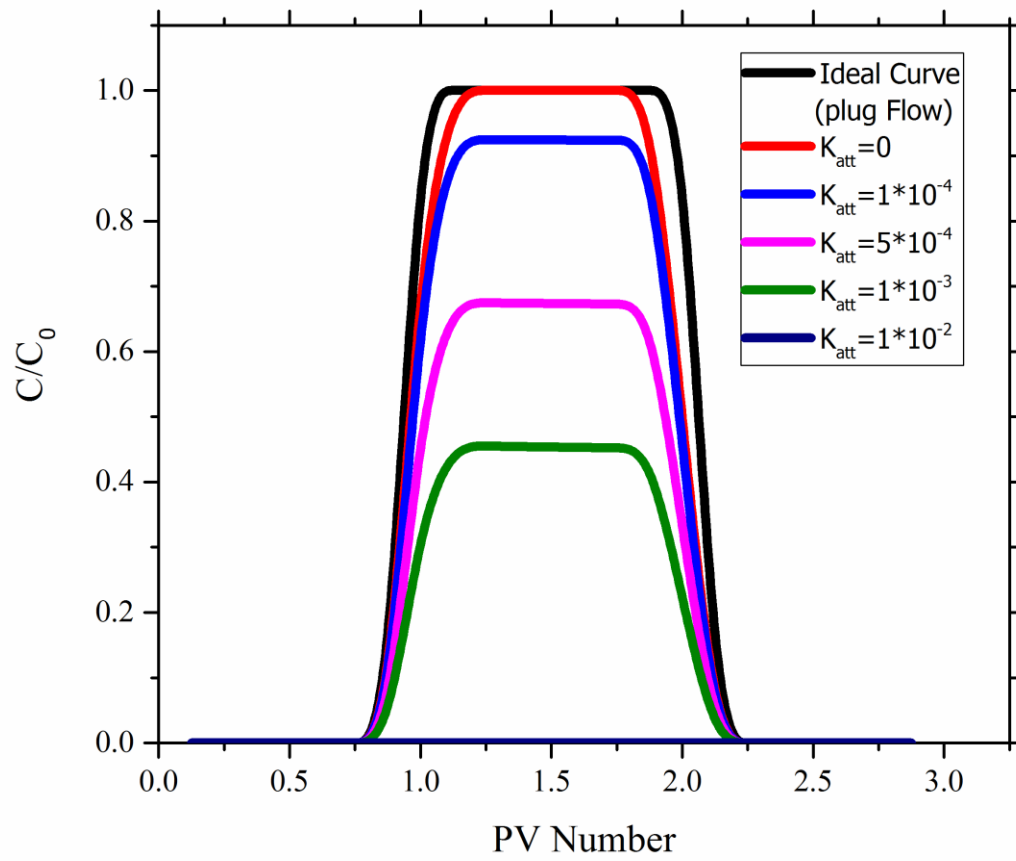


Figure 3

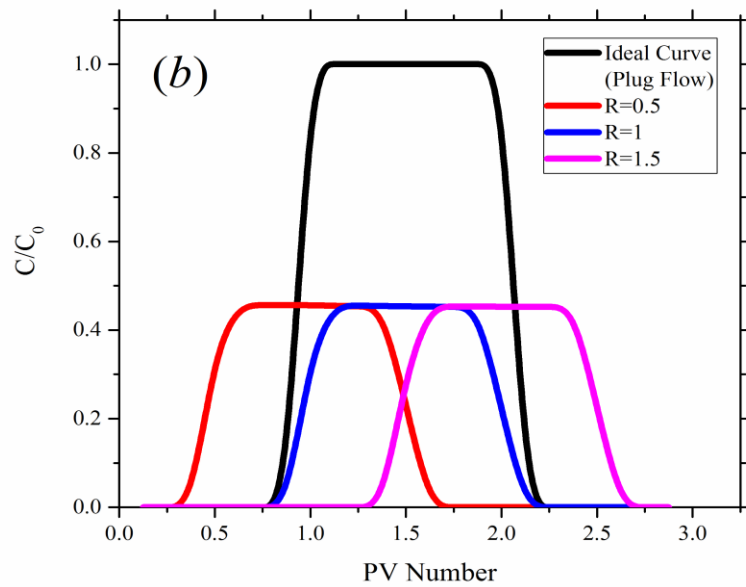
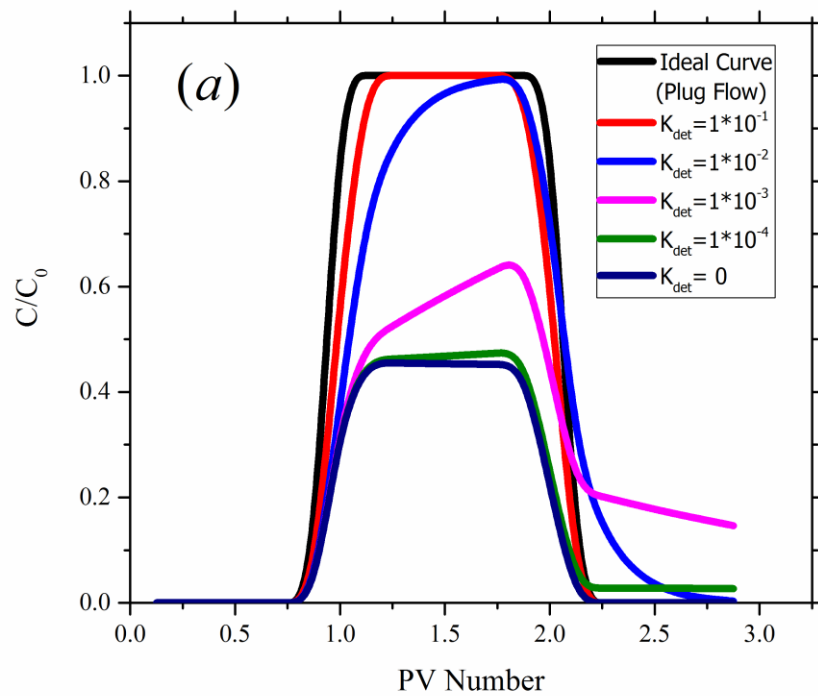


Figure 4

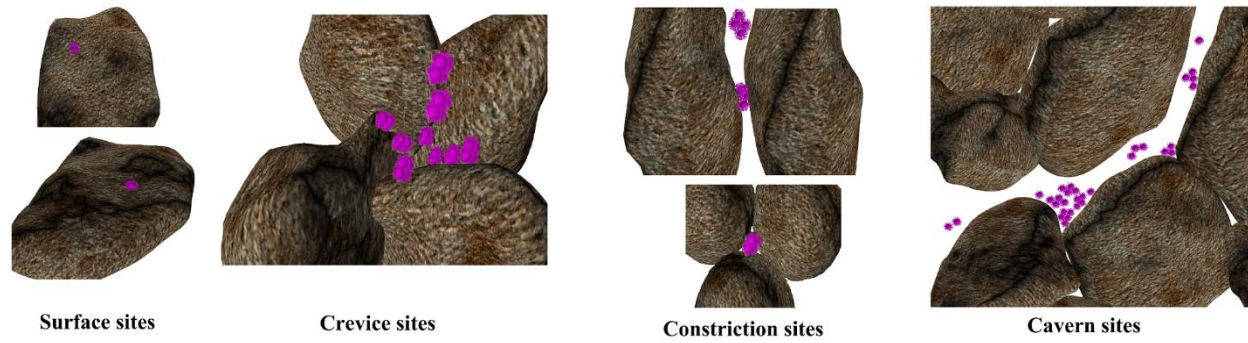


Figure 5

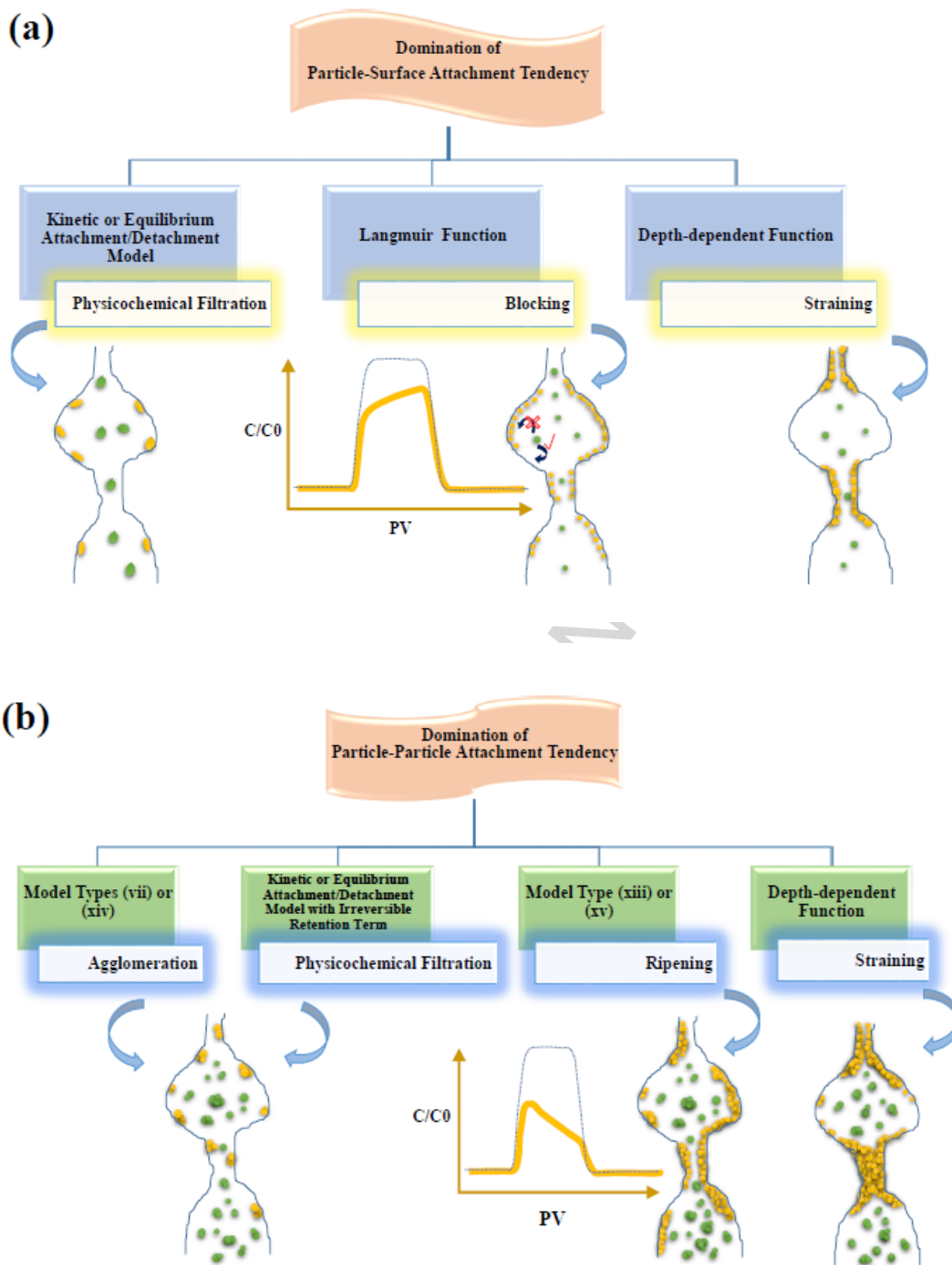
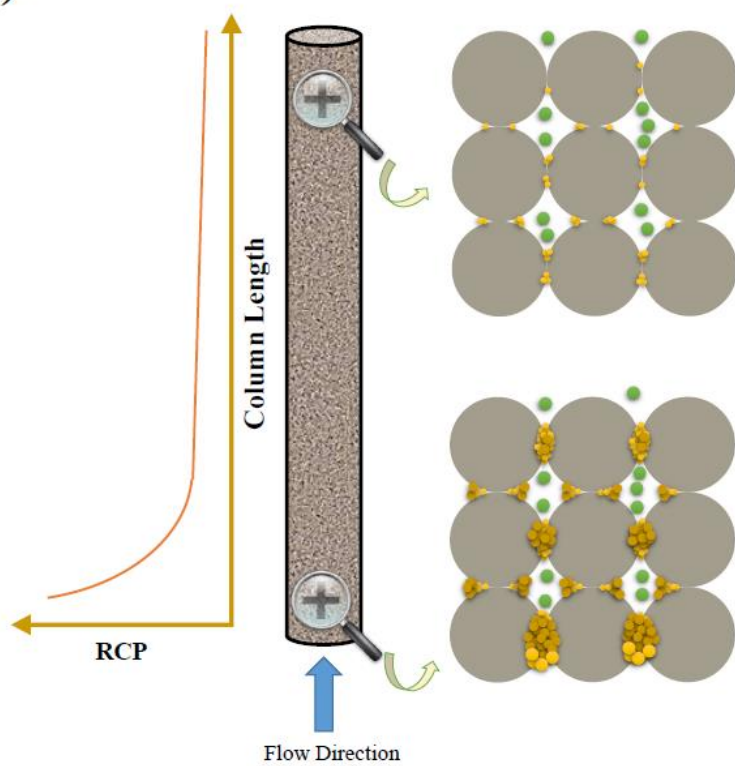


Figure 6

(a)



(b)

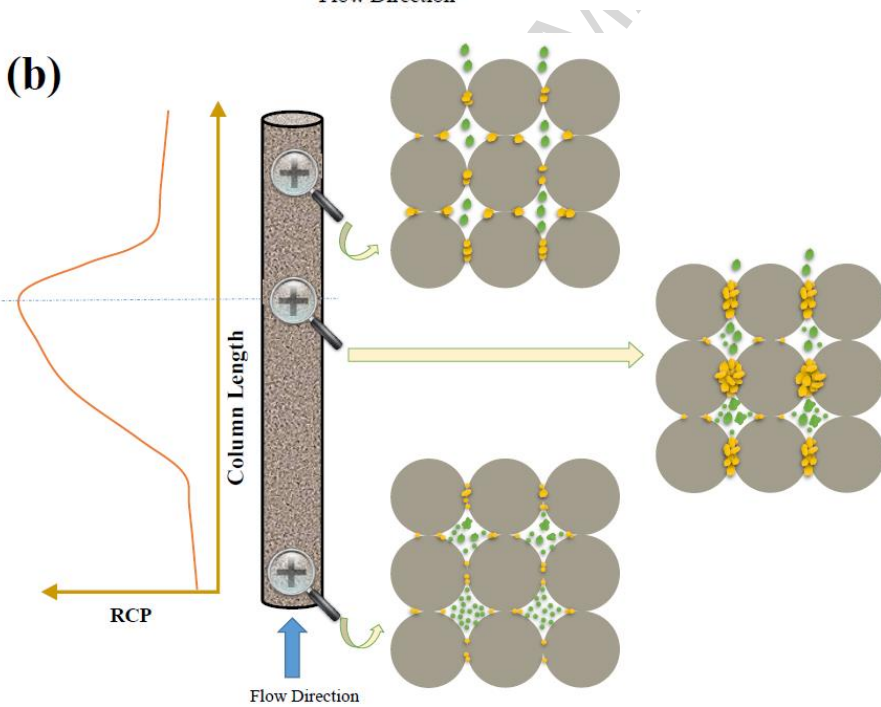


Figure 7

## Graphical abstract

